GEOMETRY, MATTER AND WAVE PROPAGATION IN LORENTZIAN WORMHOLE SPACETIMES

by

SAYAN KAR

GEOMETRY, MATTER AND WAVE PROPAGATION IN LORENTZIAN WORMHOLE SPACETIMES

A Thesis Submitted

in Partial Fulfillment of the Requirements

for the Degree of

Doctor of Philosophy

by

SAYAN KAR

to the

DEPARTMENT OF PHYSICS

INDIAN INSTITUTE OF TECHNOLOGY KANPUR

AUGUST 1994
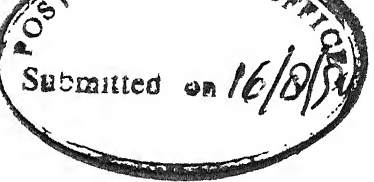
CERTIFICATE

It is certified that the work contained in this thesis entitled *"Geometry, Matter and Wave Propagation in Lorentzian Wormhole Spacetimes"*, by *"Sayan Kar"*, has been carried out under my supervision and that this work has not been submitted elsewhere for a degree.

Deshdeep Sahdev
Assistant Professor
Department of Physics
Indian Institute of Technology
Kanpur

August 1994

Acknowledgements

List of Publications/Submitted Papers

1. Lorentzian Wormholes in Einstein–Gauss–Bonnet Theory, (with Biplab Bhawal), Physical Review **D 46**,2464 (1992)

2. Evolving Wormholes and The Weak Energy Condition , Physical Review **D 49**,862 (1994)

3. Scalar Waves in a Wormhole Geometry , (with D.Sahdev and B.Bhawal), Physical Review **D 49**,853 (1994)

4. Traversable Wormholes with Traceless Matter , (with D.Sahdev), (submitted)

5. Resonances in Transmission of Massless Scalar Waves in a Class of Wormholes , (with S.N.Minwalla,D.Mishra and D.Sahdev), (submitted)

6. An Instanton Approach to Quantum Tunnelling For a Particle on a Rotating Circle , Physics Letters **A 168**,179 (1992)*

7. Quantum Energy Levels of a Particle on a Rotating Circle , (with R.S.Bandhu and C. Burragohain) , (submitted)*

* These papers do not pertain to the topic of this thesis.

Contents

List of Figures

Chapter 1

Introduction

In the late fifties, Misner and Wheeler[1] and Wheeler [2,3] introduced the notion of a wormhole while trying to understand the origin of electric charge. They considered charge free electromagnetism in a multiply–connected space and were able to interpret charge as manifest in the latter's topology . The multiply–connected space they constructed was essentially a sheet with a handle(Fig.1.1)-this was given the name of a wormhole.

Even though the Misner-Wheeler idea was quite novel and generated a fair amount of enthusiasm, it lacked an experimental basis and was perhaps a little too ambitious in nature. This probably explains the gradual decline of interest among workers in this area. The wormhole, then remained dormant for many years and reappeared only in the late eighties with the publication of the seminal papers of Hawking [4] , Giddings and Strominger [5] and Morris ,Thorne and Yurtsever (MTY) [6] .Two separate directions emerged one in an Euclidean setting and the other in a Lorentzian one. The first of these (due to Hawking, Giddings and Strominger) essentially dealt with the construction of models describing topology changing processes in Euclidean Quantum Gravity.

The other involved Lorentzian wormholes based on General Relativity(GR) and

dealt with issues related to the violation of the Energy Conditions, the occurence of closed timelike curves and the construction of time–machine models.

We shall exclusively deal with Lorentzian wormholes in this thesis.

1.1 Motivations

Since wormholes are, as of now, entirely artefacts of the human imagination it is necessary to provide some motivation for studying them. We shall restrict ourselves mainly to reasons for studying Lorentzian wormhole geometries.

(i) In order to prove the famous singularity [8] and the positive energy theorems [9] one needs to make certain assumptions on the components of the energy momentum tensor. These assumptions have come to be known as the Energy Conditions.It so happens that the matter required to support a static , spherically symmetric Lorentzian wormhole geometry violates these conditions. On the other hand, it is a well known fact that the expectation value of $T_{\mu\nu}$ taken over certain quantum states *can* violate the Energy Conditions. In fact as early as 1965 Epstein, Glaser and Yaffe[10] showed that $< T_{00} >$ for certain states can be negative. Also,the Casimir Effect provides an *experimentally* tested violation of the Energy Conditions in the quantum regime[11,12,13]. Two questions naturally arise at this point – (1) 'Are there wormholes which exist with matter satisfying the Energy Conditions?' and (2)'Can we construct a realistic model for exotic matter?'In the former case, it is clear that one has to either go beyond static and spherically symmetric metrics or consider alternative theories of gravity. On the other hand the latter query seems to have an answer only in the quantum regime which leaves us wondering whether wormholes occur naturally exclusively at Planckian scales.

(ii) In 1988 ,MTY [6] developed a time–machine model based on a traversable Lorentzian wormhole. Earlier that year Morris and Thorne[14] had discussed the

possibility of using wormholes for rapid interstellar travel–a wormhole was called traversable if the tidal forces felt by a traveller moving through it were bearable. The subsequent arrival of the wormhole time-machine led researchers to seriously consider the novel physical consequences that arise in spacetimes with closed time-like lines(CTL).Questions related to the well-definedness of the Cauchy problem [15,16] the construction of a local quantum field theory in a spacetime with CTLs [17,18,19] and the possibilities of contructing time machine models with cosmic strings [20],etc. have fascinated theoretical physicists immensely in recent times.It may be argued that such investigations are entirely academic. However, the conceptual and somewhat philosophical questions that arise in these studies are, if not impossible, difficult to ignore.

(iii) It is generally believed that in the quantum gravity era the topology of space was subject to quantum fluctuations [3]. The creation/formation of a wormhole actually requires change in topology of a spacelike section in the course of time evolution. The construction of a viable model for topology change in the Lorentzian context is however plagued by the several no-go theorems (Geroch [22] and Tipler [23]) which basically rule out the existence of such processes in the regime of GR. In Euclidean Quantum Gravity there do exist certain models which attempt to analyse these processes (see Section 1.3)and with some amount of success. However a satisfactory answer to – 'How wormholes form?' is yet to see the light of day.

(iv) Since wormholes, as of now , are far from being realistic (in the sense, say of astrophysical objects) one has to keep an open mind while asking –'How can one become aware of the presence of a wormhole?' A natural way to arrive at signatures of wormholes is to study the orbits of point particles and the propagation of waves in such geometries. Very little has been done along these lines.

(v) As a final motivation it is important to mention that the simplicity and

elegance of wormhole geometries together with the large number of deep and ill-understood issues related to them makes them a very useful teaching tool for GR. This has been illustrated beautifully by Morris and Thorne [14] .

1.2   Outline

Our concern in this thesis will be with the issues mentioned in (i) and (iv) (See 1.1). We shall now briefly outline the problems studied and then proceed towards a detailed understanding in the subsequent chapters.

The Morris–Thorne approach to constructing a wormhole is based on first choosing the metric and then investigating the resulting matter. In Chapter 3 we construct a class of wormholes which obey the tracelessness constraint on matter. The metric is not chosen initially, but arises as a solution to the tracelessness constraint under a specific choice of the redshift function A different choice of a certain constant C yields singular geometries which are used to construct Visser type wormholes. In the former case, the violation of the WEC can be restricted to a finite region of space if one does not demand a significant flare out from the throat. In the latter case matter is traceless and normal everywhere except at the throat. The human traversability of the Morris–Thorne wormholes is also discussed and bounds on the possible throat radii are obtained.

As a way of resolving the contradiction between wormhole existence and the matter required for it we extend the usual static, spherically symmetric wormholes to the nonstatic regime. The consequence of this is that, at least for arbitrarily large but finite intervals of time the required matter satisfies the Weak Energy Condition(WEC). Several examples of such geometries are constructed and the conditions necessary for avoiding WEC violation are put down in detail in Chapter 4. A model universe containing a wormhole and yet resembling the matter or

radiation–dominated flat FRW spacetime models in its asymptotic regions is also constructed.The minimum possible throat size and the nature of matter in the vicinity of the wormhole are discussed briefly.

In order to obtain better insight into specific signatures of wormholes we study the massless scalar wave equation in the background of a new one parameter family of wormhole spacetimes(Chapter 5). Exact solutions involving Modified Mathieu (in $2+1$ dimensions) and Radial Oblate Spheroidal (in $3+1$ dimensions) functions are available only for a specific member of the family ($n = 2,n$ being the parameter) and for special values of the energy of the scalar wave. Reflection and transmission coefficients are obtained both analytically and numerically in the $n = 2$ case, whereas for $n > 2$ we have only the numerical results. The plots of $|T|$ versus the energy of the scalar wave reveal the presence of certain resonances, the depth of which depends on the value of the parameter n. These can therefore be considered as possible signatures of wormholes belonging to this family, which ,in principle, can help in their identification. The above–mentioned analysis is done for both the 2+1 and 3+1 dimensional versions of the one parameter family of metrics.

It is natural to ask–what happens to the WEC violation of matter for wormholes in $D > 4$ GR or in other higher order theories. In Chapter 6 we have specifically studied Lorentzian wormholes in the Einstein–Gauss–Bonnet (EGB)theory. Since, in $D > 4$, the Einstein-Hilbert action is not unique and higher order terms contribute. The first of such terms is the Gauss–Bonnet combination. This action(i.e Einstein-Hilbert term + Gauss–Bonnet combination) also appears as the effective low energy action emerging out of String Theory. Apart from constructing solutions with specific features dependent on the dimensionality and the coupling coefficient of the Gauss-Bonnet combination, the status of the WEC is also explored in detail. A brief discussion on evolving wormhole geometries in $D > 4$ GR and EGB theories is also presented.

1.3   Brief Survey of Relevant Literature

This section briefly summarizes the basic content of some of the existing literature on wormholes. We begin with the Misner- Wheeler wormhole and then discuss Euclidean wormholes using this occasion to briefly outline the basic ideas and the important contributions in this subfield over the last few years. The final sub section, which is a little more extensive, is concerned with the Lorentzian scenario.

1.3.1   The Wheeler wormhole -'Charge is topology'

In 1925 Rainich [24] derived a remarkable result in Einstein-Maxwell theory .He showed that if certain conditions (known today as the Rainich conditions) are satisfied , the electromagnetic field strength tensor $F_{\mu\nu}$ can be written in terms of the the curvature of space. Rainich's results however remained largely unnoticed and in a later book [25]even he made no mention of them. However in the late fifties Misner and Wheeler realized the importance of Rainich's contribution. They were then involved in a serious attempt towards interpreting the basic elements of classical physics as manifestions of the curvature and topology of space. Contrary to the conventional belief that the spacetime continuum is an 'arena for the struggles of fields and particles' Wheeler declared - 'There is nothing in the world except curved and empty space. Matter, charge and electromagnetism and other fields are manisfestations of the bending of space. Physics is Geometry'. Models were provided which demonstrated the following .(a) Unquantized charge is in fact describable in terms of the source-free Maxwell field in a multiply connected space .(b) Unquantized mass is associated with a concentration of electromagnetic field energy held together by its own gravitional attraction. The wormhole geometry provided an example of the fact mentioned in (a).

Fig.1.1 shows a two dimensional section of the Wheeler wormhole as embedded
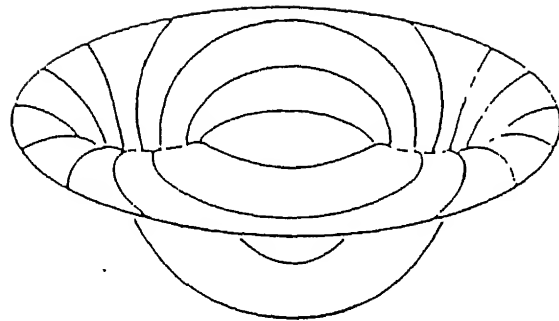
Figure 1.1: The Wheeler Wormhole

in three dimensional Euclidean space. Consider the situation when the electric field lines are trapped in the multiply connected topology of such a wormhole.Lines emerge from one mouth and enter the other .The remarkable fact is that to a person oblivious of the existence of such a handle, the mouths look like sources of positive or negative charge ,inspite of the fact that there is no charge anywhere. This led Wheeler to conclude that unquantized charge is actually manifest in the multiply connected topology of space. Wheeler's seemingly paradoxical phrase - "charge without charge "is in tune with the basic theme of Einstein's GR where the concept of "mass without mass" implies that mass is manifest in the curvature of space.

A large body of literature exists on both classical and quantum geometrodynamics(the Wheelerian term for this programme of the geometrization of physics). We shall, however, dwell no further on this.

1.3.2 Euclidean Wormholes and Topology Changing Processes

Euclidean signature wormholes are very different from their Lorentzian counterparts. The first important difference is that an Euclidean wormhole is 'intrinsically' wormhole–like whereas the Lorentzian one is 'extrinsically' so. The words 'intrinsic' and 'extrinsic' carry the same meaning as in differential geometry. A generic form of the metric tensor for an Euclidean wormhole geometry is

$$ds^2 = d\tau^2 + a^2(\tau)d\Omega_3{}^2 \tag{1.1}$$

with $a(\tau)$ having the following properties:

$$(i) \qquad \tau \to \pm \infty \qquad \Rightarrow a(\tau) \sim \tau^2 \tag{1.2}$$

$$(ii) \qquad \tau \to 0 \qquad \Rightarrow a(\tau) \sim a_0 (throat \quad radius) \tag{1.3}$$

In 1988 Giddings and Strominger [5] provided the first example of an Euclidean wormhole geometry as well as one for a topology changing process in quantum gravity. They employed Einstein gravity coupled to a rank three antisymmetric tensor field as the underlying theory. It was found that the basic requirement for an Euclidean wormhole to exist in a given theory is the existence of negative eigenvalues of the Ricci tensor. In the theory used by Giddings and Strominger [5] this was found to hold. They also studied a topology changing process from R^3 to $R^3 \oplus S^3$ and evaluated the amplitude of tunnelling from one topology to another. It happened that this amplitude was significant at Planck scales which made the paper more important in the context of Quantum Gravity. Subsequently, a lot of work has been done on Euclidean wormholes. These include scalar field Euclidean wormholes [26], magnetic Euclidean wormholes in $2+1$ and $3+1$ dimensions [27], higher dimensional analogs of the Giddings–Strominger geometry [28], Yang–Mills Euclidean

wormholes [29] to mention only a few of them. More interestingly, Coleman [7] has made an attempt at solving the age old cosmological constant problem using Euclidean wormholes. Shortly after Coleman's theory Preskill [30] investigated the consequence of similar wormhole induced effects on other constants of nature (such as 'G'). Much of the initial interest in the Coleman theory of the cosmological constant has disappeared in thewake of its failure to solve what is known as the 'large wormhole problem' which plagues its validity. Moreover, since Euclidean Quantum Gravity is itself known to have several problems in its formulation (e.g unboundedness of the Euclidean Einstein action,the question of providing a meaning to the concept of Euclidean time in the context of quantum gravity etc.) using it as a theory to study the effects of quantization is probably premature.

1.3.3 Traversable Lorentzian Wormholes

An early example of a Lorentzian wormhole geometry(in the sense in which it is used today) was provided by Ellis in 1973 [31]. He termed his geometry as a 'drainhole' .This spacetime is essentially the same as the one studied by Morris and Thorne in Box 2 of Ref [14]. Ellis obtained this geometry as an exact solution of the Einstein field equations with matter in the form of a scalar field with negative energy density. Even though the Energy Conditions of GR had already been formulated he does not mention them in his paper. However he does a very detailed study of geodesics in such geometries . Later Clement [32] investigated the scattering of plane scalar and electromagnetic waves in the Ellis geometry. We shall have more to say on the propagation of scalar waves in Ellis geometries and their generalisations in the penultimate chapter of this thesis.

We shall now briefly describe the present state of the art in Lorentzian wormhole geometries .

After the renaissance in this field in 1988, a major problem emerged concerning the nature of matter required to have such geometries. This is related to the fact that the energy conditions of GR postulated by Hawking and Penrose in the early seventies in order to prove the singularity theorems of GR are essentially violated by the matter threading a traversable wormhole. The question of confining this exotic matter to a very small region near the throat of the wormhole was addressed by Morris and Thorne [14] and later by Visser [33,34]. The Visser construction involved the suturing of two semiwormholes across a thin shell of exotic matter using the Junction Condition Formalism of GR. He used copies of the Schwarzschild geometry to make a wormhole. The advantage of the Visser construction is that in this, one is able to restrict the exotic matter to a very small region in the vicinity of the throat.

A natural line of research since the early days of GR has been to compare and contrast the effects and results in GR with those of other alternative metric theories of gravity. Infact these alternative theories serve the purpose of providing a framework for testing the validity of GR. Soon after the Morris-Thorne construction of a traversable wormhole arrived in the scene, several people attempted to resolve the issue of energy condition violation by looking into alternative models of gravity. For Brans-Dicke type theories the violation remained as long as one considered physically relevant values for the Brans-Dicke parameter ω. Hochberg [35] devoted some attention to $(R + R^2)$ type theories by reducing the relevant Lagrangians to the Einstein-Hilbert one coupled to a scalar field. Later, Ghoruku and Soma [38] dealt with the same theory in a somewhat different way by using defocussing arguments to prove the violation of the energy conditions. At about the same time Moffat and Svoboda [36] showed that in the non-symmetric theory of gravity the violation of these conditions remain. More recently, based on a suggestion of Morris and Thorne, Hochberg and Kephart [37] used squeezed states of the electromagnetic

field to arrive at a model of exotic mater in the quantum regime .It has been known for quite some time that squeezed states can entail negative energy densities. Thus matter constucted out of such states will necessarily violate the Energy conditions. We will discuss the various directions of research on Energy Conditions and their violation in the next chapter.

One of the most remarkable pieces of work on wormholes was the one on the construction of a time machine model by Morris ,Thorne and Yurtsever [6] .Further insights into wormhole −based and other time machine models was provided by Novikov [39] [40]. .Although the existence of closed timelike curves is not uncommon in GR (earlier examples include the Godel universe ,Taub-NUT space etc.) the MTY model was interesting in its own right because of its elegance and simplicity. Infact it almost made the time machine seem a realistic possibility. Sometime after the proposal of the MTY model Gott[20] proposed a time machine model using two cosmic strings moving pasteach other at a high velocity. The Gott model had the advantage of not using any exotic matter as the space is locally flat away from the strings.However it had its own drawbacks. Deser,Jackiw and t'Hooft [21] showed that Gott space could not develop from regular initial data posed on a Cauchy surface. Very recently Ori [41] has proposed a time machine model through which he has explored the interconnection between causality violation and the WEC.

The discovery of these time machine models led researchers to the study of physical phenomena in spacetimes with closed timelike curves. The Cauchy Problem was addressed for the massless scalar wave equation by Friedmann et.al [15] and Friedman and Morris [16]. The classical motion of billiard balls in spacetimes with closed timelike lines was discussed in[42] .Quantum field theory was formulated in the Gott spacetime by Boulware [17] and in a general class of multiply connected locally static spacetimes with closed timelike lines by Frolov [43]. The question of violations of unitarity for interacting quantum field theories in curved spacetime

12

with and without a time machine were dealt with in [18,19]. Particle creation due to time travel through a wormhole was discussed by Kim [44].

More importantly ,Kim and Thorne (KT) [45] analyzed the question whether quantum effects could prevent the occurence of closed timelike curves .The Cauchy Horizon (CH), which separates the region with CTL's from the region without it ,is usually unstable against classical perturbations for most of the known spacetimes with CTL's. Strangely enough for the wormhole-based time machine this is not so. However the quantum analysis by KT reveals that the vacuum polarization of a massless conformally coupled scalar field diverges near the CH. Does this divergence destroy the possibility of forming CTL's? According to KT the answer is no. They show that the vacuum polarization's gravity gives rise to metric fluctuations $\delta g_{\mu\nu}^{VP} = (l_p/D)(l_p/\Delta t)$,where l_p is the Planck length , D is the distance between the wormhole mouths and Δt is the proper time until one reaches the CH.For a microscopic wormhole with $D = 1m$,$\delta g_{\mu\nu}^{VP}$ would have grown to only $l_p/D \equiv 10^{-36}$ when one is within one Planck length of the CH. Beyond this Quantum gravity effects take over and there is no reason to believe in the results of quantum field theory in curved spacetime.This prompts KT to conjecture that the vacuum polarization's divergence gets cut off by quantum gravity effects and·spacetime remains smooth and classical and develops CTLs without any difficulty. Hawking [46], on the other hand has criticised the KT estimate of where quantum gravity invalidates quantum field theory in curved spacetime. He suggests that spacetime near the CH remains smooth and classical until one reaches $D\Delta t \equiv l_p^2$ whence $\delta g_{\mu\nu}^{VP} \equiv 1$ .Thereafter the divergence dominates and forbids the formation of CTLs. This is basically what is known as the Chronology Protection Conjecture. The issue is however far from resolved and probably will remain so till we get to know more about the theory of Quantum Gravity.

Finally a few words about the issue of topology change in the Lorentzian context,

which is ,in a certain sense related to the largely ill–understood question of wormhole formation.Progress in this field has been made very difficult by two well established no-go theorems.The first of these ,due to Geroch [22], states that if one assumes a Lorentz signature metric on a manifold with spacelike slices of different topology then there must exist either CTL's or singularities. Tipler's conclusions ten years later (the second no–go theorem), were even more drastic .He proved that if one imposes either the requirement of the WEC or the Einstein equations in addition to the assumptions of Geroch then one necessarily ends up having singularities.

However, inspite of these rather depressing but true results people have tried to construct various models for such processes. We now cite some of them. In 1973 Yodzis [51] discussed Lorentzian cobordisms from a mathematical point of view. His constructions however had singularities. Later work on topology change has been on simplistic models in $1+1$ and $2+1$ dimensions.Among these is the trousers problem in $1+1$ dimensions. Anderson and DeWitt [47] and subsequently Manogue et. al [47] studied quantum fields on the trousers manifold and concluded that such a process would lead to infinite particle production. On another front, Witten [40] has used the exactly solvable model of $2+1$ dimensional quantum gravity to evaluate topology changing amplitudes.Recently, Fujiwara et.al [50] have modelled a large number of processes in $2+1$ dimensional Euclidean Einstein gravity with a negative cosmological constant. The rules for topology changing processes in even and odd dimensions and the relationship between topology change and monopole creation has been investigated by Sorkin[48]. The interesting fact that Ashtekar's reformulation of GR allows degenerate metrics was put to use by Horowitz [52] in constructing quite a few examples of topology changing manifolds in $3+1$ dimensions.

Chapter 2

Basic Notions of Traversable Wormholes

The aim of this chapter is to provide some necessary background material relevant for the later parts of this thesis. Three topics are discussed. In section 2.1 we shall deal with the Morris-Thorne construction of a traversable wormhole. The method of 'surgical grafting' suggested by Visser is reviewed in section 2.2. Section 2.3 contains an up–to–date summary of the work done on the energy conditions, including the Morris-Thorne theorem on the violation of the Weak Energy Condition by the matter threading a Lorentzian wormhole. The final section introduces the idea of wormhole traversability and the associated notion of time travel.

2.1 The Morris-Thorne approach

In general relativity the interrelationship between matter and geometry is well known. Normally when one solves the Einstein field equations an initial assumption is made regarding the nature of the matter to be inserted on the R.H.S. The latter must satisfy certain physical requirements and possibly certain equations of

14

state. These together constrain the components of the energy-momentum tensor. Thus, given a certain kind of matter one looks for the resulting geometry. Morris and Thorne [14] did exactly the opposite while framing the notion of a Lorentzian wormhole. They first imposed certain restrictions on the components of the metric tensor, to ensure that it fulfilled the minimum requirements for having a Lorentzian wormhole geometry. Thereafter, they turned towards an analysis of the type of matter that would be necessary in order to have such a spacetime structure. We recall here these conditions on the metric. In section 2.3 the analysis of the resulting matter stress-energy will be carried out in detail.

Let us consider the case of a static , spherically symmetric metric generically given by

$$ds^2 = -e^{2\Phi(r)}dt^2 + \frac{dr^2}{1 - \frac{b(r)}{r}} + r^2 d\Omega_2^2 \qquad (2.1)$$

$\Phi(r)$ and $b(r)$ are two unknown functions, namely the 'redshift' and 'shape' functions respectively. $d\Omega_2^2$ is the line element on a two-sphere.

In order to avoid the presence of horizons/singularities $\Phi(r)$ should be such that $e^{2\Phi(r)}$ is finite and never zero in the given domain of r. (A detailed proof of this result for general static spherically metrics can be found in Vishveshwara [53])

As suggested by its name the function $b(r)$ characterizes the shape of the space-like slice. It turns out that if we wish to have a wormhole, $b(r)$ must satisfy the following requirements:

$$(i) \qquad \frac{b(r)}{r} \leq 1 \ \ with \ \ b(r = b_o) = b_o \qquad (2.2)$$

$$(ii) \qquad \frac{b(r)}{r} \to 0 \ \ as \ \ r \to \infty \qquad (2.3)$$

(i) guarantees that the signature of the metric is Lorentzian and implies that there exists a minimum value of r which defines the throat of the wormhole ($r = b_o$). (ii) guarantees the asymptotic flatness of the metric.

16

A better way of understanding the significance of these conditions is to embed a spacelike slice (say a two-dimensional section given by $t =$const., $\theta = \pi/2$) in a higher dimensional Euclidean space. The metric on R^3 in cylindrical coordinates is given as

$$ds^2 = dr^2 + dz^2 + r^2 d\Phi^2 \tag{2.4}$$

If $z(r)$ (the embedding function)describes the profile of the two-dimensional section as viewed in R^3, then by comparison with equation (2.1) one can write down the differential equation which relates $z'(r)$ and $b(r)$. This turns out to be

$$\left(\frac{dz}{dr}\right)^2 = \left[\frac{1}{1 - \frac{b(r)}{r}} - 1\right] \tag{2.5}$$

Thus, given a $b(r)$ one can in principle integrate the above to obtain $z(r)$. What do conditions (i) and (ii) tell us about $\left(\frac{dz}{dr}\right)^2$? The first implies that $\left(\frac{dz}{dr}\right)^2 \to \infty$ as $r \to b_o$. (ii) leads to the fact that $\left(\frac{dz}{dr}\right)^2 \to 0$ as $r \to \infty$. For a well behaved $b(r)$ with no zeros anywhere the function $z(r)$ would generally look as shown in Figure 2.1.

One can write the above metric in an alternative way by using the proper radial distance function $l(r)$:

$$l(r) = \pm \int_{b_0}^{r} \frac{dr}{\sqrt{1 - \frac{b(r)}{r}}} \tag{2.6}$$

Assuming $l(r)$ to be invertible Eq 2.1.1 can be written as

$$ds^2 = -e^{\chi(l)} dt^2 + dl^2 + r^2(l) d\Omega^2 \tag{2.7}$$

Note the fact that the function $l(r)$ has a range $-\infty \leq l \leq \infty$. $l \to \pm\infty$ refer to the two asymptotically flat regions. At the throat $r = b_o$, $l = 0$. The conditions on $b(r)$ translate into conditions on $r(l)$. These are $l \to \pm\infty$, $r^2 \to l^2$ and $l \to 0$, $r^2(l) \to b_o^2$. In a similar way, the conditions on $\Phi(r)$ translate into identical ones for $\chi(l)$.
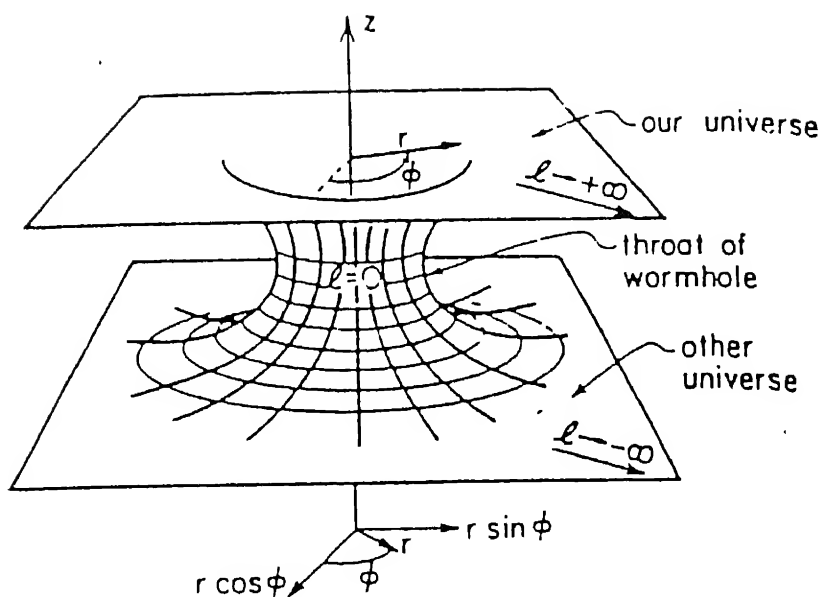
Figure 2.1: $z(r)$ versus r for a general wormhole

A few examples are in order now. Assume for simplicity $\Phi(r) = 0$. Consider the choice

$$b(r) = \frac{b_o^2}{r} \tag{2.8}$$

For this case $z(r)$ turns out to be

$$z(r) = b_o \cosh\left(\frac{r}{b_o}\right) \tag{2.9}$$

which represents a catenoid. In terms of the l coordinate one can write the metric as

$$ds^2 = -dt^2 + dl^2 + (b_o^2 + l^2)d\Omega^2 \tag{2.10}$$

This simple example was first investigated by Ellis [31] and used subsequently by Morris and Thorne [14] to illustrate the notion of a wormhole. One important feature of this metric is that its 2+1 dimensional version has spacelike sections which when embedded in R^3 have zero mean curvature implying that they are minimal surfaces.

Another choice of $b(r)$ could be $b(r) = b_o^m r^{1-m}$ with $0 < m \leq 1$. The $m = 1$ case is the Schwarzschild wormhole. Way back in 1916, shortly after the discovery of the Schwarzschild solution, Flamm [54] noticed the wormhole–like features of the Schwarzschild solution. For other values of m one gets Lorentzian wormholes with different shapes some of which have been discussed in [14].

The conditions on $b(r)$ and $\Phi(r)$ are not too restrictive and with some intelligent guesswork one can easily construct wormholes at will. In many cases, however the exact functional form of $l(r)$ or $z(r)$ may not be easy to obtain.

2.2 The Visser approach

In 1989, Visser [33,34] proposed an elegant new method for constructing traversable wormholes. This is based on what he termed as 'Schwarzschild surgery'. It is known

that spacelike sections of the Schwarzschild or the Reissner-Nordstrom geometry have the features of a wormhole. The only problem with them is the existence of horizons and singularities. This makes the wormhole non-traversable. In order to avoid the existence of a horizon Visser used two copies of the Schwarzschild geometry with the $r \leq 2m$ region removed. This gives two submanifolds which are geodesically incomplete and have a boundary given by the timelike hypersurfaces $r_{1,2} = a > 2m$. These two manifolds were joined across a surface layer to obtain a geodesically complete manifold resembling a wormhole connecting two asymptotically flat regions. The metric on this geometry obviously had a kink and therefore its first derivatives were discontinuous. The construction is based on the Junction Condition Formalism[72,73] using which the surface stress energy at the the throat turns out to be

$$S^i{}_j = \mathcal{K}^i{}_j - \delta^i{}_j \mathcal{K} \tag{2.11}$$

where $\mathcal{K}_{ij} = K_{ij}{}^+ - K_{ij}{}^-$ and

$$K_{ij}{}^{\pm} = \frac{1}{2} g_{ik} \left(\frac{dg_{kj}}{d\eta} \right)_{\eta \to \pm 0} \tag{2.12}$$

where $K_{ij}^{\pm}$ are the second fundamental forms evaluated in the regions above and below the surface layer.η is the coordinate normal at the junction.The surface stress energy has to satisfy a condition of pressure balance and a further constraint reflecting the fact that stress energy may be exchanged between the layers. For the static,spherically and reflection symmetric cases under consideration these constraints are automatically satisfied and $\mathcal{K}_{ij}$ is diagonal with components by $\mathcal{K}^r{}_r$, $\mathcal{K}_\theta{}^\theta$ and $\mathcal{K}_\theta{}^\theta$. Denoting the components of $S_i{}^j$ which are likewise diagonal, as $-\sigma, -\xi, -\xi$ we get, the following expressions for the Schwarzschild space example discussed by Visser [34]:

$$\sigma = -\frac{\sqrt{1 - 2m/a}}{4\pi a}, \qquad \xi = \frac{1}{4\pi a}\frac{1 - m/a}{\sqrt{1 - 2m/a}} \qquad (2.13)$$

where $r = a > 2m$ is the point where the geometry is cut off. The energy density of the surface layer is seen to violate the WEC.

Apart from providing a novel method for constructing Lorentzian wormholes, Visser also did a stability analysis of his geometries by making the throat of the wormhole dynamic. It turned out that such wormholes are essentially unstable - they either grow very large or collapse to a singularity. The examples dealt with in [33] include non spherically symmetric constructions and a special wormhole through which a traveller can move through without encountering the region of exotic matter.

2.3 The Energy Conditions and Lorentzian Wormholes

The proofs of the singularity theorems of General Relativity (GR) are based on the assumption that the energy momentum tensor of matter satisfies certain restrictions which go by the name of the Energy Conditions. Apart from the singularity theorems, the proof of the positive energy theorem of GR also relies on an assumption on matter which is essentially a special version of the Energy Condition (The Dominant Energy Condition). These conditions are far from being artificial. In fact, all known forms of classical matter obey some version or the other of the Energy Conditions. We shall now elaborate on these conditions and review some of the work done on them.

We begin with the focussing theorem for timelike and null geodesics. The Raychaudhuri equation [55] governs the rate of change of the expansion θ of null or

timelike geodesic bundles. This is given as

$$\frac{d\theta}{d\lambda} = -\frac{1}{n}\theta^2 - R_{\mu\nu}\xi^\mu\xi^\nu - 2\sigma^2 \qquad (2.14)$$

where λ is the affine parameter, $n = 2$ or 3 according to whether the geodesics are null or timelike and σ^2 is a nonnegative quantity (obtained from the shear of the congruence being considered). ξ^μ denotes the tangent vector to the geodesics. A focal point of the congruence/bundle is defined as one at which $\theta(\lambda) \to \infty$ as $\lambda \to \lambda_o$ from above or $\theta(\lambda) \to -\infty$ as $\lambda \to \lambda_o$ from below. Now, if $R_{\mu\nu}\xi^\mu\xi^\nu \geq 0$ then one can write

$$\frac{d\theta}{d\lambda} + \frac{1}{n}\theta^2 \leq 0 \qquad (2.15)$$

Integrating the above one gets

$$\frac{1}{\theta} \geq \frac{1}{\theta_o} + \frac{1}{n}\lambda \qquad (2.16)$$

where θ_o is the value of θ at $\lambda = 0$. If θ_o is negative somewhere (that is the congruence is initially converging) then $\frac{1}{\theta}$ must pass through a zero as $\theta \to -\infty$ within a finite value of λ given by $\lambda \leq +\frac{n}{|\theta_o|}$. The convergence of the geodesics here indicates the existence of a singularity in the expansion of the congruence and not in the underlying spacetime. However the focussing theorem together with certain other global arguments actually implies the existence of singularities. We shall not deal with those theorems the details of which are available in Wald [76], Hawking and Ellis[8].

The important point to note in the above is the fact that the focussing of geodesics relies largely on the validity of $R_{\mu\nu}\xi^\mu\xi^\nu \geq 0$. From the Einstein field equations we can translate this into a statement on the matter stress energy - $T_{\mu\nu}\xi^\mu\xi^\nu \geq 0$. This is an energy condition. We shall now enunciate the energy conditions which are well known in the literature – the Weak Energy Condition, the Strong Energy Condition and the Averaged Weak Energy Condition.

2.3.1 The Weak Energy Condition

This is probably the simplest of the Energy Conditions. It states that for all non-spacelike ξ^μ, $T_{\mu\nu}\xi^\mu\xi^\nu \geq 0$. For a diagonal $T_{\mu\nu}$ written in an orthonormal basis $(t_\mu, x_\mu, y_\mu, z_\mu)$ with t_μ timelike we have

$$T_{\mu\nu} = \rho t_\mu t_\nu + \tau x_\mu x_\nu + p_1(y_\mu y_\nu) + p_2(z_\mu z_\nu) \tag{2.17}$$

The condition translates into $\rho \geq 0$, $\rho + \tau \geq 0$, $\rho + p_i \geq 0$ $(i = 1, 2)$. It can be shown that the basic statement of this energy condition is the fact that the energy-density of matter is positive in all frames of reference.

2.3.2 The Strong Energy Condition

The statement of this condition is

$$T_{\mu\nu}\xi^\mu\xi^\nu \geq -\frac{1}{2}T \tag{2.18}$$

where ξ^μ are timelike as before and T denotes the trace of the energy momentum tensor. In the same way as for the WEC one can show that the above condition translates into the following set of inequalities $\rho + \tau + \sum_{i=1}^{2} p_i \geq 0$, $\rho + \tau + p_i \geq 0$ $(i = 1, 2)$.

2.3.3 The Dominant Energy Condition

This condition states that for all future directed, timelike ξ^μ, the quantity $T_\nu^\mu\xi^\nu$ should be a future directed timelike or null vector. Physically the quantity $T_\nu^\mu\xi^\nu$ represents the energy momentum 4-current density of matter as seen by an observer with 4-velocity ξ^μ. Thus the dominant energy condition means that the speed of energy flow of matter is always less than the speed of light. The Dominant Energy Condition translates into the following inequalities $\rho \geq |\tau|$, $\rho \geq |p_i|$ $i = 1, 2$.

2.3.4 The Averaged Weak Energy Condition

In the late seventies Tipler [58] suggested a new energy condition which was not local but global. He considered the inequality

$$\int_{\lambda_1}^{\lambda_2} T_{\mu\nu}\xi^\mu\xi^\nu d\lambda \geq 0 \qquad (2.19)$$

and showed that this requirement was sufficient in order to prove the singularity theorem. Weaker versions have been discussed by Borde [59]. The Penrose theorems for open universes which relied on the WEC have been extended by assuming the AWEC (Roman[13]).

We now review the work done on the consequences of violations of these conditions. This will in turn lead us to the latest example - the case of the Lorentzian wormholes.

In the earlier half of this century, the general belief was that the trace of the energy momentum tensor of matter T_α^α should be always greater than or equal to zero. This led to the fact that $p \leq \frac{\rho}{3}$. In 1962 Zel'dovich [56]constructed a model quantum field theory with a vector boson and demonstrated that for this case $p = \rho$. It turned out later that equations of state like $p = \rho$ had to be taken into account seriously while dealing with the matter residing at the core of neutron stars.

A major drawback of the cosmological models in GR is the inevitable presence of a singularity, which implies the collapse of the whole of spacetime. Several attempts were made in the seventies towards resolving this crisis. One suggested way out was the introduction of violations in the Energy Conditions. The works of Parker and Fulling[60] , Murphy [61], and Bekenstein [62] were all related to the construction of nonsingular cosmologies based on EC violating energy momentum tensors. Even the currently fashionable inflationary cosmologies which rely primarily on the presence of a Higgs–like field require SEC violating matter during the inflationary era. This follows from the fact that the massive scalar field energy momentum tensor violates

24

the SEC.

Similarly, for the case of stellar collapse one can attempt to avoid the black hole singularity by considering a violation of the WEC. This was studied in some detail by Bergmann and Roman [68].

Around the time when Penrose published his first singularity theorem (1965) researchers in axiomatic field theory, namely Epstein, Glaser and Yaffe [10] proved the important result that the expectation value of T_{00} taken over certain specific quantum states can actually be negative.Examples of WEC violating energy momentum tensors are abundant in the context of quantum field theory. The most dramatic of these is the case of the Casimir effect[11,12,13]. The renormalized stress energy tensor of the electromagnetic field confined between two perfectly conducting, parallel capacitor plates violates both WEC and SEC. In quantum field theory in curved spacetime the well known examples include the $\langle T_{\mu\nu} \rangle$ in spacetimes with moving mirrors[63,64] , massive Dirac particles in Kerr-Newman geometry [65], interacting field theories [66] and the squeezed vacuum states of light . The last of these, like the Casimir effect is once more an example which has been verified experimentally [67].

After the discovery of wormholes serious attemps to understand the validity of the averaged energy condition in the quantum field theoretic context have been made in the papers by Klinkhammer[69], Yurtsever [70] and Wald and Yurtsever [71].

We now turn to the case of traversable wormholes and the nature of the matter that threads such a geometry. Our analysis here will be confined to static spherically symmetric metrics. The form of the metric is the same as in (i). The unknown functions $b(r)$ and $\Phi(r)$ will be assumed to satisfy the necessary conditions for the geometry to represent a Lorentzian wormhole. We define an energy momentum tensor which is diagonal with components in the static observers frame given by

$T_{oo} = \rho(r)$, $T_{11} = \tau(r)$, $T_{22} = T_{33} = p(r)$. The Einstein field equations relate the metric functions with the components of the energy momentum tensor. These are

$$\rho(r) = \frac{b'}{r^2} \tag{2.20}$$

$$\tau(r) = -\frac{b}{r^3} + \frac{2\Phi'}{r}\left(1 - \frac{b}{r}\right) \tag{2.21}$$

$$p(r) = \cdot\frac{b - b'r}{2r^3} + \left(1 - \frac{b}{r}\right)\left(\Phi'' + \Phi'^2 + \Phi'\frac{-b'r + b}{2r(r - b)} + \frac{\Phi'}{r}\right) \tag{2.22}$$

where we have taken $8\pi G = c^2 = 1$. Recall that we have already constrained $b(r)$ and $\Phi(r)$ in order to 'make' a wormhole. Thus the functional forms of ρ, τ, p are in principle known to us.

We now check whether the WEC is satisfied by the energy momentum tensor. The first inequality $\rho \geq 0$ simply implies that $b' \geq 0$. The second one is non trivial. It is given as

$$\rho + \tau = \cdot\frac{b'r - b}{r^3} + \frac{2\Phi'}{r}\left(1 - \frac{b}{r}\right) \geq 0 \tag{2.23}$$

The question is whether this is satisfied for all r.

We know from the embedding of spacelike slices that

$$\frac{dr}{dz} = \pm\left(\frac{r - b}{b}\right)^{\frac{1}{2}} \tag{2.24}$$

Therefore

$$\frac{d^2r}{dz^2} = \frac{b - b'r}{2b^2} \tag{2.25}$$

Now at the throat ($r = b_o$) the function $r(z)$ (which is just the inverse of $z(r)$) has to have a minimum. Therefore $r''(z)|_{r=b_o} > 0 \Rightarrow b - b'r|_{r=b_o} > 0$ strictly. On the other hand, assuming that Φ' is everywhere finite we have $b'r - b|_{r=b_o} \geq 0$ as the condition emerging from the energy condition. Hence we have a contradiction. We cannot have a wormhole with the required matter satisfying the WEC. This simple result is known as Morris-Thorne theorem on the nature of the matter threading a

static traversable wormhole. Similarly for Visser type wormholes the surface stress energy at the joint violates the WEC as has been shown earlier in 2.2.

We have already discussed the possibile violation of WEC by matter energy momentum in the context of quantum field theory. Morris and Thorne had suggested that these examples typified the matter required to make a traversable wormhole. However, as we shall show later in this thesis, there is another way out. If one considers evolving wormholes one can avoid WEC violation at least for finite intervals of time. Such evolving geometries which may grow very large or collapse altogether can be further considered as a part of the expanding universe, and made quite realistic.

2.4   Traversability and Time Machine Models

We now move on to the notion of human traversability of a Lorentzian wormhole geometry and thereafter discuss the time machine model introduced by Morris, Thorne and Yurtsever using traversable wormholes.

Consider the science-fiction like scenario in which we imagine a human being starting off at one asymptotically flat region, moving through the wormhole and ending up in the other asymptotically flat region. Since gravitational forces near the throat may be quite large it is possible that the person might get crushed while attempting such a traversal. Thus it is necessary to construct a set of constraints which when obeyed would make a wormhole traversable in the human sense.

Since gravitational forces are characterized by the values of the Riemann curvature tensor components (through the equation of geodesic deviation) at different points in the spacetime, one ends up constraining these components in order to make a wormhole traversable for human beings. Assume a traveler starting out from one asymptotic region. If v denotes the four velocity of the traveler, then

the orthonormal frame associated with him is related to the static observer's frame by a simple Lorentz transformation. The requirement that the traveler does not feel an acceleration more than one Earth gravity leads to another constraint. Stated mathematically these conditions read as:

$$(i)(a)\, |R_{\hat{1}'\hat{0}'\hat{1}'\hat{0}'}| = \left|\left(1 - \frac{b(r)}{r}\right)\left(-\Phi'' + \frac{b'r - b}{2r(r-b)}\Phi' - \Phi'^2\right)\right| \le \frac{g_{\oplus}}{c^2 2m}$$

$$\cong \frac{1}{(10^{10}cm)^2} \tag{2.26}$$

$$(b)\, |R_{\hat{2}'\hat{0}'\hat{2}'\hat{0}'}| = \left|\frac{\gamma^2}{2r^2}\left(\beta^2\left(b' - \frac{b}{r}\right) + 2(r-b)\Phi'\right)\right| \le \frac{g_{\oplus}}{c^2 2m}$$

$$\cong \frac{1}{(10^{10}cm)^2}$$

$$\tag{2.27}$$

$$(ii)\, \left|\exp\left(-\Phi\right)[\frac{d}{dr}(\gamma \exp\left(\Phi\right))]\sqrt{1 - \frac{b}{r}}\right| \le \frac{g_{\oplus}}{c^2} \cong \frac{1}{.97L.yr} \tag{2.28}$$

where the hatted frame is that of the static observer and the primed one denotes the traveler's basis set.

Criterion (i) (a) quite generally constrains the form of Φ and $b(r)$. (i) (b) then puts an upper limit at any point of the journey on the allowed values of (v/c). A velocity exceeding this limit will result in unbearable tidal forces. Lastly, the acceleration constraint given in (ii) contains two terms. The first one given by $(1 - \frac{b}{r})^{\frac{1}{2}} \exp\left(-\Phi\right)\gamma\frac{d\exp\left(-\Phi\right)}{dr}$ is due to gravitational free fall, while the other, i.e., $(1 - \frac{b}{r})^{\frac{1}{2}}\frac{d\gamma}{dr}$ results from nongravitational forces which could, in principle, be controlled and adjusted by the traveller. This condition in general puts additional constraints on the allowed values of b_0 and γ. Morris and Thorne have also discussed further constraints such as restriction of the traversal time (in the static observer's

as well as the traveler's frame) to a maximum of one year. However, this is not a necessity in making the wormhole traversable.

Once we have a traversable wormhole we can very easily convert it into a time machine. This was shown by MTY [6] in 1988.

Consider the wormhole as depicted in Figure 2.2 where 1 and 2 denote the two mouths of the wormhole. If one accelerates Mouth 1 to a light–like velocity for a short while and then brings it back to its old position - a time delay ΔT is introduced in the clock at 1 relative to the clock at 2. Thus, traveling from Mouth 1 to Mouth 2 sufficiently fast through the wormhole and back to Mouth 1 across the asymptotically flat region leads to backward time travel as seen by the inertial observer. The opposite motion, i.e., from Mouth 2 to Mouth 1 through wormhole and back gives rise to future time travel.

MTY were able to write down a metric that represents such generic relative motions of the wormhole mouths. This is given as

$$ds^2 = -(1 + glF\cos\theta)e^{2\Phi}dt^2 + dl^2 + r^2(l)d\Omega_2^2 \tag{2.29}$$

where $F(l) = 0$ for $l \leq 0$ and $F(l)$ rises smoothly from 0 to 1 as one moves rightward from the throat to Mouth 1. $g(t)$ is the acceleration of Mouth 1 as measured in its own asymptotic rest frame. The coordinate transformations from wormhole coordinates to Minkowski coordinates (X, Y, Z, T with $ds^2 = -dT^2 + dX^2 + dY^2 + dZ^2$)in the neighbourhoods of Mouth 1 and Mouth 2 are

$$T = T_1 + v\gamma l\cos\theta, \quad Z = Z_1 + \gamma l\cos\theta \tag{2.30}$$

$$X = l\sin\theta\cos\phi, \quad Y = l\sin\theta\sin\phi \tag{2.31}$$

$$T = t, \quad Z = Z_2 + l\cos\theta \tag{2.32}$$

$$X = l\sin\theta\cos\phi, \quad Y = l\sin\theta\sin\phi \tag{2.33}$$
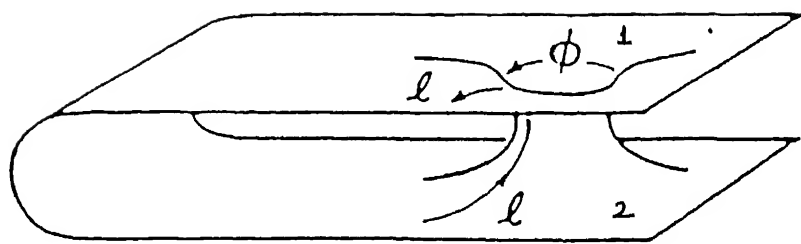
Figure 2.2: The wormhole in a topologically different representation

where $Z = Z_1(t)$, $T = T_1(t)$ is the world line of Mouth 1 with $V = \frac{dZ_1}{dT_1}$ and $dt^2 = dT_1^2 - dZ_1^2$. Z_2 is the time independent location of the Mouth 2 It can be shown that the matter required for the above metric violates all versions of the energy conditions. MTY used the Casimir stress energy to generate the required exotic matter at the throat of the wormhole.

The fact that a wormhole spacetime can be converted into a time machine means that it can be made to possess closed-timelike curves. We have briefly summarized the research on such geometries earlier in the introduction. Popular accounts on time travel can be found in Thorne's latest book [77] and the consequences of time travel in the context of quantum physics have been discussed by Deutsch and Lockwood [78]. We shall now leave this fascinating topic and concentrate more on the geometry, matter content and wave propagation in wormhole geometries without closed timelike curves, in the next four chapters.

Chapter 3

Two New Examples of Wormhole Geometries

The basic criteria for constructing a traversable wormhole geometry have been discussed in detail in the previous chapter. Our aim here is to provide certain specific examples. In the first section we introduce a one–parameter family of wormhole geometries. The parameter defining a member of the family controls the rate of change of the embedding function -in other words it increases/decreases the flaring out of the geometry in the neighborhood of the throat.The motivation for discussing this simple class of wormholes is that we shall be using them later (Chapter 5) as backgrounds for studying the propagation of scalar waves.

The second section is concerned with another class of static spherically symmetric geometries with the required matter satisfying the tracelessness constraint.Both Morris Thorne and Visser type wormholes are discussed with emphasis on their embeddings, the required matter and their traversability.

31

3.1 A One Parameter Family of Wormholes

The one-parameter family of wormholes to be introduced in this section is essentially an extension of the Ellis geometry. The metric for these geometries is generically represented as follows

$$ds^2 = -dt^2 + dl^2 + r^2(l)d\Omega^2 \tag{3.1}$$

Here $d\Omega^2 = d\theta^2$ in $2+1$ dimensions and $d\Omega^2 = d\theta^2 + \sin^2\theta d\phi^2$ in $3+1$ dimensions and $r(l) = (b_0^n + l^n)^{\frac{1}{n}}$. One can easily generalise this metric to higher dimensions($D > 4$). n is the parameter which is assumed to take on only even values. The choice of even n is based on the requirement that the function $r(l)$ be smooth everywhere (i.e. it has no discontinuities in its derivatives in the given domain of l i.e. $[-\infty, \infty]$. If n were odd then one can in principle replace the $r(l)$ given above by $r(l) = (b_0^n + |l|^n)^{1/n}$. In this case the metric has a kink and thus to make a wormhole one has to use the Junction Condition Formalism of GR. We shall however work with even 'n' only.

The metric in 3.1 can be written in an alternative form by using the radial coordinate 'r'. The form of the metric will be

$$ds^2 = -dt^2 + \frac{dr^2}{1 - \frac{b(r)}{r}} + r^2 d\Omega^2 \tag{3.2}$$

where $b(r)$ is given by the following expression

$$b(r) = r\left[1 - \left(1 - \left(\frac{b_0}{r}\right)^n\right)^{2-2/n}\right] \tag{3.3}$$

Notice that the form given in 3.3 satisfies the usual Morris-Thorne conditions for a Lorentzian wormhole geometry.

The essential features of the geometry can be understood more clearly by considering the embedding of its two-dimensional spacelike slices in R^3

The embedding function $z(r)$ satisfies

$$\left(\frac{dz}{dr}\right)^2 = \frac{b(r)}{r - b(r)}$$ (3.4)

with the $b(r)$ being given by 3.3 .In Fig 3.1 we have plotted the R.H.S of Eqn 3.4 as a function of r for different values of n. For the class of geometries under consideration here , each member has the same throat radius b_0 , but different profiles $z(r)$. Geometries with larger values of n flare out less quickly than those with small n i.e the spacetime takes on increasingly the aspect of long uniform tunnel connecting two flat spaces (see Fig 3.1). It should also be mentioned that the $n = 2$ case in $2 + 1$ dimensions has a spacelike section which when embedded in R^3 has zero mean curvature implying that it is a minimal surface . For $n > 2$ the spacelike slices are no longer so.

Finally we turn to the matter that would be necessary to have such geometries. For this we need to write down the Einstein Field equations.Defining as before a diagonal energy momentum tensor with components ρ, τ, p we have the following.

$$\rho(l) = \frac{1}{(b_0^n + l^n)^{2/n}} - \frac{2(n - 1)l^{n-2}b_0^n + l^{2n-2}}{(b_0^n + l^n)^2}$$ (3.5)

$$\tau(l) = \frac{l^{2n-2}}{(b_0^n + l^n)^2} - \frac{1}{(b_0^n + l^n)^{2/n}}$$ (3.6)

$$p(l) = \frac{(n - 1)l^{n-2}b_0^n}{(b_0^n + l^n)^2}$$ (3.7)

Given ρ, τ, p one would naturally like to check the WEC inequalities . It is easily seen that for all n ,l the inequality $\rho + \tau \geq 0$ is violated.The other two inequalities are also violated but not throughout the entire domain of l .Therefore this class of wormholes can be supported only by 'exotic' matter. Note that for all n the matter satisfies the equation of state

$$\rho + \tau + 2p = 0$$ (3.8)
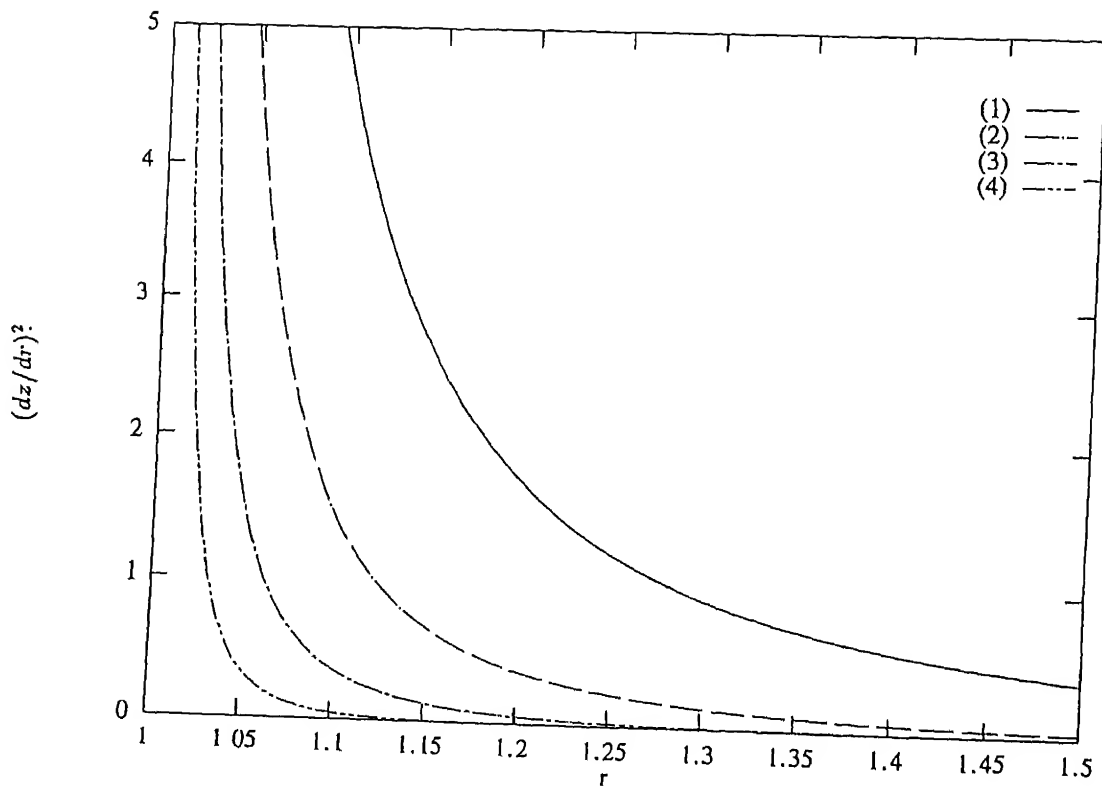
Figure 3.1: The embedding of spacelike slices for the one parameter family discussed in Sec.3.1: $(\frac{dz}{dr})^2$ is plotted as a function of r for different n values (1) $n = 4$ (2) $n = 10$ (3) $n = 20$ (4) $n = 40$.

3.2 Traversable Wormholes With Traceless Matter

Among the prescriptions for obtaining wormholes,two approaches exist in the literature. In [14] Morris and Thorne obtain static spherically symmetric wormhole geometries by appropriately constraining the metric tensor.Only later do they investigate the resulting matter and find it to be exotic.Visser [33,34], on the other hand obtains a wormhole by connecting two identical copies of various well-known asymptotically flat spacetimes using the Junction Condition Formalism of General Relativity.

In this section we obtain wormholes as solutions to the Einstein equations in the following sense.We start with the Morris–Thorne metric which contains two unknown functions $\Phi(r)$ and $b(r)$.We calculate the matter density $\rho(r)$ and the radial and angular pressures $\tau(r)$ and $p(r)$ respectively.These are completely determined,through Einstein's equations,in terms of $b(r)$, $\Phi(r)$ and their derivatives.We now require ρ,τ and p to satisfy a certain constraint(equation of state) and as a result obtain a differential equation in $b(r)$ and $\Phi(r)$.This equation is second order and nonlinear in Φ but first order and linear in $b(r)$.To proceed further we make a specific choice of $\Phi(r)$, consistent with the requirements that the metric be asymptotically flat and free of horizons and singularities.We substitute this $\Phi(r)$ into the constraint equation and solve for $b(r)$(to within an arbitrary constant of integration).With both Φ and $b(r)$ in hand ,we analyze the geometry in question as to its shape, traversability and matter content. It should be emphasized that only specific combinations of the constraint equation and of $\Phi(r)$, will result in a shape function $b(r)$ representing a wormhole.Among the various possibilities available, we have chosen tracelessness of the energy momentum tensor for our investigation here.It is worth mentioning that traceless matter can either satisfy or violate the

WEC.Perfect fluids with $p = \frac{\rho}{3}$ satisfy it whereas the Casimir stress energy is well-known to be WEC violating [11,12,13] .Our choice for the redshift function is fairly simple-$\Phi = -\frac{\alpha}{r}, \alpha > 0$.For all $r > 0$ exp 2Φ is finite and nonzero which implies the nonexistence of horizons and singularities.

It turns out that with the above choices,the resulting shape function actually does represent a class of traversable wormholes.We analyse the nature of the matter (WEC) and the embedding of the spacelike slices. Another class of asymptotically flat solutions made possible by a different choice of the constant of integration is used to construct Visser type wormholes.It so happens that for these Visser type wormholes the exotic surface stress energy is not traceless. Finally, human traversability of these spacetimes is discussed.It leads to lower bounds on the throat radius of the wormhole.

3.2.1   The Field Equations,Solutions and Wormholes

We begin with a spherically symmetric static metric parametrized in terms of two unknown functions $\phi(r)$ and $b(r)$(the 'redshift' and 'shape' functions respectively).

$$ds^2 = -e^{2\Phi(r)}dt^2 + \frac{dr^2}{1 - \frac{b(r)}{r}} + r^2 d\Omega_2^2 \tag{3.9}$$

From the Einstein field equations (Eq 2.20,2.21,2.22) with $\rho(r)$, $\tau(r)$ and $p(r)$ as the diagonal components of the energy-momentum tensor in the static observer's frame of reference, we obtain, using the tracelessness constraint $-\rho + \tau + 2p = 0$ the following relation between $b(r)$ and $\Phi(r)$:

$$\Phi'' + \Phi'^2 + \frac{2\Phi'}{r} + \Phi' \frac{(b - b'r)}{2r(r - b)} - \frac{b'}{r(r - b)} = 0 \tag{3.10}$$

For $\Phi = 0$ the above equation has a simple solution $b(r) = b_0$, where b_0 is a constant.This is the familiar horizon–free Schwarzschild wormhole with the coefficient

of dt^2 in the metric set to one.Its matter stress energy is somewhat peculiar in the sense that the energy density is zero while $\tau = -2p$.

Wih a redshift function $\Phi = \frac{-\alpha}{r}$ however, Eq.(5) reduces to the following first order differential equation for $b(r)$.

$$b' + b[\frac{2\alpha^2 - \alpha r}{r^2(\alpha + 2r)}] = \frac{2\alpha^2}{r(\alpha + 2r)} \tag{3.11}$$

This integrates straightforwardly to

$$b(x) = \alpha \frac{F_4(x) + C \exp 2(x - 2)}{x^5} \equiv \alpha \tilde{b}(x) \tag{3.12}$$

where $x = 2 + \frac{\alpha}{r}$, C is the constant of integration and $F_4(x)$ is given as

$$F_4(x) = [x^4 + 2x^3 + 3x^2 + 3x + 1.5] \tag{3.13}$$

We first note that this shape function satisfies the asymptotic flatness condition i.e $\frac{b(r)}{r} = \tilde{b}(x)(x - 2) \to 0$ as $r \to \infty (x \to 2)$ irrespective of the choice of C.However, $\frac{b(r)}{r} = \tilde{b}(x)(x - 2) \leq 1$ i.e we have a Morris–Thorne type wormhole ,only if C satisfies the following inequality at all points in the domain of x $[2 \leq x \leq x_0$ $(\alpha(x_0 - 2)^{-1} \leq r \leq \infty)]$

$$0 < C \leq \exp 2(2 - x) \frac{x^3 + 3x^2 + 4.5x + 3}{x - 2} \tag{3.14}$$

The equality holds for $x = x_0$ which marks the position of the throat .A plot of the equality relation is given in Fig 3.2(curve (1)).Thus x_0 fixes C but not the absolute size of the throat which depends further on the parameter α.

For $C > 0$ $b(x)$ is positive.The curves (1), (2) and (3) in Fig 3.3 show the plots for $b(x)$ for three different values of C.As we reduce C the throat moves inwards in r.Finally for $C = 0$, $\frac{b(r)}{r} = \tilde{b}(x)(x - 2)$ equals one only for $r = 0(x = \infty)$ and, instead of a wormhole , we end up with a singular geometry. This is because the redshift function diverges as $r \to 0$.
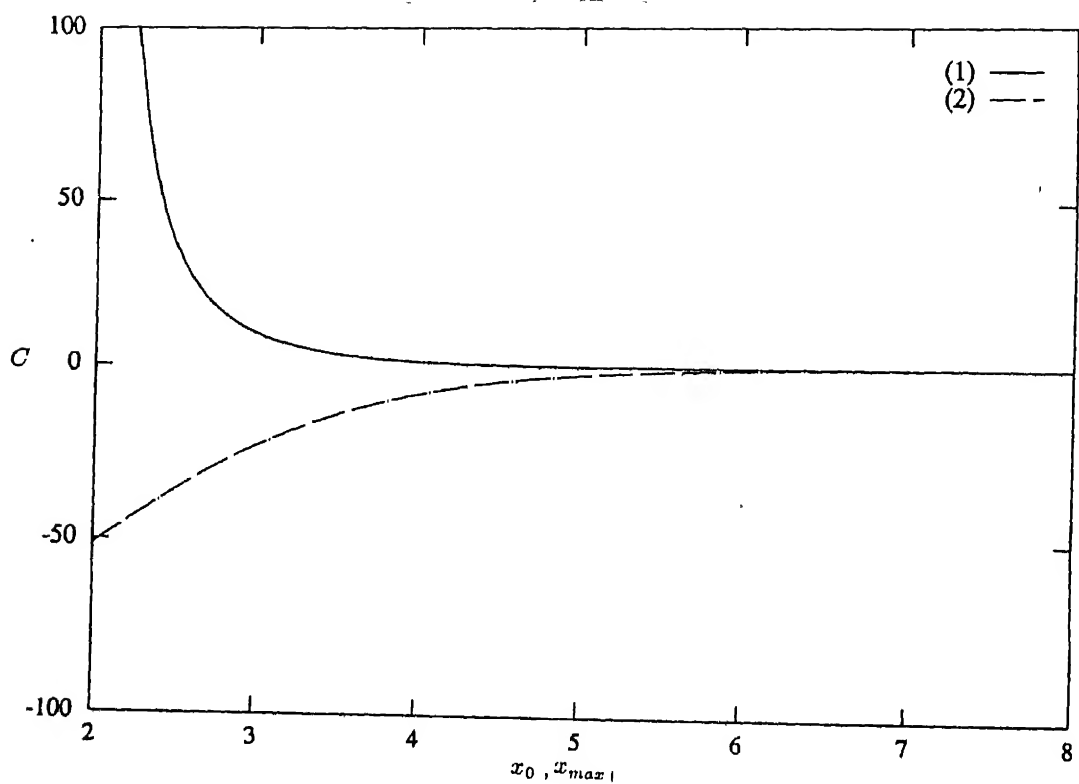
Figure 3.2: (1) C as a function of x_0 as given in Eq. 3.14; (2) C as a function of x_{max} as given in Eq. 3.15
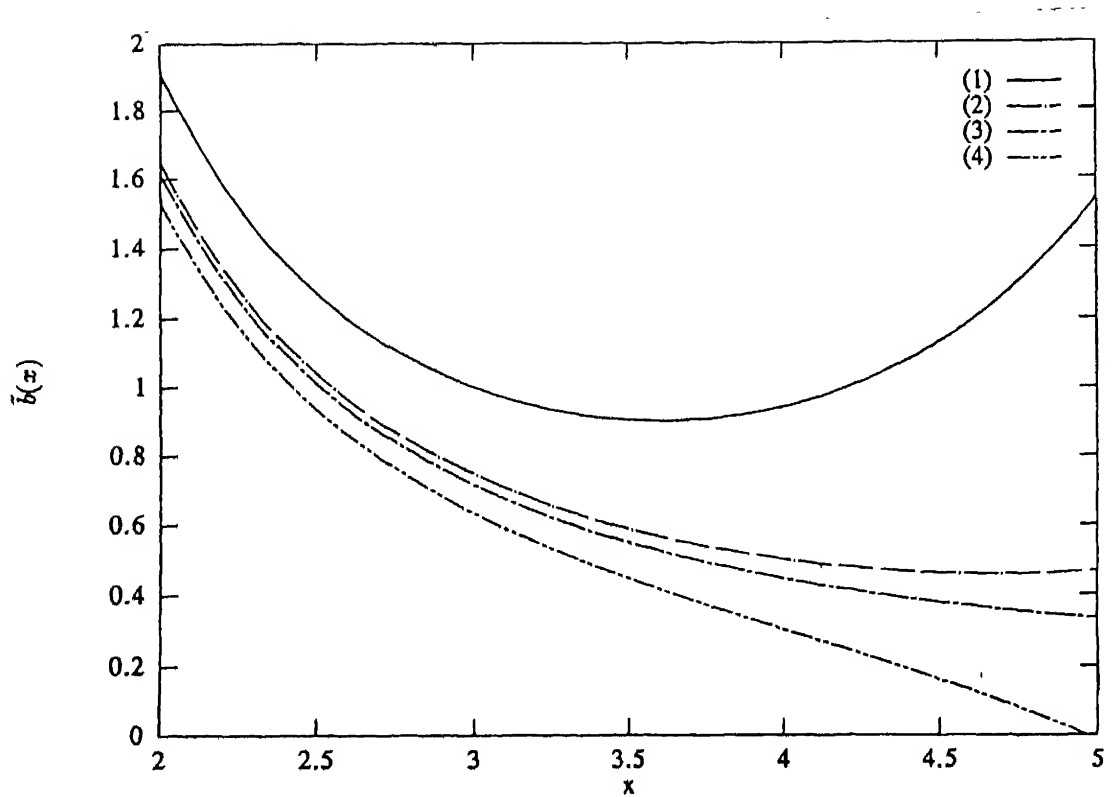
Figure 3.3: $\tilde{b}(x)$ as a function of x for C values :(1) $C = 9.541$ (2) $C = 1.218$ (3) $C = .1863$ (4) $C = -2.5$

If C is negative then $b(x)$ can be positive only upto a certain x_{max} where it has a zero. The values of C and the corresponding x_{max} are shown in curve (2) of Fig. 3.2 which obeys the following equation.

$$C = -F_4(x)exp[2(2-x)] \qquad (3.15)$$

The fact that this curve has a minimum signifies that beyond a certain C value $b(x)$ is negative for all x. Curve (4) in Fig. 3.3 shows a plot of $b(x)$ for a negative C value lying above the minimum.

The geometries discussed above are ofcourse better understood in terms of the embeddings of their spacelike slices. In Fig 3.4 we plot the quantity $(\frac{dz}{dr})^2$ versus x. We see that (1) ,(2) and (3) are the usual Morris-Thorne wormholes. The fourth curve which results from a $b(x)$ with $C < 0$ has a altogether different shape in embedding space. Here the embedding function has a point of inflexion and the geometry curves inwards instead of 'flaring out' beyond the throat. (as happens for the usual wormhole). Later in this section, sections of these geometries will be used to construct Visser type wormholes .

At this stage it is worthwhile to analyse the nature of the matter that threads these various geometries. Tracelessness has been imposed as a constraint and has led to the solutions discussed above .However, as mentioned earlier, tracelessness alone does not say anything about the status of the WEC. We shall now explicitly check the WEC inequalities for the cases of interest here.

For the geometries under discussion here the WEC inequalities turn out to be as follows:

$$\rho \geq 0 \quad \Rightarrow \quad \frac{(x-2)^4}{x\alpha^2}[2 - \tilde{b}(x)(2x-5)] \geq 0 \qquad (3.16)$$

$$\rho + \tau \geq 0 \quad \Rightarrow \quad \frac{(x-2)^3}{x\alpha^2}[4(x-1) - \tilde{b}(x)(4x^2 - 12x + 10)] \geq 0 \qquad (3.17)$$
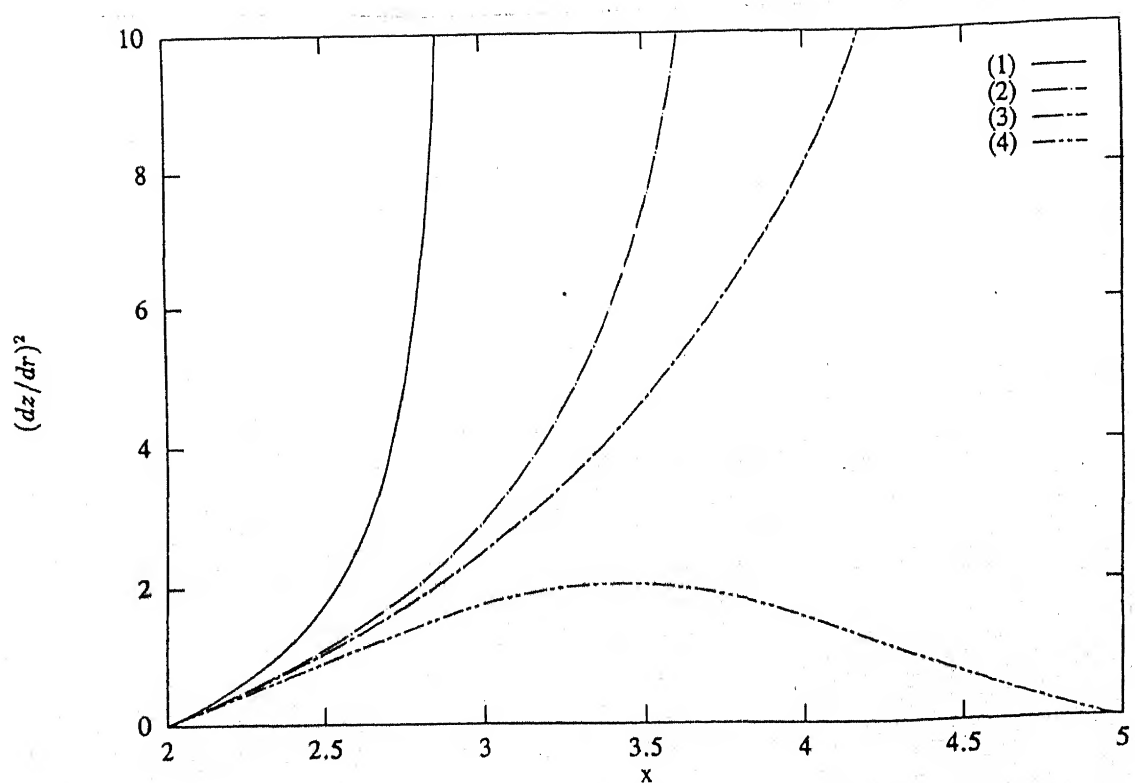
Figure 3.4: Embedding of spacelike slices for the geometries discussed in Sec.3.2:$(dz/dr)^2$ plotted against x for C values (1) $C = 9.541$ (2) $C = 1.218$ (3) $C = .1863$ (4) $C = -2.5$

$$\rho + p \geq 0 \quad \Rightarrow \quad \frac{(x-2)^3}{x\alpha^2}[4(x-3) - \tilde{b}(x)(4x^2 - 24x + 30)] \geq 0$$

$$(3.18)$$

Figs 3.5,3.6,3.7 are the plots for the left hand sides of these inequalities as functions of x.In two of the $C > 0$ cases(curves (1) and (2)) only the second of these is seen to be violated and that too only near the throat. In other words, one can localize the WEC violating stress energy to a small region in space by appropriately choosing C.To see how small this region can be and what the geometry looks like within it we note from Fig3.6that for the case with $x_0 = 5(C = .1863)$(curve (2)) violation begins at $x = 4.54(r = .3931\alpha)$ and continues upto the throat $x = 5(r = .3333\alpha)$.Thus the region of violation is about $.060\alpha$ which is certainly less than the throat radius itself. However, the geometry flares out very little from the throat-the tangent to the embedding curve $z(r)$ makes an angle of 78 degrees at the point where WEC violation ends.On the other hand ,if $C = 1.218 x_0 = 4$ WEC violation starts at about $x = 3.49(r = .671\alpha)$.The throat is at $x = 4(r = .5\alpha)$.Therefore, the region of violation turns out to be $.17\alpha$ which is just one-third of the throat radius.The angle made by the embedding curve is about 70 degrees.For $x_0 = 3$ we see (curve (3)) that the WEC is violated everywhere.In [14] Morris and Thorne showed that if one wishes to have a large flare out from the throat(say of 45 degrees) over a region small compared to the throat radius then one must have b' and hence ρ negative at the throat.However if b' is positive everywhere then all that the Morris-Thorne analysis says is that a 45 degree flare out from the throat is impossible over a very small region.One can check this with a little effort for the geometries discussed here.Moreover,we notice that for our geometries (for which b' is positive everywhere) the region of WEC violation can be microscopic only if the outward flare within is very slight.

For $C \leq 0$ the matter satisfies the WEC in the entire domain $[2, x_{max}]$ of x(curves
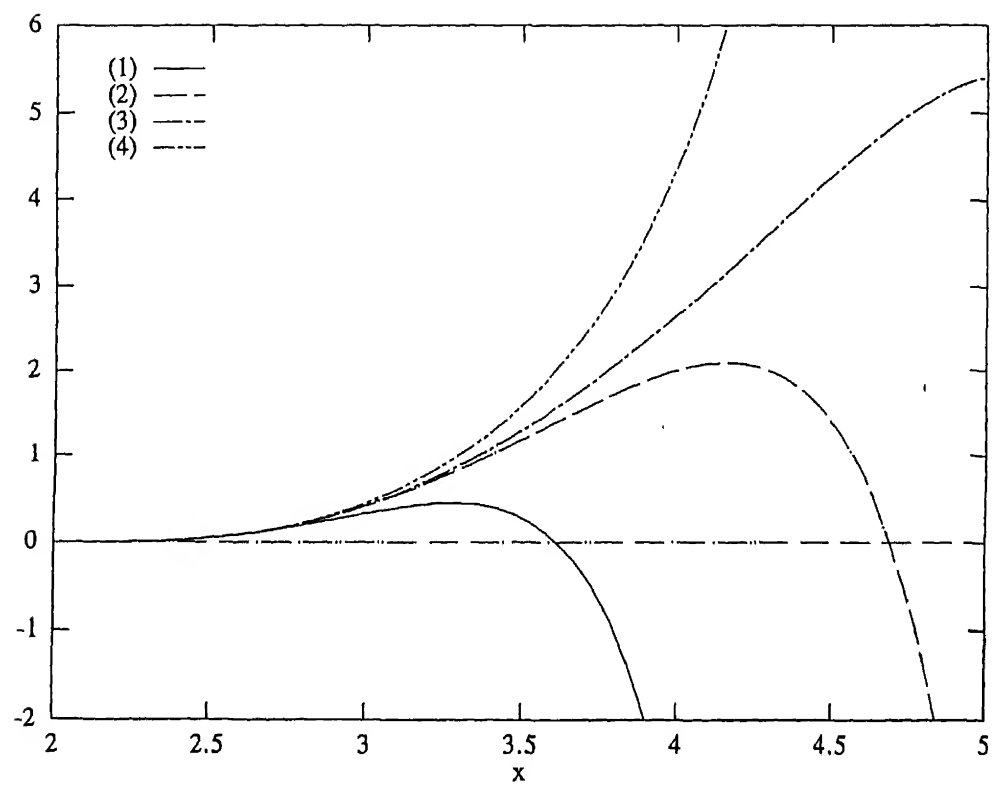
Figure 3.5: The $\rho \geq 0$ inequality for different C values (1) $C = 9.541$ (2) $C = 1.218$ (3) $C = .1863$ (4) $C = -2.5$
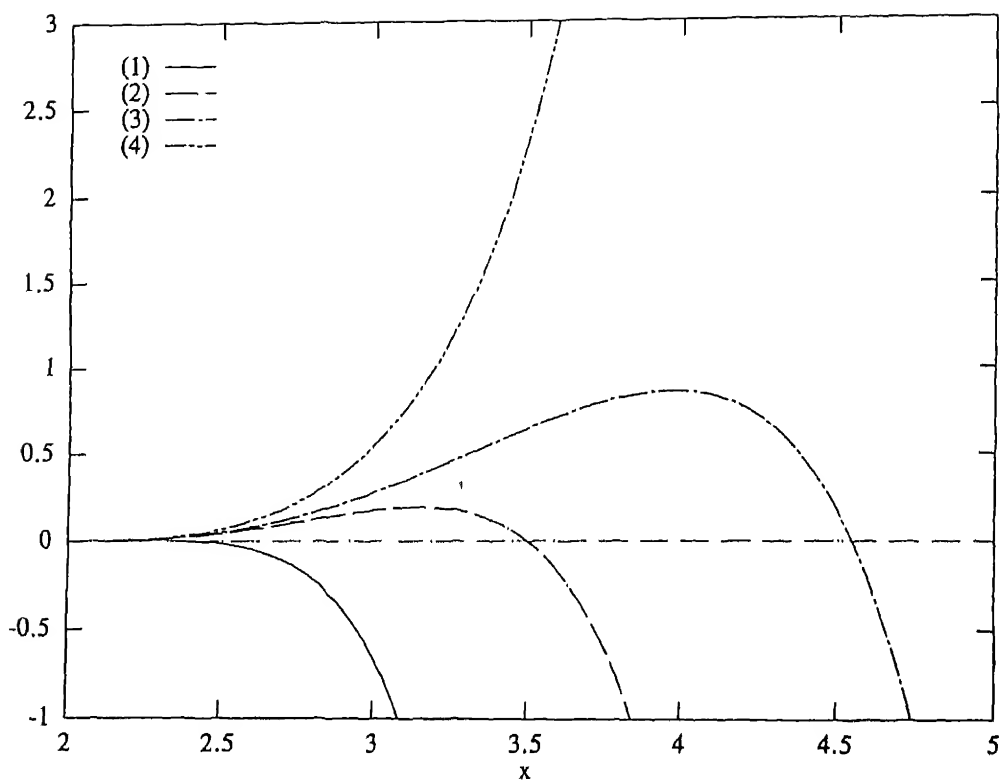
Figure 3.6: The $\rho + \tau \geq 0$ inequality for different C values (1) $C = 9.541$ (2) $C = 1.218$ (3) $C = .1863$ (4) $C = -2.5$
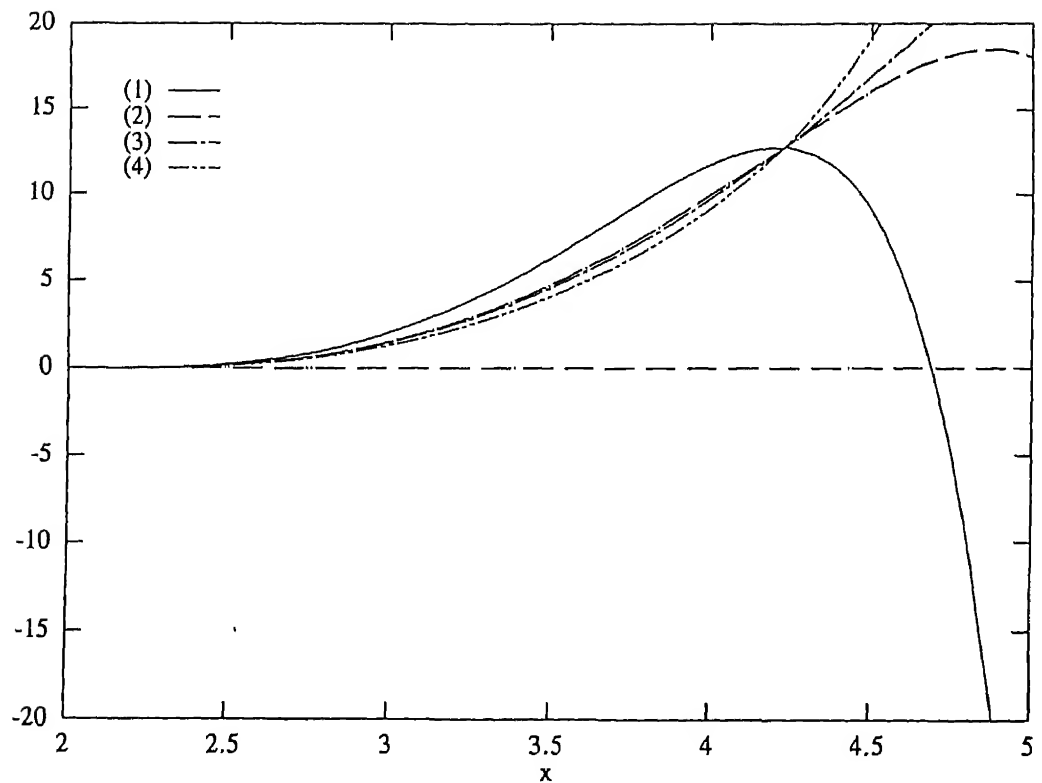
Figure 3.7: The $\rho + p \geq 0$ inequality in for different C values (1) $C = 9.541$ (2) $C = 1.218$ (3) $C = .1863$ (4) $C = -2.5$

(iii) and (iv)).However,since the geometries for $C < 0$ are not by themselves worm-holes one has to suture two identical copies and 'make' a wormhole a la Visser [34,33] This basically employs the Junction Condition Formalism of GR . Using the expressions for the surface stress energy mentioned in Sec. 2.2 we obtain ,

$$\sigma = -\frac{1}{2\pi b_0}, \qquad \xi = -\frac{(\alpha + b_0)}{4\pi b_0^2} \tag{3.19}$$

where b_0 is the point in r where we cut the geometry off.

Notice that we can neither make the surface stress energy traceless nor keep it from violating the energy conditions .

3.2.2   Traversability

We turn finally to the question of human traversability of the wormholes introduced here. In Sec.2. we have outlined the relevant criteria.These include the tidal forces felt by a traveller across his body and the accelerations experienced by him.For our metric these conditions read :

$$(i)(a)\frac{(x-2)^3}{x\alpha^2}\left|[4 - \tilde{b}(x)5(x-2)]\right| \leq \frac{1}{(10^{10}cm)^2} \tag{3.20}$$

$$(b)\frac{\gamma^2(x-2)^3}{x\alpha^2}|[\{(x-2)\beta^2 + x\} - \tilde{b}(x)\{R_2(x)\beta^2 + x(x-2)\}]|$$
$$\leq \frac{1}{(10^{10}cm)^2} \tag{3.21}$$

$$(ii)\frac{1}{\alpha}\left|(x-2)^2\sqrt{1 - \tilde{b}(x)(x-2)}(\gamma - \frac{d\gamma}{dx})\right| \leq \frac{1}{.97L.Yr} \tag{3.22}$$

where $R_2(x) = x^2 - 4x + 5, \qquad \beta = \frac{v}{c}$

Let us first consider a traveller moving with a constant nonrelativistic velocity (i.e., $\gamma \approx 1$). In this case the second constraint above puts the most stringent restriction on the allowed values of α.Fig 3.12 shows a plot for the function of

x appearing in the L.H.S of this inequality for two values of $C(C = .1863$ and $C = 1.218)$.The maximum value of this function is about 1.5 for the former case and .8 for the latter.On the other hand ,for the first two inequalities the maximum values of the relevant functions are 5.3 and .92 for $C = .1863$ and 2 and .4 for $C = 1.218$.These are seen from the curves (1) and (2) in Figs 3.8 and 3.9.Thus the minimum permissible throat radius which is consistent with the traversability constraints turns out to be .51 L.yr and .39 L.yr for the C values .1863 and 1.218 respectively.

If, on the other hand, our traveller is capable of adjusting his velocity (as he moves across the wormhole) in such a way that $\gamma(x) = \exp(x) = \exp(2 + \alpha/r)$ he will feel no acceleration whatsoever right through the journey. However, he will have to move at an almost lightlike speed throughout, with very subtle variations resulting out of the very specific choice of $\gamma(x)$.For this case the first constraint yields nothing new.The third constraint is satisfied automatically by virtue of the specific choice of γ.It is the second constraint which yields the lower bound on the throat radius.As before we plot the function of x that appears on the L.H.S for the two C values.The maximum occurs around 40000 and 3000 for $C = .1863$ and $C = 1.218$ respectively(Fig3.11,3.10).Thus the minimum permissible throat radius is about 6.6×10^{11} cm and 2.73×10^{11} cm for the smaller and larger C values respectively.

3.3   Remarks and Conclusions

Since Section 3.1 essentially contains background material relevant for Chapter 5 we shall put down here our concluding remarks on the geometries discussed in Section 3.2.

The main question addressed in Section 3.2 is whether there exist nontrivial
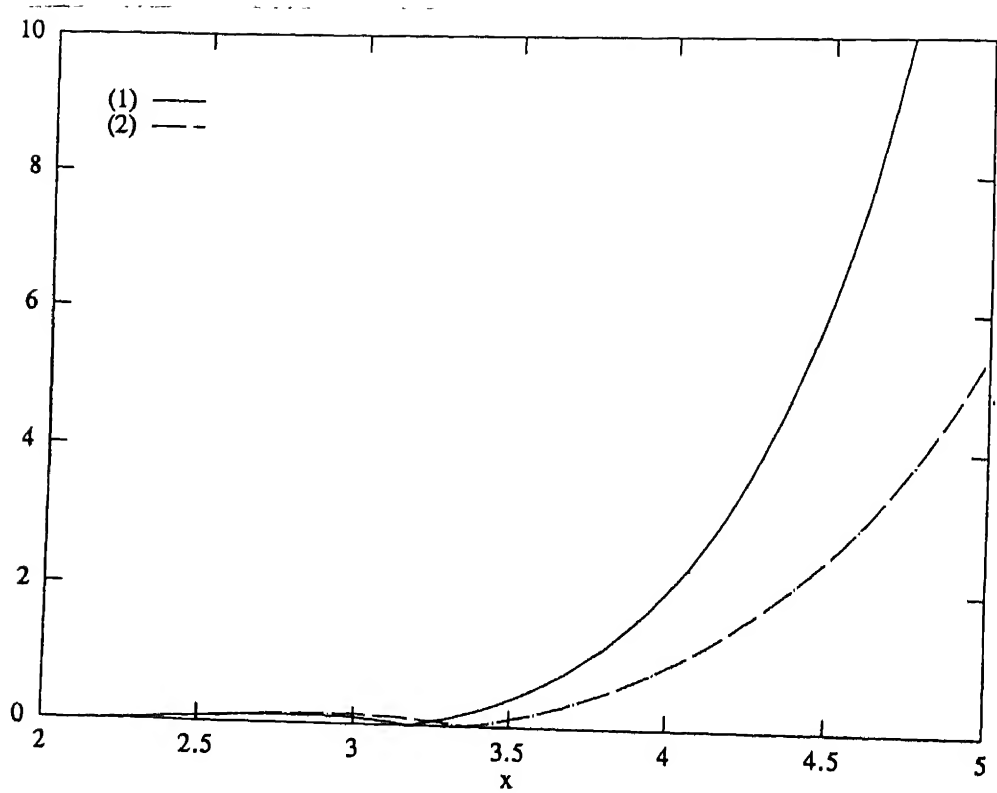
Figure 3.8: The L.H.S of the traversability in Eq 3.20 for C values (1) $C = 1.218$ (2) $C = .1863$
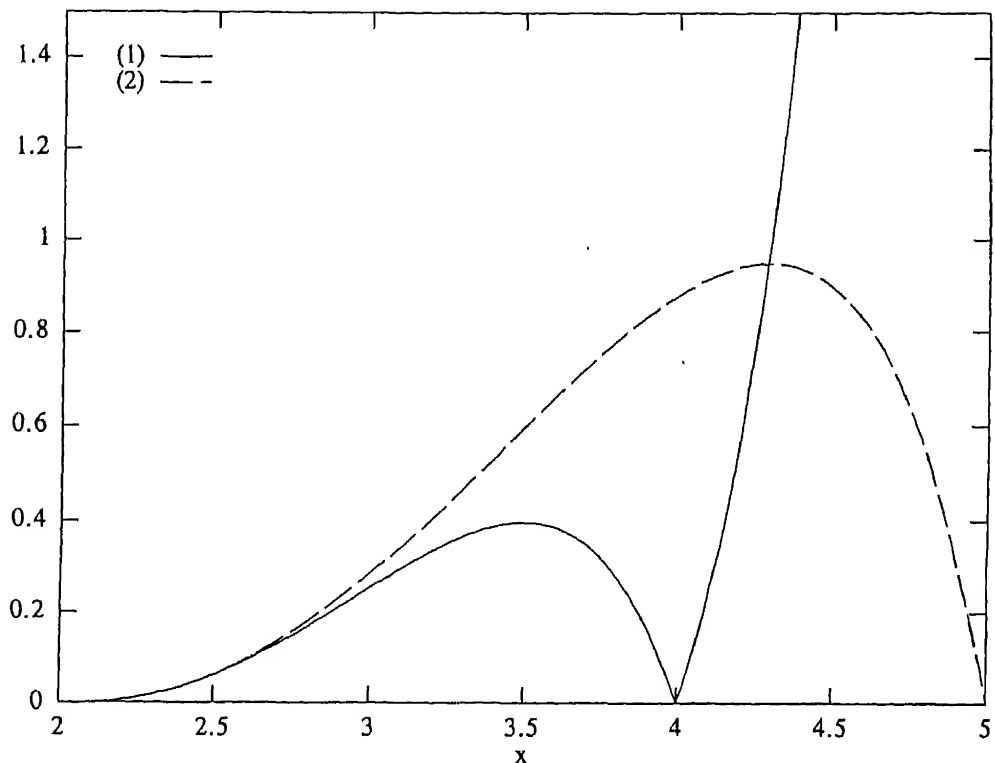
Figure 3.9: The L.H.S of the traversability in Eq 3.21 for C values (1) $C = 1.218$ (2) $C = .1863$ and nonrelativistic velocities.
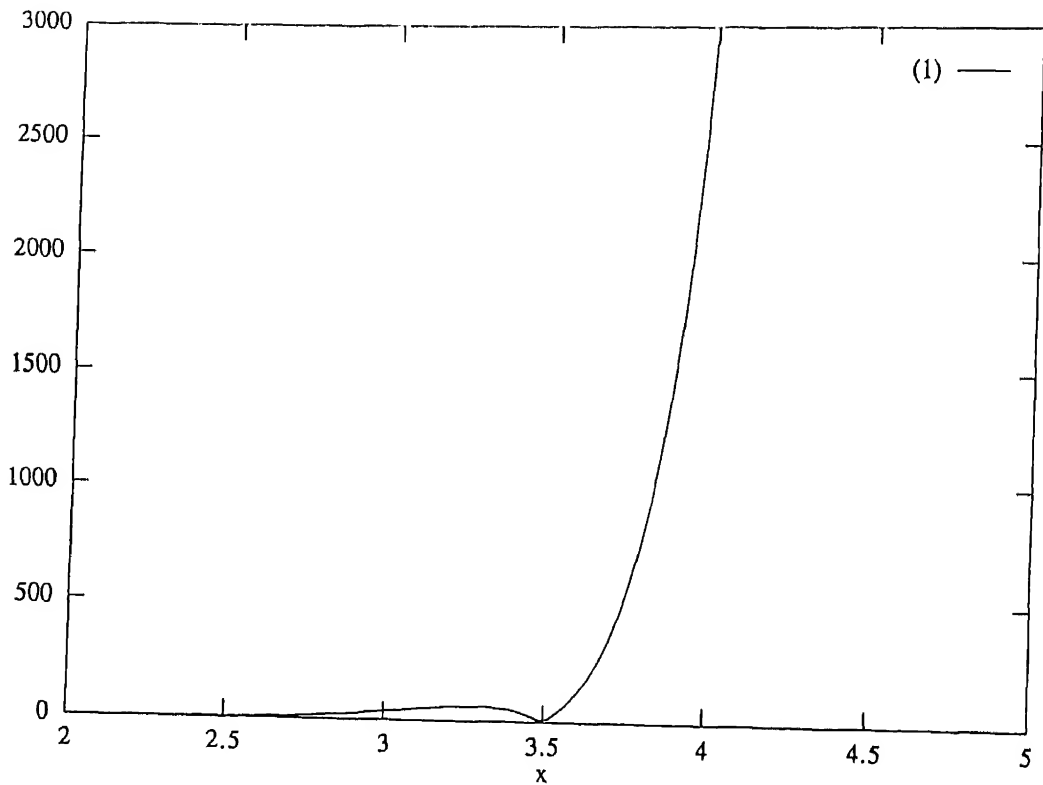
Figure 3.10: The L.H.S of the traversability in Eq 3.21 for the C value (1) $C = 1.218$ and relativistic velocities.
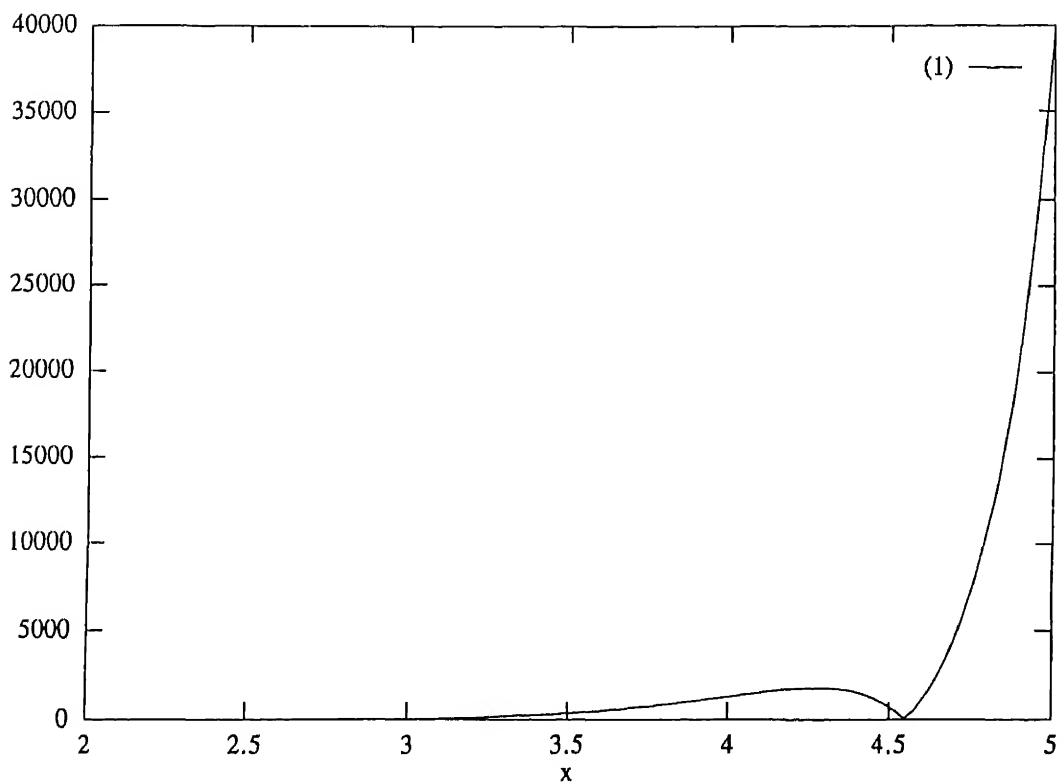
Figure 3.11: The L.H.S of the traversability in Eq 3.21 for the C value (1) $C = .1863$ and relativistic velocities.
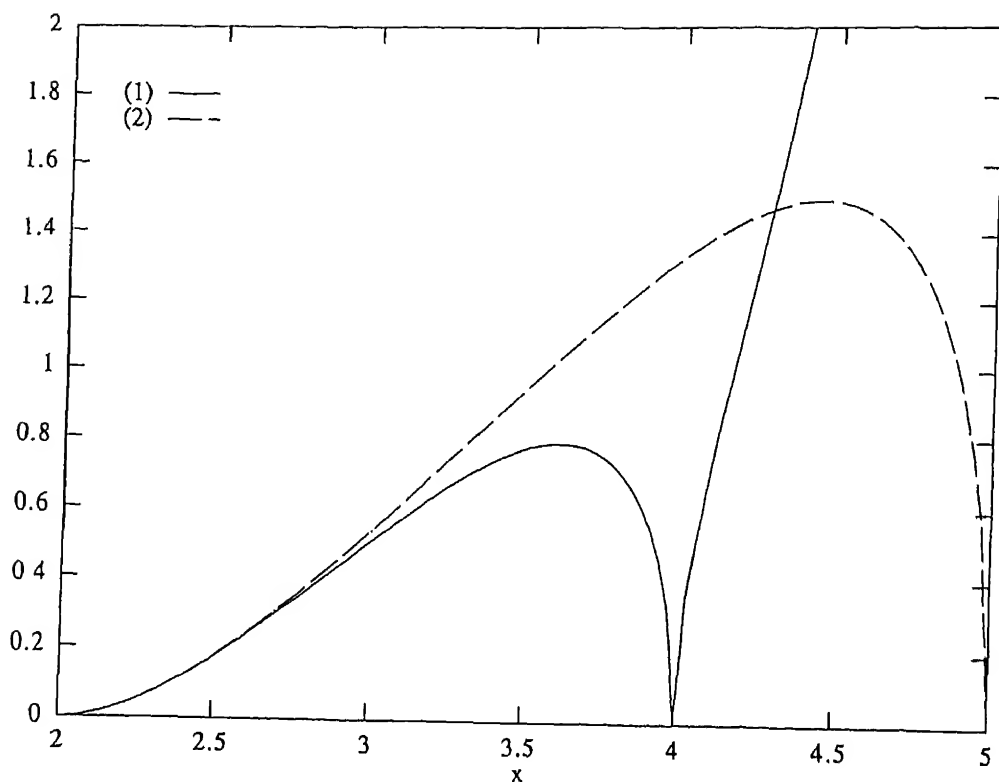
Figure 3.12: The L.H.S of the traversability in Eq 3.22 for C values (1) $C = 1.218$ (2) $C = .1863$ for nonrelativistic velocities.

traversable wormhole solutions which obey a certain physical requirement on the matter stress energy. We have been able to find such spacetimes for matter satisfying the tracelessness constraint. Our solutions depend on a parameter C. For positive values of C, these solutions represent Morris–Thorne wormholes with exotic matter. As C decreases the exoticity becomes confined to an ever smaller region around the throat which also reduces in size. For $C = 0$ both throat and WEC violating region shrink to zero. For $C < 0$ WEC violation disappears altogether but the geometry no longer remains that of a wormhole either. This illustrates clearly the intimate relationship between exotic matter and the wormhole shape. The $C < 0$ solutions , being asymptotically flat can nevertheless be used to construct Visser-type wormholes through the Junction Condition Formalism of GR. Finally an analysis of the traversability of the Morris -Thorne type geometries yields a certain lower bound on the throat radius. This, for a traveller moving with an extreme relativistic velocity turns out to be around $10^{11} - 10^{12}$ cm for the C values in the range .1-10. On the other hand , for the case of non relativistic velocities the size of the wormhole can be as large as .51light years.

One assumption we have made regards the choice of the redshift function. One can check that for a somewhat more general choice $-\Phi(r) = -(\frac{\alpha}{r})^n$ it is difficult to integrate the resulting differential equation and arrive at a closed form solution which would represent a wormhole. The case $n = .5$ is easily integrable but yields a solution which is not asymptotically flat.

Finally a remark about other constraints on matter. We have tried obtaining wormholes by imposing 'isotropic pressures' as a restriction. One can arrive at asymptotically flat geometries of the type discussed in this paper for the $C < 0$ case with the same choice of the redshift function. Unfortunately these can be used only to construct Visser type wormholes. The exotic matter at the throat cannot be made to satisfy the condition of isotropic pressures at any cost unlike the case for traceless

stress energy discussed here.

Chapter 4

Evolving Lorentzian Wormholes

In the previous chapters most of our efforts in understanding Lorentzian wormholes and WEC violations have been concentrated on static geometries. The only place where a nonstatic geometry was mentioned was in the time-machine constructions due to Morris,Thorne and Yurtsever [6] and Novikov [39]. The aim here is to show that within classical general relativity there exist Lorentzian wormholes which are nonstatic and which do not require WEC violating matter to support them. These wormholes,as will be shown, exist for a finite (but arbitrarily small or large) time interval and represent evolving geometries. During its evolution the shape of the wormhole changes in the embedding space–the throat radius expands or contracts and the rate of change of the embedding function increases or decreases. One can draw an analogy between these geometries and the usual FRW universe ($k = 1$). The spacelike sections of the former are topologically $R \otimes S^2$ while those of the latter are S^3. In the spirit of this, one can therefore think of these spacetimes as constituting 'wormhole universes'. The only other papers which deal with evolving wormholes are due to Hochberg and Kephart [74] and Roman [75].While the former discusses a possible resolution of the horizon problem using a network of dynamic (evolving) wormholes possibly present in the early universe, the latter considers

55

an evolving geometry with an inflationary scale factor. It should also be mentioned that Visser in [34] has discussed the stability of his wormholes by making the throat dynamic (i.e time dependent).

4.1 Evolving Wormholes And The Weak Energy Condition

We begin our analysis with the following ansatzen for the metric and the energy-momentum tensor.

$$ds^2 = \Omega^2(t)[-dt^2 + \frac{dr^2}{1 - b(r)/r} + r^2 d\Omega_2^2] \tag{4.1}$$

$$T_{oo} = \rho(r,t), \quad T_{11} = \tau(r,t), \quad T_{22} = T_{33} = p(r,t) \tag{4.2}$$

Here $\Omega^2(t)$ is the conformal factor, finite and positive definite throughout the domain of 't'. One can also write the metric in 4.1 using 'physical time' instead of 'conformal time'. This would mean replacing t by $\tau = \int \Omega(t)dt$ and therefore $\Omega(t)$ by $R(\tau)$ where the latter is the functional form of the metric in the τ coordinate. However, at the moment we use 'conformal time'. Translating all the results for t into those for τ is a trivial exercise. $\rho(r,t), \tau(r,t)$ and $p(r,t)$ are the components of the energy momentum tensor in the frame given by the one-form basis

$$e^o = \Omega(t)dt, \quad e^1 = \frac{\Omega(t)dr}{\sqrt{1 - b(r)/r}}, \quad e^2 = \Omega(t)r d\theta, \quad e^3 = \Omega(t)r \sin\theta d\phi \tag{4.3}$$

$d\Omega_2^2$ is the line element on the two-sphere. $b(r)$ is the usual 'shape function' as defined by Morris and Thorne [3]. It will be assumed to satisfy all the conditions required for a spacetime to be a Lorentzian wormhole; i.e., $\frac{b(r)}{r} \leq 1; \frac{b(r)}{r} \to 0$ as $r \to \infty$; at $r = b_o, b(r) = b_o; r > b_o$. The Einstein field equations with the ansatz (1) and (2) turn out to be (units $8\pi G = c = 1$).

$$\rho(r,t) = \frac{1}{\Omega^2}\left[3\left(\frac{\dot{\Omega}}{\Omega}\right)^2 + \frac{b'}{r^2}\right] \tag{4.4}$$

$$\tau(r,t) = \frac{1}{\Omega^2}\left[-2\frac{\ddot{\Omega}}{\Omega} + \left(\frac{\dot{\Omega}}{\Omega}\right)^2 - \frac{b}{r^3}\right] \tag{4.5}$$

$$p(r,t) = \frac{1}{\Omega^2}\left[-2\frac{\ddot{\Omega}}{\Omega} + \left(\frac{\dot{\Omega}}{\Omega}\right)^2 + \frac{b - b'r}{2r^3}\right] \tag{4.6}$$

The dots denote derivatives with respect to t and the primes derivatives with respect to r. The WEC ($T_{\mu\nu}u^\mu u^\nu \geq 0\, \forall$ nonspacelike u^μ) reduces to the following inequalities for the case of a diagonal energy-momentum tensor

$$\rho \geq 0, \quad \rho + \tau \geq 0, \quad \rho + p \geq 0 \quad \forall(r,t) \tag{4.7}$$

From Eq 4.4, 4.5, 4.6 one can write down three inequalities which have to be satisfied if the WEC is not violated. These are

$$\frac{1}{\Omega^2}\left[3\left(\frac{\dot{\Omega}}{\Omega}\right)^2 + \frac{b'}{r^2}\right] \geq 0 \tag{4.8}$$

$$\frac{1}{\Omega^2}\left[-2\frac{\ddot{\Omega}}{\Omega} + 4\left(\frac{\dot{\Omega}}{\Omega}\right)^2 - \frac{b - b'r}{r^3}\right] \geq 0 \tag{4.9}$$

$$\frac{1}{\Omega^2}\left[-2\frac{\ddot{\Omega}}{\Omega} + 4\left(\frac{\dot{\Omega}}{\Omega}\right)^2 + \frac{b + b'r}{2r^3}\right] \geq 0 \tag{4.10}$$

Several important facts should be noted here in comparison with the case of a static geometry. Eq 4.8 is trivially satisfied if $b' \geq 0$ irrespective of the geometry being static/ nonstatic. However, if it is nonstatic then one can satisfy Eq 4.8 even for the case when $b' \leq 0$. Infact, one obtains the inequality

$$\frac{|b'|}{r^2} \leq 3\left(\frac{\dot{\Omega}}{\Omega}\right)^2 \tag{4.11}$$

For every $t = constant$ slice Eq 4.11 has to hold, which means

$$\frac{|b'|}{r^2} \leq min\left[3\left(\frac{\dot{\Omega}}{\Omega}\right)^2\right] \tag{4.12}$$

where min denotes the minimum value of the function in the given time interval.

For a static geometry Eq 4.9 can never be satisfied, as shown by Morris and Thorne [14]. But, for a nonstatic geometry with $b' \geq 0$ one can satisfy Eq 4.9. We require

$$\left[2\left(\frac{\dot{\Omega}}{\Omega}\right)^2 - \frac{\ddot{\Omega}}{\Omega} \right] \geq \frac{b - b'r}{2r^3} \qquad (4.13)$$

Stated explicitly Eq 4.13 implies that the value of $(b - b'r)/r^3$ for all r must be less than or equal to the minimum value of the function $\left[2\left(\frac{\dot{\Omega}}{\Omega}\right)^2 - \frac{\ddot{\Omega}}{\Omega} \right]$, in the corresponding domain of 't'. However, we need

$$F(t) = 2\left[2\left(\frac{\dot{\Omega}}{\Omega}\right)^2 - \frac{\ddot{\Omega}}{\Omega} \right] > 0 \qquad (4.14)$$

Eq 4.14 can be written in a more precise form by introducing a function $\chi(t) = \Omega/\dot{\Omega}$. We have

$$\frac{d\chi}{dt} > (-1) \qquad (4.15)$$

With $b' \geq 0$ and Eq 4.13 holding one clearly sees that Eq 4.9 is satisfied. Therefore from this very simple analysis it is clear that nonstatic spherically symmetric Lorentzian wormhole geometries can exist with the required matter not violating the WEC. However, the fact that $\Omega(t)$ be finite everywhere and must satisfy the condition Eq 4.13 implies that these wormholes exist for finite intervals of time (arbitrarily small or large). For finite and bounded Ω which is everywhere nonzero this can be proved as follows. The finiteness and boundedness of $\Omega(t)$ implies that it can have only a specific class of functional forms. These include (i) functions which have no extremum and asymptotically approach the constant limiting values (e.g. $A + B \tanh \omega t$) (ii) functions which have one extremum and asymptotically approach constant limiting values (e.g. $A + Be^{-\omega t^2}$) (iii) oscillatory functions which may or may not approach the limiting values (e.g $\sin \omega t + a$). In all the three cases

where the functions asymptotically approach limiting values $F(t)$ tends to zero at $t \rightarrow \pm\infty$ and the WEC is violated. For a purely oscillatory function there exists more than one extremum and at the minimum $F(t)$ is clearly negative.Thus WEC violations can be avoided only for finite intervals of time if one chooses a finite and bounded $\Omega(t)$.

Before we construct explicit examples it is necessary to discuss briefly the embedding in R^3 of a $\theta = \pi/2$, $t = t_0$ slice, where t_0 lies in the interval in which the wormhole exists. Since our geometry is nonstatic each such slice will be different - more precisely the value of the function $\Omega(t)$ at $t = t_0$ will dictate the shape and features of this slice, which will thus change as we alter t_0. The metric on such a slice takes the form

$$\bar{ds}^2 = \Omega^2(t_0) \left[\frac{dr^2}{1 - \frac{b(r)}{r}} + r^2 d\phi^2 \right] \tag{4.16}$$

Define

$$\tilde{r} = \Omega(t_0)r \tag{4.17}$$

Thus 4.16 takes the form

$$\bar{ds}^2 = \frac{d\tilde{r}^2}{\frac{1 - a(\tilde{r})\Omega(t_0)}{\tilde{r}}} + \tilde{r}^2 d\phi^2 \tag{4.18}$$

where $a(\tilde{r})$ is the functional form of $b(r)$ in the $\tilde{r}$ coordinate. The minimum value of $\tilde{r}$ which determines the throat radius is evaluated from

$$a(b_0)\Omega(t_0) = \tilde{b}_0 \tag{4.19}$$

This clearly shows the dependence on $\Omega(t)$.Using the mathematics of embedding we can write the following differential equation for the spacelike slice at $t = t_0$.

$$\frac{dz(\tilde{r})}{d\tilde{r}} = \left[\frac{a(\tilde{r})\Omega(t_0)}{\tilde{r} - a(\tilde{r})\Omega(t_0)} \right]^{\frac{1}{2}} \tag{4.20}$$

where $z(\tilde{r})$ is the embedding function. Integrating 4.20 one can obtain the $z(\tilde{r})$ for the slice at $t = t_0$.

(iii) $\Omega(t) = \sin \omega t$

The scale factor is the same as the one that arises in the closed FRW cosmology which starts with a 'bang' and ends with a 'crunch'.Instead of the usual S^3 spacelike sections we have wormhole metrics on $R \otimes S^2$ .The expression for $F(t)$ turns out to be

$$F(t) = 2\omega^2(2\cot^2 \omega t + 1) \tag{4.23}$$

One can easily check that $F(t)$ has a minimum at $\omega t = \frac{\pi}{2}$ .Hence the constraint on the allowed values of b_o turns out to be the same as in the previous case i.e $b_0^2 \omega^2 \geq \frac{1}{2}$ .One can also say that the lifetime of this wormhole universe is $\frac{\pi}{\omega}$ .The time interval for which this universe can exist without collapsing into a singularity is $\frac{m\pi}{\omega} < t < \frac{(m+1)\pi}{\omega}$.

(iv) $\Omega(t) = (\omega t)^\nu$ ν integral or fractional

This case is important because the scale factors that arise in the dust-filled or radiation dominated FRW cosmologies with flat spacelike sections are obtained by considering special values of the ν used above. We shall deal with these special cases later in a separate section.

For general ν the expression for $F(t)$ is given as

$$F(t) = \frac{2\nu(\nu + 1)}{t^2} \tag{4.24}$$

Therefore as $t \to \pm\infty$ $F(t) \to 0$. The constraint on b_0 turns out to be dependent on t .

$$b_0^2 \geq max\left(\frac{t^2}{2\nu(\nu + 1)}\right) \tag{4.25}$$

Thus the evolving wormhole with this type of scale factor can exist only for a finite interval of time (similar to the previously discussed cases). The lower bound on b_0 is decided by the maximum time t upto which we wish the wormhole to exist with the matter threading the geometry satisfying the WEC.Beyond this time the matter

62

will violate the WEC. As we shall see later this condition sets the most stringent restriction on the size of the wormhole.

We now move on to a special class of scale factors which exhibit 'flashes' of WEC violation. This essentially means that the matter threading the wormhole violates the Energy Conditions only for small intervals of time and is normal at all other times. Whether such matter is physically possible is as yet unknown. However , the intervals during which the WEC is violated can be chosen to be very small (this obviously leads to a constraint on the throat radius). We shall deal with two representative examples. Many more can constructed without much of a problem.

(a) $\Omega(t) = \sin \omega t + a$ $a > 1$

This scale factor reminds us of the 'bounce' type solutions in cosmology which were constructed in order to avoid the big–bang singularity. For a nonstatic wormhole with the scale factor chosen as above the function $F(t)$ turns out to be :

$$F(t) = 2\omega^2 \left[\frac{2 - \sin^2 \omega t + a \sin \omega t}{(\sin \omega t + a)^2} \right] \tag{4.26}$$

This function is plotted in Fig 4.1.

Note that $F(t)$ goes to zero in the vicinity of $\omega t = 3\pi/2$,stays negative for a while and then subsequently becomes positive again.This happens once in every period , i.e at ωt values given by $(2n+1)\pi/2$.Thus the WEC will be violated during those intervals of time.The time domain over which the WEC is violated is ,as mentioned before , related to the throat radius parameter of the wormhole.One chooses this interval in the following way. Assume a minimum ,positive and finite value of $F(t)$,say F_0.In the neighborhood of the point where $F(t)$ is zero , this value occurs at points say $\omega t_0 - \delta$ and $\omega t_0 + \delta$.If the shape function is assumed as constant $(b(r) = b_0)$ then the relation between the throat radius parameter and the minimum value of $F(t)$ turns out to be :

$$b_0^2 \geq \frac{1}{F_0} \tag{4.27}$$
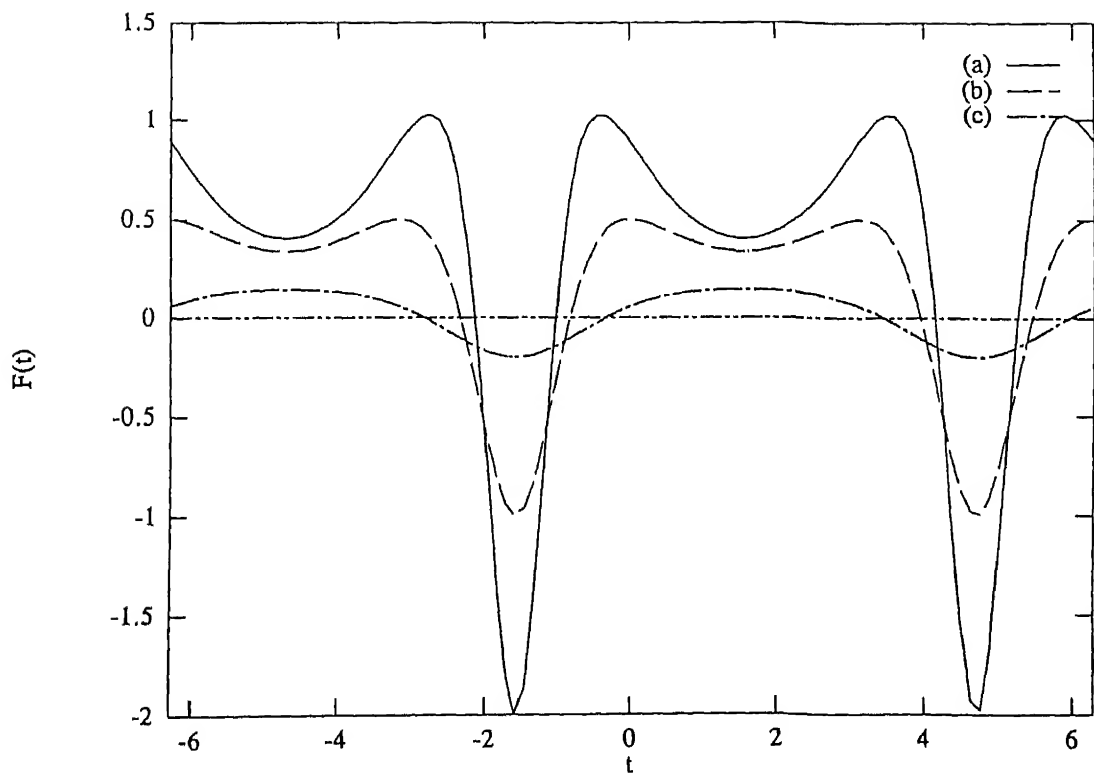
Figure 4.1: F(t) vs t for $\Omega(t) = \sin t + a$ $(a)\omega = 1, a = 1.5 (b)\omega = 1, a = 2 (c)\omega = 1, a = 6$

Hence the interval during which the WEC is violated is 2δ . The smaller this time interval the larger the minimum allowed value of b_0.

(b) $\Omega(t) = \frac{t^2+a^2}{t^2+b^2}$ $b > a > 0$

In this case also the scale factor is such that the geometry is never singular.Asymptotically it becomes a static wormhole.The function $F(t)$ turns out to be

$$F(t) = \frac{4(b^2 - a^2)(3t^2 - a^2)}{(t^2 + b^2)(t^2 + a^2)^2}$$

(4.28)

This function is shown plotted in Fig 4.2. At $t = \pm a/\sqrt{3}$ $F(t) = 0$.For $-a/\sqrt{3} < t < a/\sqrt{3}$ $F(t)$ is negative.One can carry out an analysis similar to the one for (a) the only difference being that WEC violation occurs here only in the neighborhood of the interval mentioned above and at $\pm\infty$.

Further examples can be constructed by choosing other forms of $\Omega(t)$. Two worth mentioning follow from constraints on the matter stress energy for an evolving wormhole geometry. For the perfect fluid with $p = \frac{\rho}{3}$ we end up with the scale factor of a closed FRW universe while for traceless matter in general i.e matter obeying only $-\rho + \tau + 2p = 0$ we get a linear $\Omega(t)$ i.e $\Omega(t) = at + b$.

4.3   A Wormhole in a Flat FRW universe

A probable realisation of an evolving wormhole could be obtained by thinking of it as part of an asymptotically FRW universe i.e. by imagining the asymptotically flat parts of an evolving wormhole geometry as constituting a flat FRW spacetime .Mathematically one therefore chooses a metric which represents an evolving wormhole with the scale factor identical to either the matter or the radiation dominated
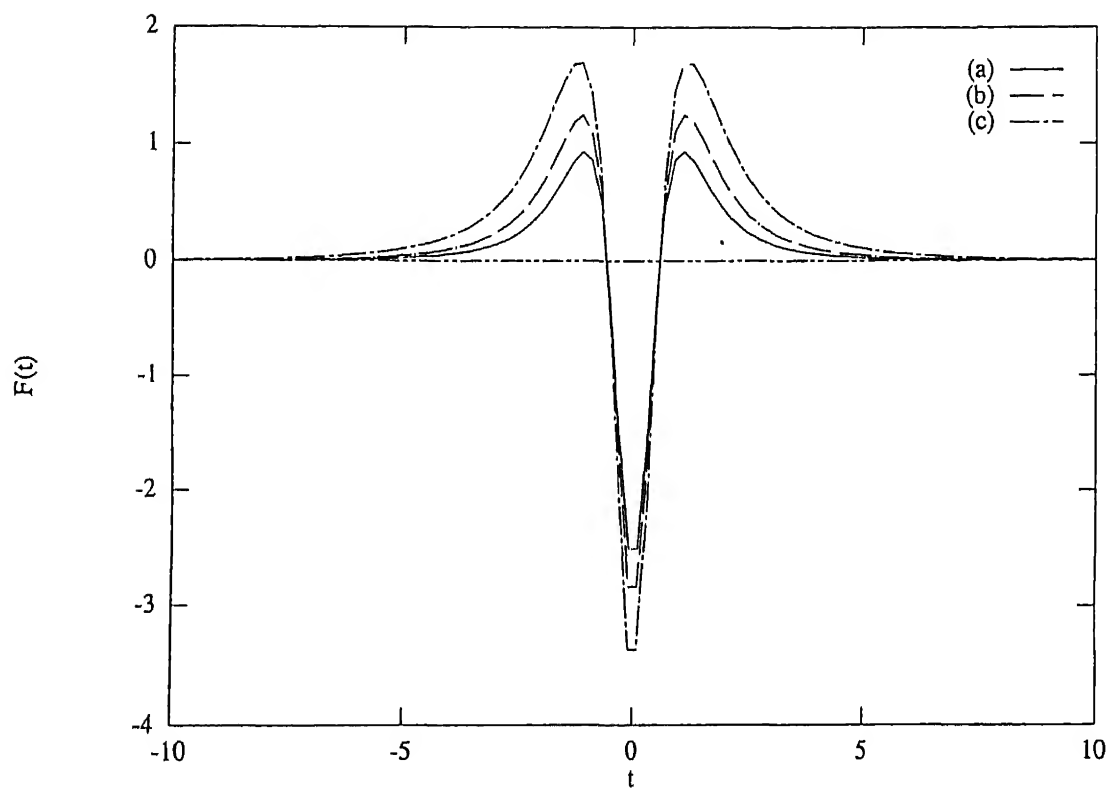
Figure 4.2: F(t) vs t for $\Omega(t) = \left(\frac{t^2+a^2}{t^2+b^2}\right)$ $b > a > 0 (a) a = 1, b = 1.5 (b) a = 1, b = 2 (c) a = 1, b = 3$

66

FRW model. Thus

$$ds^2 = -d\tau^2 + \tau^n \left(\frac{dr^2}{1 - \frac{b(r)}{r}} + r^2 d\Omega_2^2 \right) \qquad (4.29)$$

where we have changed our time coordinate from the conformal time used in the earlier discussions to real time. The exponent n takes on the values $\frac{1}{2}$ and $\frac{2}{3}$ in accordance with the radiation and matter dominated cases of the flat FRW universe. The Einstein equations lead to the following expressions for the matter density and the pressures.

$$\rho(r,\tau) = \frac{b'}{(\tau)^{2n} r^2} + \frac{3n^2}{c^2 \tau^2} \qquad (4.30)$$

$$p_1(r,\tau) = -\frac{b}{(\tau)^{2n} r^3} - \frac{n(3n-2)}{(c\tau)^2} \qquad (4.31)$$

$$p_2(r,\tau) = \frac{b - b'r}{2r^3 (\tau)^{2n}} - \frac{n(3n-2)}{(c\tau)^2} \qquad (4.32)$$

The WEC inequality $\rho + p_1 \geq 0$ reduces to the following :

$$\frac{b'r - b}{r^3 (\tau)^{2n}} + \frac{2n}{(c\tau)^2} \geq 0 \qquad (4.33)$$

As expected all the essential properties of the matter stress energy of the flat FRW model follow from the expressions for ρ, p_1 and p_2. As $r \to \infty$, only the τ dependent terms survive, and we get $\rho = \rho_{FRW} = \frac{4}{3(c\tau)^2}$, $p_1 = p_2 = 0$ for dust and $\frac{\rho}{3} = p_1 = p_2 = \frac{1}{4(c\tau)^2}$ for pure radiation.

Secondly, the pressures become increasingly disparate as we approach the throat $(p_2 - p_1 = \frac{3b - b'r}{2(\tau)^{2n} r^3} \geq 0)$. From the geometrical viewpoint this is because the curvature s in the $\theta\phi$ directions is different from that in the r direction. Thus, inside the wormhole, matter is subject to anisotropic stresses and to remain in equilibrium it must respond by generating anisotropic strains.

Lastly let us look at the WEC conditon mentioned earlier. For concreteness and simplicity we choose $b(r) = b_0$. From the WEC inequality $\rho + p_1 \geq 0$ we arrive at the

condition $b_0 R(\tau) \geq \frac{(c\tau)}{\sqrt{2n}}$. This quite simply leads to the statement that the throat radius $b_0 R(\tau)$ at time τ must exceed the horizon size $c\tau$ (upto a constant factor given by $\sqrt{1/2n}$ which is of O(1),being exactly equal to 1 and $\frac{\sqrt{3}}{2}$ for pure radiation and dust respectively). Now for an FRW evolution the horizon always moves faster that the scale $R(\tau)$ and hence eventually overtakes $b_0 R(\tau)$, causing WEC violation to begin at the throat and slowly spread outward.Furthermore, since wormholes presumably arise through quantum gravitational processes, they can reasonably be assumed to form in the Planckian era,with a radius ,which is typically of Planck size at Planck time. If their subsequent evolution is FRW–like ,WEC violation occurs within a few Planck times.To avoid this ,the wormhole must inflate to a size much larger than the horizon.This is precisely what happens in the early universe (inflationary epoch).However, as we have shown earlier an inflationary scale factor leads to WEC violation at all times.

4.4   Concluding Remarks

We have shown in this chapter that wormholes with normal matter are a realistic possibility even in the domain of classical GR. The existence of these geometries for a finite interval of time with matter satisfying the WEC seems a little disturbing although it is definitely better than the situation for static geometries. Consequences of the presence of such an evolving wormhole in the flat FRW model have been outlined in brief.

We have not dealt with the question of human traversability in the context of these evolving geometries. Such an analysis, is however, not too difficult. One has to replace the static observer's frame in the case of a static wormhole with the comoving frame for the evolving geometry. Then one carries out a simple Lorentz transformation to go into the frame of the traveller. The Riemann tensor

components are obtained in this traveller's frame and they lead to the tidal force constraints. A similar analysis also holds for the acceleration constraint. The major difference is that all constraints depend on time and one has to find by extremization the time at which the inequalities yield the most stringent condition. After this extremization with respect to time one has to extremize w.r.t r to obtain the final condition which when satisfied would make the wormhole traversable.

Since evolving wormholes are nonstatic , the study of quantum field theory in these backgrounds may result in particle creation. The relevant calculation would be fruitful to pursue. It requires, however, the exact solutions of the scalar wave/Maxwell or Dirac equations which at first sight may be rather difficult to obtain. Numerical analyses can nevertheless be done to provide hints into the number density and distributions of the created particles.

Chapter 5

Scalar Waves in Wormhole Geometries

We now turn towards the propagation of massless scalar waves in a one parameter family of wormholes. A number of papers have been written on various aspects of wormholes and some of these have been mentioned and discussed in the various preceding Chapters of this thesis. However, questions related to geodesics and to scalar, spin-half, electromagnetic and gravitational perturbations seem to have attracted very little attention. The few existing pieces of work along these lines include the investigations of Friedman et.al [15] and Friedman and Morris [16] on the Cauchy problem for the scalar wave equation in wormhole–based spacetimes with CTLs. Our focus here, is however, somewhat different. We consider scalar wave propagation through static wormholes without CTLs.To this end, we first define a one–parameter family of wormholes which are essentially generalizations of the geometry discussed extensively by Ellis [31](see also Box 2 in [14]).A certain parameter $n \geq 2(n$ even) defines this family (for a detailed analysis of these geometries see Section 3.1). The scalar wave equation (massless) is written down and separated. It turns out that the radial equation for the coordinate l for $n = 2$ is a

Modified Mathieu equation in 2+1 dimensions. In 3+1 dimensions the 'l' equation is the radial equation that appears when the Helmholtz equation is separated in oblate spheroidal coordinates. Both equations can be solved exactly. We discuss their solutions and use them to understand the scattering of scalar waves through the wormhole. The reflection and transmission coefficients for $n = 2$ are evaluated analytically for certain specific values of the energy of the scalar wave. For $n > 2$ exact solutions of the corresponding radial equations are not available and we adopt numerical methods to obtain $|R|^2$ and $|T|^2$.

For the sake of convenience we recall from Sec.3.1 the metrics to be used as backgrounds for our investigations here .These are-

$$ds^2 = -dt^2 + d\ell^2 + (b_o^n + l^n)^{\frac{2}{n}} d\theta^2 \qquad (2+1) dimensions \qquad (5.1)$$

$$ds^2 = -dt^2 + dl^2 + (b_o^n + l^n)^{\frac{2}{n}} [d\theta^2 + \sin^2\theta d\phi^2] \quad (3+1) dimensions \qquad (5.2)$$

In the above $l \to +\infty$ and $l \to -\infty$ correspond to the upper and lower asymptotically flat regions. $l = 0$ is the throat region.It has be shown that the matter required to have such a geometry violates the WEC .

5.1 Massless Scalar Wave Equation,Separation Of Variables ,Equivalent One Dimensional Problems

The massless scalar wave equation is given by

$$g^{\mu\nu}\nabla_\mu\nabla_\nu\Phi = 0 \qquad (5.3)$$

where ∇_μ denotes the covariant derivative. We shall discuss the 2+1 and 3+1 dimensional cases separately.

2+1 Dimensions

Using standard methods of separation of variables we find that the equations for the t, l and θ coordinates reduce to the following. We assume

$$\Phi(t, l, \theta) = T(t)L(l)\Theta(\theta) \tag{5.4}$$

Then,

$$\frac{d^2\Theta}{d\theta^2} + m^2\Theta = 0 \tag{5.5}$$

$$\frac{d^2T}{dt^2} + \omega^2 T = 0 \tag{5.6}$$

$$(b_0^n + l^n)^{\frac{2}{n}}\frac{d^2L}{dl^2} + l^{n-1}(b_0^n + l^n)^{\frac{2}{n}-1}\frac{dL}{dl} + [\omega^2(b_0^n + l^n)^{\frac{2}{n}} - m^2]L = 0 \tag{5.7}$$

The first two of these equations are simple. The third equation can be reduced to the following alternative forms. If we define a function $g(l)$ such that

$$L(l) = \frac{g(l)}{(b_0^n + l^n)^{1/2n}} \tag{5.8}$$

then Eq 5.7 reduces to

$$\frac{d^2g}{dl^2} + [\omega^2 - V(l)] = 0 \tag{5.9}$$

where

$$V(l) = \frac{2(n-1)b_0^n l^{n-2} - l^{2n-2}}{4(b_0^n + l^n)^2} + \frac{m^2}{(b_0^n + l^n)^{2/n}} \tag{5.10}$$

This is the equivalent one dimensional Schrodinger–type equation with the role of energy being played by ω^2 and the potential function being given by Eq.5.10 . The allowed values of m are discrete in order that $\Theta(\theta)$ be single- valued. The effective potential is plotted for $n = 2$ in Fig 5.1 and for other values of n and m in Fig 5.2 and 5.3. These are generically barrier type potentials asymptotically

going to zero. For n increasing with m fixed the barrier becomes progressively flat at the top. However at $l = \pm b_0$ there appear spikes which increase in height with increasing n.We recall from Chapter 3 that as n increases the geometry becomes more and more like a uniform tunnel which suddenly opens out into flat space in the vicinity of $l = \pm b_0$.This sharp change in the embedding features at $l = \pm b_0$ is the root cause of the spikes in the potentials.On the other hand, if n is fixed and m varies the barrier height changes–this is clear from the functional form of the potential

The $n = 2$ case is rather special. If one uses the transformation

$$l = b_o \sinh \xi \tag{5.11}$$

one can reduce Eq 5.7 to the following equation

$$\frac{d^2}{d\xi^2} L(\xi) - (a - 2q \cosh 2\xi) L(\xi) = 0 \tag{5.12}$$

where $a = m^2 - \frac{\omega^2 b_o^2}{2}$ and $q = \frac{\omega^2 b_o^2}{4}$. The equation in 5.12 is known as the Modified Mathieu equation with parameters satisfying $a + 2q = m^2$.

3+1 Dimensions

In 3+1 Dimensions one can similarly get

$$\Phi(t, l, \theta, \phi) = T(t)L(l)\Theta(\theta)P(\phi) \tag{5.13}$$

The corresponding equations for $T(t), L(l), \Theta(\theta)$ and $P(\phi)$ turn out to be the following

$$\frac{d^2 T}{dt^2} + \omega^2 T = 0, \tag{5.14}$$

$$(b_0^n + l^n)^{\frac{2}{n}} \frac{d^2 L}{dl^2} + 2l^{n-1}(b_0^n + l^n)^{\frac{2}{n}-1} \frac{dL}{dl} + (\omega^2 (b_0^n + l^n)^{\frac{2}{n}} - p(p+1))L = 0 \tag{5.15}$$
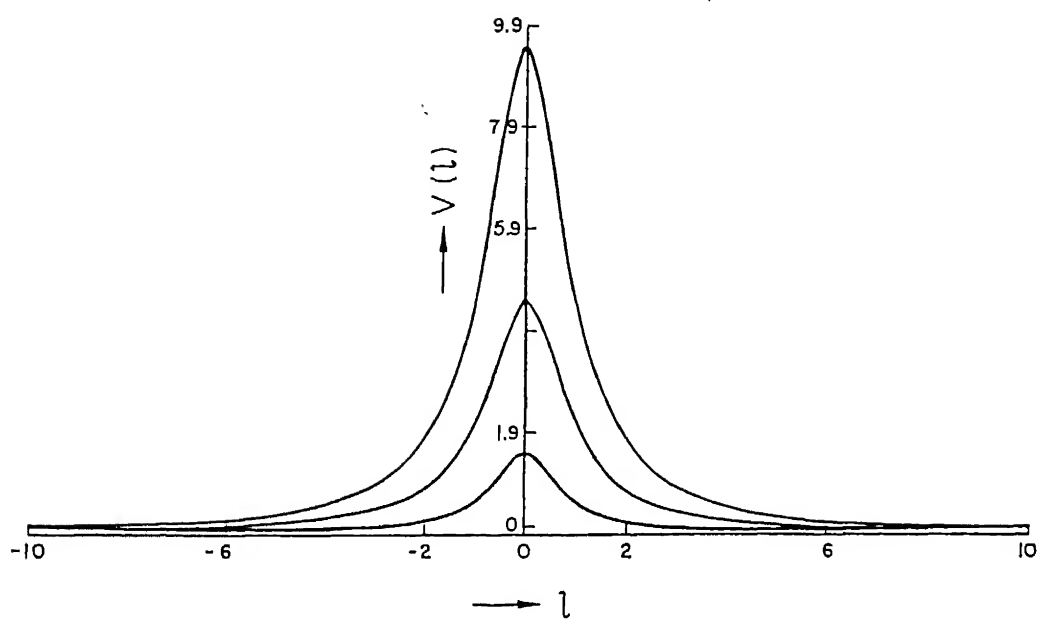
Figure 5.1: Effective Potential for $n = 2(2+1)$ case with $m = 1, 2, 3$ for the three curves with succesively increasing values of the barrier at $l = 0$
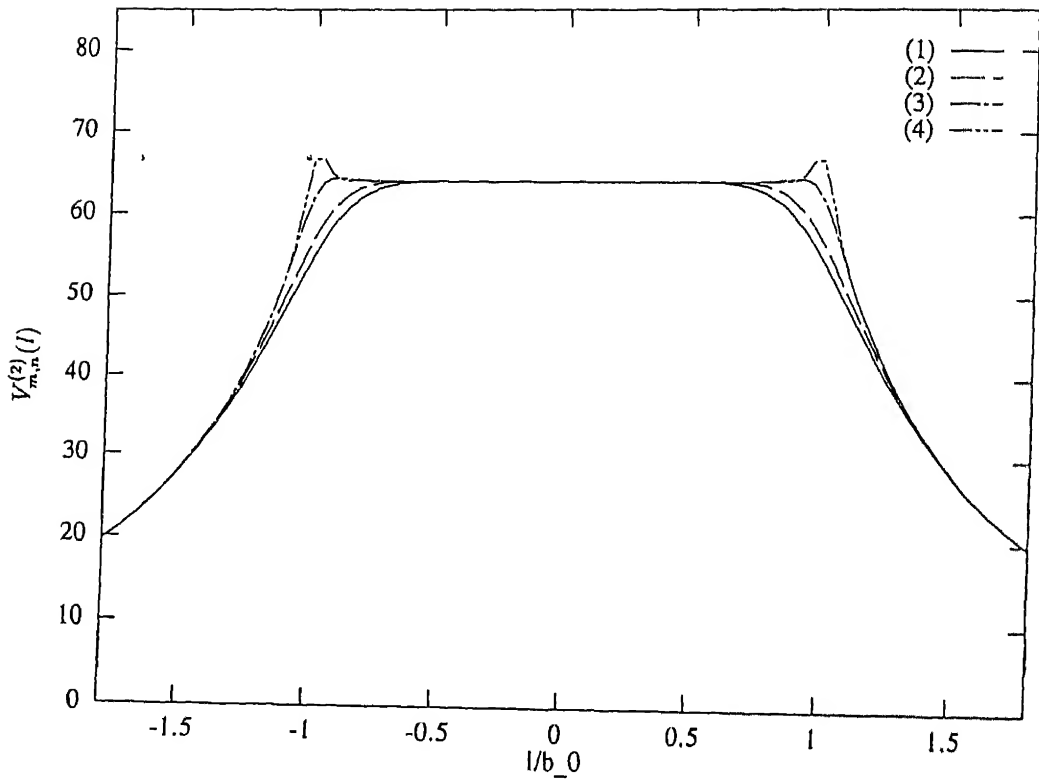
Figure 5.2: Effective Potential (2+1case) for $m = 8$ and $(1)n = 8, (2)n = 10, (3)n = 20, (4)n = 40$
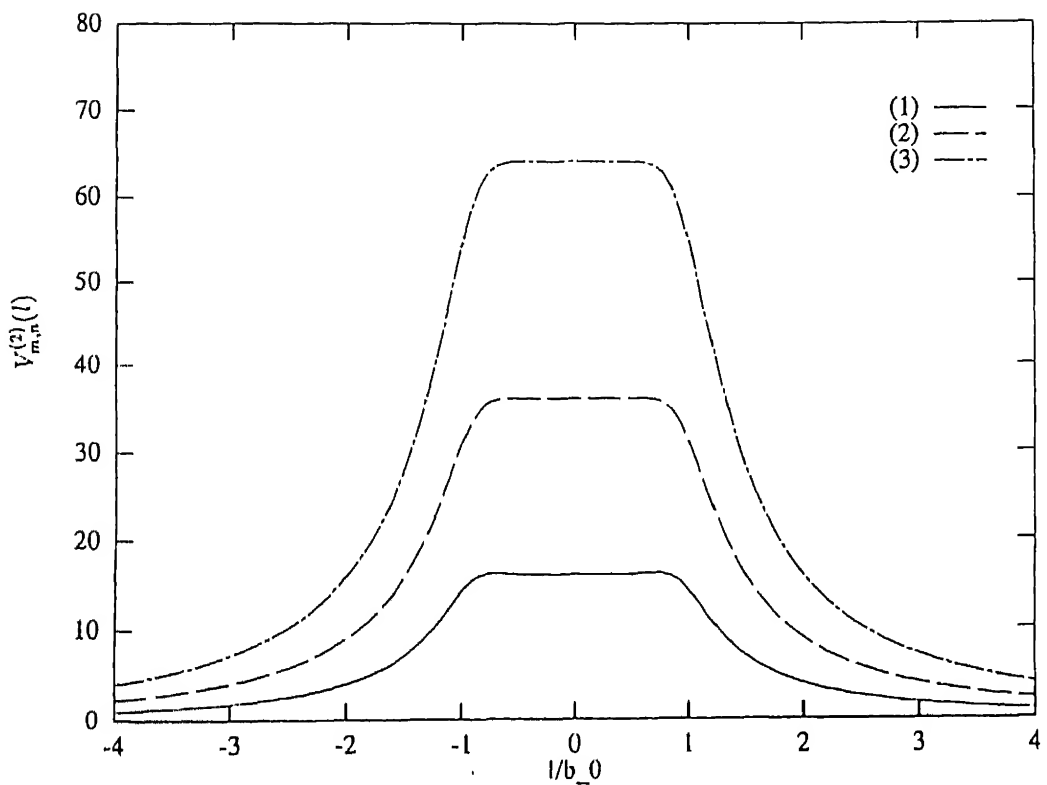
Figure 5.3: Effective Potential (2+1 case) for $n = 8$ and $(1)m = 4, (2)m = 6, (3)m = 8$

$$\frac{1}{\sin\theta}\frac{d}{d\theta}\sin\theta\frac{d\Theta}{d\theta} + \left(p(p+1) - \frac{m^2}{\sin^2\theta}\right)\Theta = 0 \tag{5.16}$$

$$\frac{d^2 P}{d\phi^2} + m^2 P = 0 \tag{5.17}$$

The solutions to the angular equations comprise the spherical harmonics. As in the 2+1 dimensional case the radial (l) equation can also be reduced to an equivalent Schrodinger type equation of the form

$$\frac{d^2 F}{dl^2} + [\omega^2 - V(l)] = 0 \tag{5.18}$$

where

$$V(l) = \frac{(n-1)b_0^n l^{n-2}}{(b_0^n + l^n)^2} + \frac{p(p+1)}{(b_0^n + l^n)^{\frac{2}{n}}} \tag{5.19}$$

and

$$L(l) = \frac{F(l)}{(b_0^n + l^n)^{\frac{1}{2n}}} \tag{5.20}$$

The $n = 2$ case, as before, is special. Indeed, by introducing $\xi = \frac{l}{b_o}$ we can write 5.15 in the form

$$(1 + \xi^2)\frac{d^2 L}{d\xi^2} + 2\xi\frac{dL}{d\xi} + (\omega^2 b_o^2(1 + \xi^2) - p(p+1))L = 0 \tag{5.21}$$

The Helmholtz equation $(\nabla^2 + k^2)\psi = 0$ when separated in oblate spheroidal coordinates (see Appendix I) yields a radial equation of the form

$$(1 + \xi^2)\frac{d^2 V_{mn}}{d\xi^2} + 2\xi\frac{dV_{mn}}{d\xi} + [-\lambda_{mn} + k^2\xi^2 - \frac{m^2}{1 + \xi^2}]V_{mn} = 0 \tag{5.22}$$

For $m = 0$ this equation is exactly the same as Eq 5.15 with the identifications

$$\lambda_{on} = p(p+1) - \omega^2 b_0^2 \qquad , k^2 = \omega^2 b_o^2 \tag{5.23}$$

Therefore $\lambda_{on} + k^2 = p(p+1)$ is a constraint on the allowed values of λ_{on} which are essentially functions of k^2.
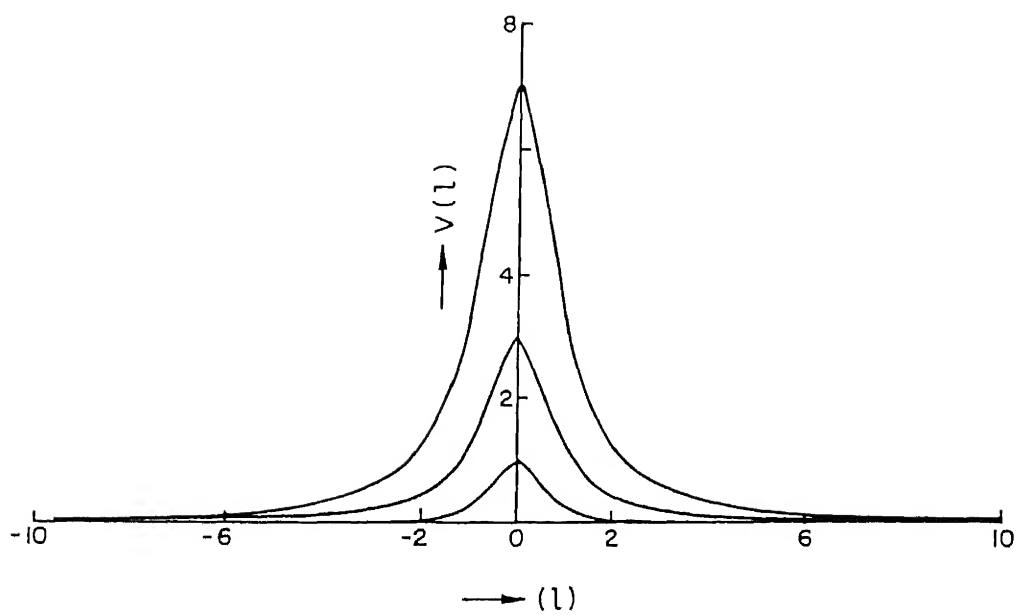
Figure 5.4: Effective Potential for $n = 2(3 + 1$ case) with $p = 0, 1, 2$ for the three curves with succesively increasing values of the barrier at $l = 0$
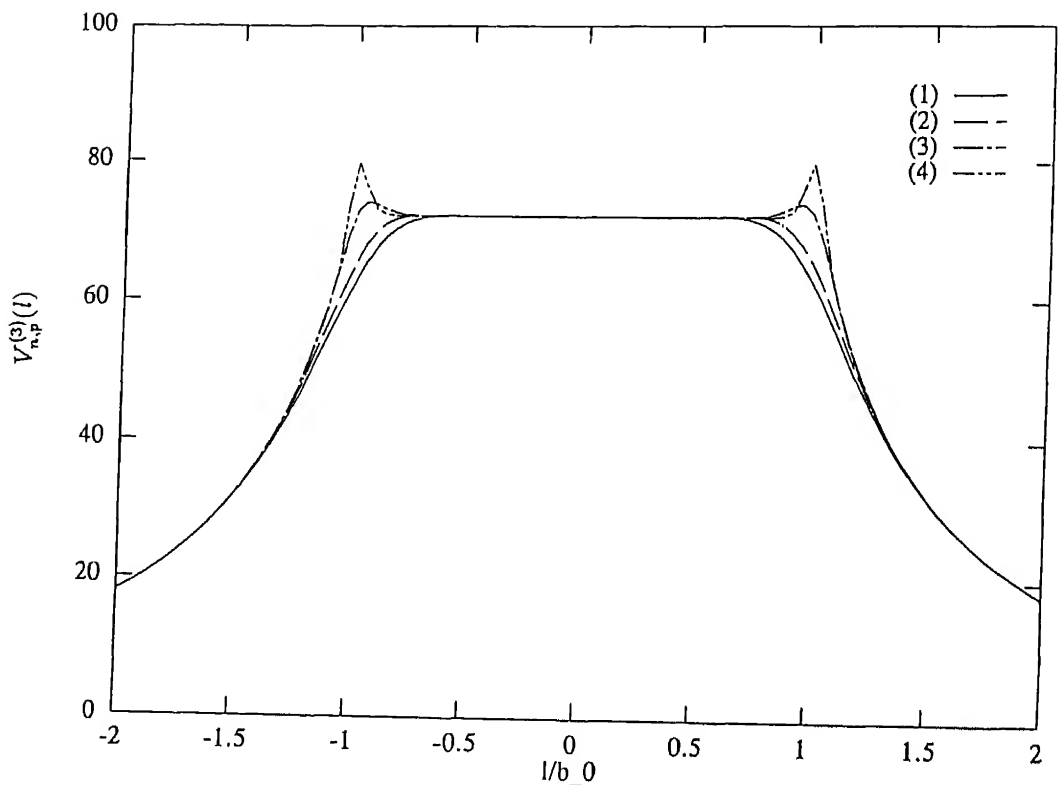
Figure 5.5: Effective Potential (3+1case) for $p = 8$ and $(1)n = 8, (2)n = 10, (3)n = 20, (4)n = 40$
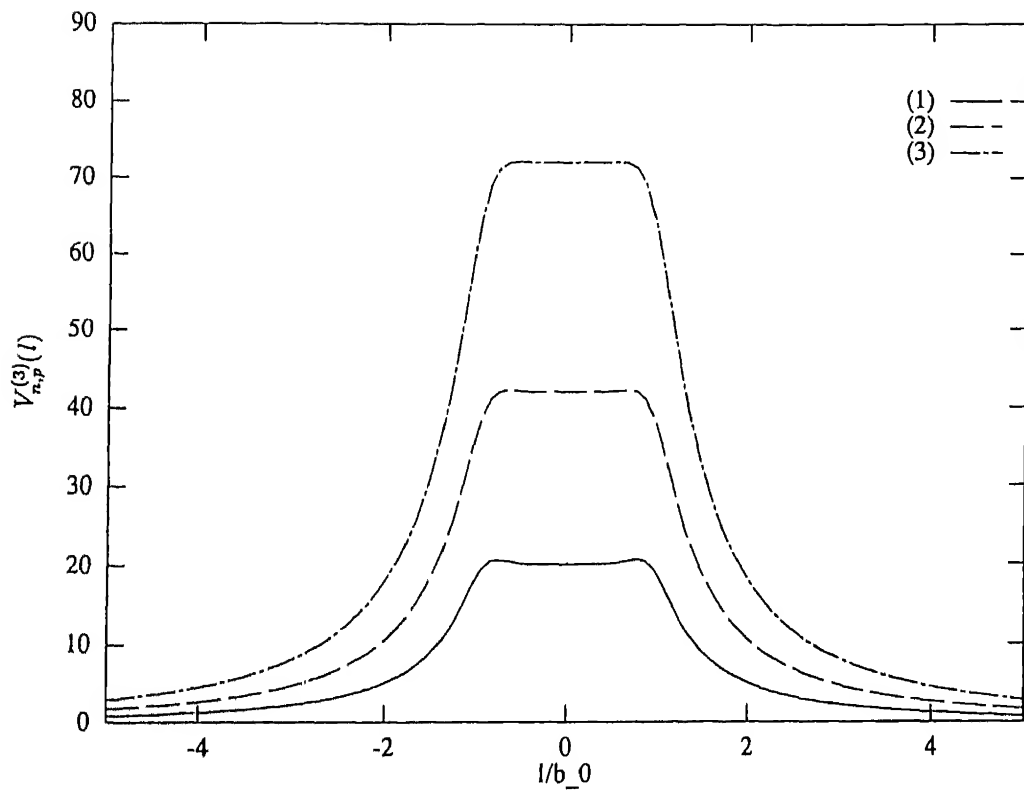
Figure 5.6: Effective Potential (3+1 case) for $n = 8$ and $(1)p = 4, (2)p = 6, (3)p = 8$

The potential functions for the $3 + 1$ dimensional cases are plotted in Fig 5.4 ($n = 2$) and Fig 5.5, 5.6 ($n > 2$). For all n these are barrier-type potentials with the barrier situated at $l = 0$. We have, therefore, reduced the study of scalar waves to a one dimensional scattering problem in traditional quantum mechanics. The reflection and transmission coefficients across the barrier can now be evaluated . However, before undertaking this evaluation it is essential to understand certain important characteristic features of the functions occurring in the exact solutions for the $n = 2$ cases. These are dealt with in the subsequent section.

5.2   The Exact Solutions in 2+1 and 3+1 Dimensions n=2

The full solution of the wave equation in 2+1 dimensions will be as follows (see Appendix I).

$$\Phi(t, l, \theta) = e^{\pm i\omega t} e^{\pm im\theta} \begin{cases} A & Mc^{(1)}{}_{2n,2n+1} + B & Mc^{(2)}{}_{2n,2n+1} \\ C & Ms^{(1)}{}_{2n,2n+1} + D & Ms^{(2)}{}_{2n,2n+1} \end{cases} \tag{5.24}$$

where $Mc^{(1)}{}_{2n,2n+1}$ and $Mc^{(2)}{}_{2n,2n+1}$ constitute a fundamental system for the l coordinate equations with characteristic values $a_{2n}, a_{2n+1} while M s^{(1)}{}_{2n,2n+1}, M s^{(2)}{}_{2n,2n+1}$ form the ssecond fundamental system with characteristic values b_{2n}, b_{2n+1}. The known solutions of the Modified Mathieu equation are essentially of two types – of integral order and of fractional order. In the above we have written down the solutions for integral order only. Thus we have restricted ourselves to values of (a, q) that lie on the characteristic lines. These values corespond to the points of intersection of the characteristic curves and the straight lines $a + 2q = m^2$. Other values of (a, q) which lie on the lines $a + 2q = m^2$ but fall in the regions between the a_i and b_{i+1} curves

give rise to the Modified Mathieu functions of fractional order. It is worthwhile to note that for $m = 0$ there are known solutions for positive values of q. The diagram shown in Fig I.1 illustrates the facts discussed above. Additional details about the Modified Mathieu functions can be found in Appendix I. It is necessary to realise that all information regarding the reflection and transmission of scalar waves can be obtained by properly analysing the solutions of the l–coordinate differential equation. The asymptotic forms of the various solutions are essential ingredients for understanding scattering phenomena. We discuss below the asymptotic forms of $Mc^{(1)}$ and $Mc^{(2)}$ as $l \to +\infty$ and $l \to -\infty$ in some amount of detail. We shall work exclusively with the solutions corresponding to the characteristic values a_{2n}, i.e. with $Mc_{2n}^{(1)}$ and $Mc_{2n}^{(2)}$ only. The analyses for the other cases is very similar and will therefore be omitted. Using the Bessel function series representations for the functions $Mc_{2n}^{(1)}$ and $Mc_{2n}^{(2)}$ we first analyze the limit $l \to \infty (\xi \to \infty)$. The series for $Mc_{2n}^{(1)}$ is valid for all $\xi (-\infty < \xi < \infty)$ whereas for $Mc_{2n}^{(2)}$ it is valid only for $\xi > 0$. Moreover, $Mc_{2n}^{(1)}$ is an even function whereas $Mc_{2n}^{(2)}$ is neither even nor odd. Their asymptotic forms are as follows:

(a) For $\xi \to \infty (l \to \infty)$

$$Mc_{2n}^{(1)} \to ([ce_{2n}(o,q)]^{-1} \sum_{k=o}^{\infty} (-1)^n A_{2k}^{2n}(q)) (\frac{1}{\pi \sqrt{q} \cosh \xi})^{1/2} \cos(2\sqrt{q} \cosh \xi - \pi/4)$$

$$(5.25)$$

$$Mc_{2n}^{(2)} \to ([ce_{2n}(o,q)]^{-1} \sum_{k=o}^{\infty} (-1)^n A_{2k}^{2n}(q)) (\frac{1}{\pi \sqrt{q} \cosh \xi})^{1/2} \sin(2\sqrt{q} \cosh \xi - \pi/4)$$

$$(5.26)$$

(b) For $\xi \to -\infty (l \to -\infty)$

$$Mc_{2n}^{(1)} \to [ce_{2n}(o,q)]^{-1} \sum_{k=o}^{\infty} (-1)^n A_{2k}^{2n}(q) (\frac{1}{\pi \sqrt{q} \cosh \xi})^{1/2} \cos(2\sqrt{q} \cosh \xi - \pi/4)$$

$$(5.27)$$

$$Mc_{2n}^{(2)} \to [cc_{2n}(o,q)]^{-1} \sum_{k=o}^{\infty} (-1)^n A_{2k}^{2n}(q) \left(\frac{1}{\pi\sqrt{q}\cosh\xi}\right)^{1/2}$$

$$[-\sin(2\sqrt{q}\cosh\xi - \pi/4) - 2f_{e,2n}\cos(2\sqrt{q}\cosh\xi - \pi/4] \qquad (5.28)$$

where ce_{2n} is the ordinary Mathieu function evaluated at $\xi = 0$ and

$$f_{e,2n} = -Mc_{2n}^{(2)}(o,q)/Mc_{2n}^{(1)}(o,q) \qquad (5.29)$$

$f_{e,2n}$ are known as the joining factors and are tabulated in [79] and [80]. In obtaining Eq. 5 28, we have used the analytical extension of $Mc_{2n}^{(2)}$ to $\xi < 0$ (see Appendix I for details).

A remark about the allowed values of (a,q) or $\omega^2 b_o^2$ is in order now. We note that solutions to the l equations are possible only for certain ranges (bands) of energies of the scalar wave The edges of the bands lie on the characteristic curves and therefore correspond to integral order solutions. The region within the curves a_i and b_{i+1} lying on $a + 2q = m^2$ but excluding the end points corresponds to fractional order Modified Mathieu functions $Ce_{2n+\beta}, Se_{2n+\beta}$ which can coexist for identical a values $a_{2n+\beta}$. However, while discussing the scattering of scalar waves we shall consider only those values of the energy which lie on the characteristic lines. In other words, we deal with only the integral order Modified Mathieu functions.

In 3+1 dimensions the situation is quite similar. The full solution to the scalar wave equation is now of the form

$$\Phi(t,l,\theta,\phi) = e^{\pm i\omega t} Y_{pm}(\theta,\phi) \begin{cases} A & V_{no}^{(1)}(\xi) + B & V_{no}^{(2)}(\xi) & n & even \\ C & V_{no}^{(1)}(\xi) + D & V_{no}^{(2)}(\xi) & n & odd \end{cases} \qquad (5.30)$$

We have written both sets of solutions (i.e for n odd and n even) using the same symbols $V_{no}^{(1)}$, $V_{no}^{(2)}$. It should be noted, however, that the functional series representations for n odd and n even are not entirely identical.

In this case also we have a constraint on the allowed values of λ_{on} (this is the condition $\lambda_{on} = -k^2 + p(p+1)$). Therefore, we have to draw the lines $\lambda_{on} = -k^2 + p(p+1)$ on the $\lambda_{on} - k^2$ plot for the characteristic curves (Fig I2). Each value of p gives a certain straight line which cuts the $n = 0, 1, ..$ curves at specific points. These points denote the specific values of k^2 at which we have the solutions $V_{on}^{(1)}$ and $V_{on}^{(2)}$.

The asymptotic forms for $V_{on}^{(1)}$ and $V_{on}^{(2)}$ can be written down from ref [81]. These are as follows. For $\xi \to -\infty$ we use the fact that $V_{on}^{(2)}$ is neither even nor odd and define joining factors by which we analytically extend the solutions to the $\xi < 0$ region.

The asymptotic forms for $\xi \to +\infty$

$$V_{no}^{(1)}(\xi) \to \frac{q_{no}}{k\xi} \sin k\xi \qquad n \quad even \tag{5.31}$$

$$V_{no}^{(1)}(\xi) \to -\frac{iq_{no}}{k\xi} \cos k\xi \qquad n \quad odd \tag{5.32}$$

$$V_{no}^{(2)}(\xi) \to -\frac{q_{no}}{k\xi} \cos k\xi \qquad n \quad even \tag{5.33}$$

$$V_{no}^{(2)}(\xi) \to -\frac{iq_{no}}{k\xi} \sin k\xi \qquad n \quad odd \tag{5.34}$$

while those for $\xi \to -\infty$ are

$$V_{no}^{(1)}(\xi) \to \frac{q_{no}}{k\xi} \sin k\xi \qquad n \quad even \tag{5.35}$$

$$V_{no}^{(1)}(\xi) \to \frac{iq_{no}}{k\xi} \cos k\xi \qquad n \quad odd \tag{5.36}$$

$$V_{no}^{(2)}(\xi) \to -\frac{q_{no}}{k\xi} \cos k\xi - 2h_{e,n}\frac{q_{no}}{k\xi} \sin k\xi \qquad n \quad even \tag{5.37}$$

$$V_{no}^{(2)}(\xi) \to -\frac{iq_{no}}{k\xi} \sin k\xi - 2ic_{e,n}\frac{q_{no}}{k\xi} \cos k\xi \qquad n \quad odd \tag{5.38}$$

where

$$h_{e,n} = -\frac{V_{no}^{(2)}(0)}{V_{no}^{(1)}(0)}, \qquad c_{e,n} = \frac{V_{no}^{(2)}(0)}{V_{no}^{(1)}(0)} \tag{5.39}$$

and q_{no} are constants the exact forms of which are irrelevant for our purpose.

We now have all the essential material to analytically study the scattering problem in both 2+1 and 3+1 dimensions for $n = 2$. It will be shown that the reflection and transmission coefficients depend on the 'joining factors'. In 3+1 dimensions, we are unaware of the existence of fractional order solutions, stability zones and associated characteristics similar to the 2+1 dimensional case. Furthermore, the 'joining factors' for $3 + 1$ dimensions are not tabulated as they are for $2 + 1$ dimensions.

5.3   Scattering ,Reflection and Transmission Coefficients for the n=2 Case

In order to deal with the scattering of scalar waves it is necessary to go back to the equivalent one dimensional Schrodinger equations derived from the original l coordinate equation . The relationship between the functions $L(l)$ and $g(l)$ has been stated earlier. The solution $L(\xi)$ can be written in terms of 'l' using the inverse relationship $\xi = \sinh^{-1}(l/b_o)$. The two linearly independent solutions to the Schrodinger equations are therefore given as

$$g^{(i)}(l) = (b_0^2 + l^2)^{1/4} Mc_{2n}^{(i)}(\xi, q) \tag{5.40}$$

where i takes the values 1 and 2. In the previous section we had discussed the asymptotic forms of $Mc_{2n}^{(i)}$. The corresponding asymptotic forms for $g^{(i)}(l)$ turn out to be:

$l \to +\infty$

$$g^{(1)}(l) = \frac{2}{\pi\omega}^{1/2} A_1 \cos(\omega l - \pi/4) \tag{5.41}$$

$$g^{(2)}(l) = \frac{2}{\pi\omega}^{1/2} A_1 \sin(\omega l - \pi/4) \tag{5.42}$$

$l \to -\infty$

$$g^{(1)}(l) = \frac{2}{\pi\omega}^{1/2} A_1 \cos(\omega l - \pi/4) \qquad (5.43)$$

$$g^{(2)}(l) = \frac{2}{\pi\omega}^{1/2} A_1[-\sin(\omega l - \pi/4) - 2f_{e,2n}\cos(\omega l - \pi/4)] \qquad (5.44)$$

where

$$A_1 = [ce_{2n}(0,q)]^{-1}(-1)^n \sum_{k=0}^{\infty} A_{2k}^{2n} \qquad (5.45)$$

Now, as $l \to \infty$ we want only a right-moving transmitted wave. The linear combination of interest is therefore given by

$$\lim_{l\to\infty} \left[g^{(1)}(l) + ig^{(2)}(l)\right] = \bar{A}_1 e^{-i\pi/4} e^{i\omega l} \qquad (5.46)$$

where we now have set

$$\bar{A}_1 = A_1(\frac{2}{\pi\omega})^{1/2} \qquad (5.47)$$

At $l \to -\infty$ we have an incident wave and a reflected wave. Thus,

$$\lim_{l\to-\infty} \bar{A}_1 \left[-if_{e,2n}e^{-i\pi/4}e^{-i\omega l} + (1 - if_{e,2n})e^{i\pi/4}e^{i\omega l}\right] \qquad (5.48)$$

Hence the reflection and transmission coefficients are given by

$$R = \frac{-f_{e,2n}}{1 - if_{e,2n}}, \qquad T = \frac{-i}{1 - if_{e,2n}} \qquad (5.49)$$

It is easy to see from Eq. 5.49 that

$$|R|^2 + |T|^2 = 1 \qquad (5.50)$$

A similar analysis can be done for the $Mc_{2n+1}^{(1)}, Mc_{2n+1}^{(2)}$ and the $Ms^{(1)}, Ms^{(2)}$ functions. Thus for certain specific values of the energy (obtained from points common to the characteristic curves and the lines $a + 2q = m^2$ we have the R and T given by Eq. 5.49 . Using the tables given in [79] and [80] we can now evaluate

m	s_m	$f_{e,r}, f_{o,r}$	$|T|^2$
1	2.25 (a_0)	.2867	.9241
2	4.25 (a_1)	.9280	.1753
	18.5 (a_0, b_1)	.0025	.9999
3	7.75 (a_2)	2.099	.1850
	11.25 (b_2)	.3610	.8847
	13.25 (a_1)	.1666	.9730
4	12.00 (a_3)	5.801	.0290
	13.75 (b_3)	2.806	.0994
	18.00 (a_2)	.5272	.7866
	33.75 (a_1, b_2)	.0059	.9999
5	16.75 (a_4)	21.48	.9989
	17.00 (b_4)	18.76	.0022
	25.00 (a_3)	1.105	.4505
	33.00 (b_3)	.1129	.9874
	34.25 (a_2)	.0835	.9931

Table 5.1: Table of analytical values for $|T|^2$ for different m and s_m

the R and T for those values explicitly. A short table of values is given in Table 5.1. The values of $|R|$ there suggest that both 'near perfect' reflection as well as transmission are possible.

In 3+1 dimensions the solution of the scattering problem is similar. We shall only be dealing with the case for which 'n' is even. The relationship between $L(\xi)$ and $F(\xi)$ is given in 5.20 . The asymptotic forms for $F_n^{(1)}(\xi)$ and $F_n^{(2)}(\xi)$ as $\xi \to \pm\infty$ are given below.

$$F_n^{(1)}(\xi) \to \frac{q_{no}}{k} \sin k\xi \tag{5.51}$$

$$F_n^{(2)}(\xi) \to -\frac{q_{no}}{k} \cos k\xi \tag{5.52}$$

The linear combination at $\xi \to \infty$ which gives us a purely right moving transmitted wave is $F_n^{(1)}(\xi) + iF_n^{(2)}(\xi)$. Indeed

$$\lim_{l \to \infty}[F_n^{(1)}(\xi) + iF_n^{(2)}(\xi)] \to \frac{-iq_{no}}{k}e^{ik\xi} \tag{5.53}$$

where q_{no} are constants given in [81].

As in the 2+1 dimensional case, for $\xi \to -\infty$ we will have the joining factors coming into the picture. Therefore,

$$\lim_{l \to -\infty}\frac{iq_{no}}{k}[(1 - ih_{e,n})e^{ik\xi} + ih_{e,n}e^{-ik\xi}] \tag{5.54}$$

The reflection and transmission coefficients turn out to be

$$R = \frac{+ih_{e,n}}{1 - ih_{e,n}} \qquad T = \frac{-1}{1 - ih_{e,n}} \tag{5.55}$$

Once again it is clear from 5.58 that $\mid R \mid^2 + \mid T \mid^2 = 1$.

5.4 Reflection and Transmission For the $n > 2$ Cases

For $n = 2$ we have seen that at least for certain values of ω^2 there exist exact solutions with the help of which one can evaluate the reflection and transmission coefficients. Unfortunately analytical solutions are not available for the $n > 2$ cases. We therefore use numerical methods to study reflection and transmission in the $n > 2$ cases. The analytical results for the $n = 2$ case serve as checks on the correctness of the method. Appendix II details the method briefly.

The most striking feature of the transmittivity for $n > 2$ is a series of resonances which become progressively weak as we increase the energy to higher and higher values. The positions of the resonances depend on the value of m^2 (in $2 + 1$ dimensions) and $p(p + 1)$ (in $3 + 1$ dimensions). For a fixed m or p one notices that the

88

resonances become more and more prominent with increasing n. Since n characterizes the geometry we can say that the resonances are signatures of wormhole–like features. The more the wormhole resembles an uniform tunnel which rapidly opens out into flat space , the larger is the depth of the resonance. It should also be mentioned that with increasing m or p but with n fixed the resonances become more and more prominent.This feature is related to the increase in the barrier height with increasing m or p.All of these features are best captured in terms of the transmittivity plots.Figs 5.7,5.8 and Figs 5.9,5.10are the plots for $|T|^2$ versus $\omega^2 b_0^2$ for the various cases mentioned above–i.e n constant,m varying;n varying,m constant; n constant,p varying;n varying,p constant respectively.

5.5   Concluding Remarks

(i) The primary motivation of this Chapter has been to use scalar waves as a method of studying the properties of wormholes. To this end we have solved exactly the massless Klein-Gordon equation in one specific wormhole background(the $n = 2$ case) both in $2 + 1$ and $3 + 1$ dimensions. The plots of the effective potentials arising out of the radial equations reveal that these are barrier type potentials. Hence we have been able to study analytically the reflection and transmission of incident circular and spherical waves. In 2+1 dimensions, the solutions of the Modified Mathieu equation have enabled us to evaluate the reflection coefficient for specific values of the quantity ωb_o. In fact, we have also seen that unless ωb_o lies within certain ranges and satisfies $a + 2q = m^2$ we are unable to write down explicit solutions. For these specific range of values of ωb_o the scattering of scalar waves can be understood using known solutions to the wave equation (which are finite at infinity). The values of $|T|^2$ given in Table 5.1 confirms the physically obvious fact that for higher values of $\omega(b_o$ fixed) the transmission exceeds reflection. The
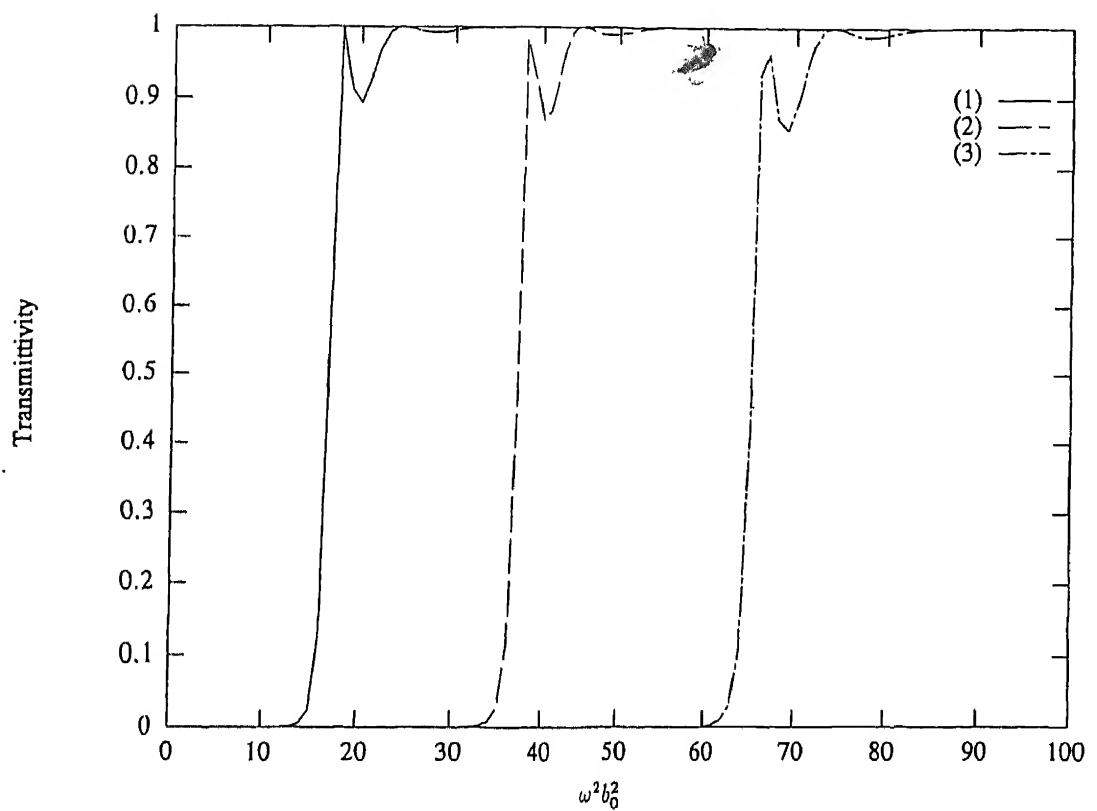
Figure 5.7: $|T|^2$ for $n = 8$ and (1) $m = 4$ (2) $m = 6$ (3) $m = 8$
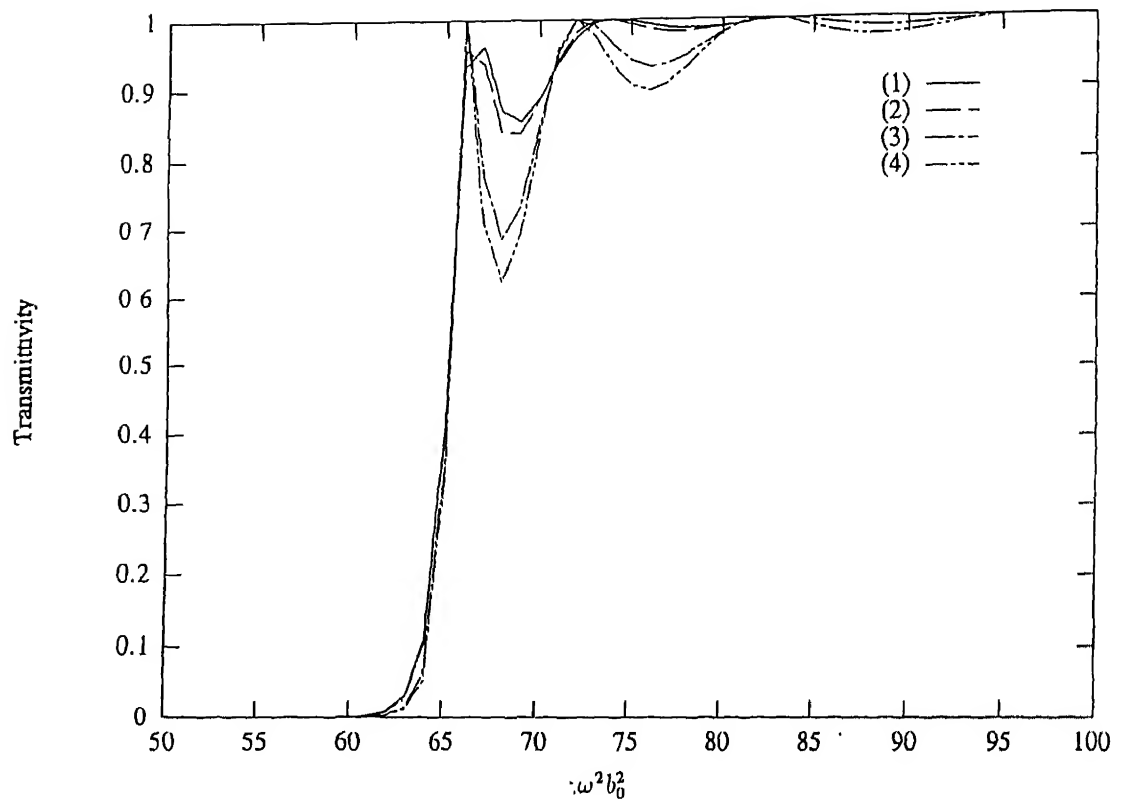
Figure 5.8: $|T|^2$ for $m = 8$ and (1) $n = 8$ (2) $n = 10$ (3) $n = 20$ (4) $n = 40$
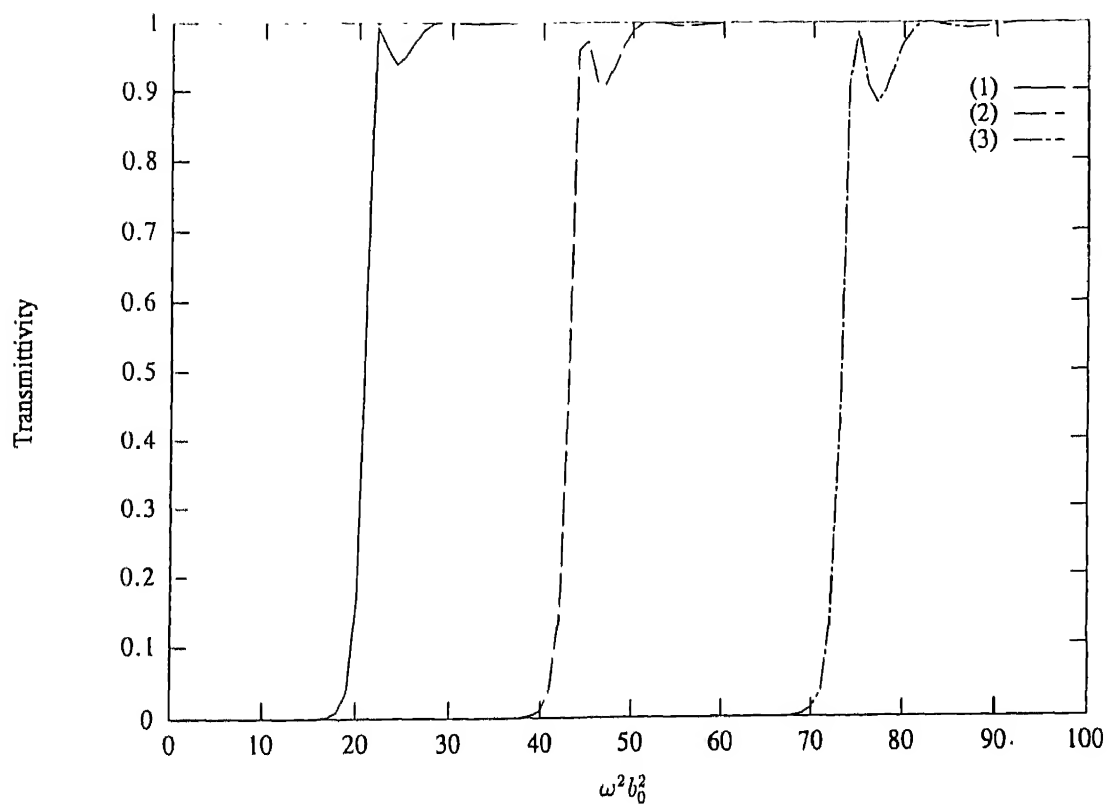
Figure 5.9: $|T|^2$ for $n = 8$ and (1) $p = 4$ (2) $p = 6$ (3) $p = 8$
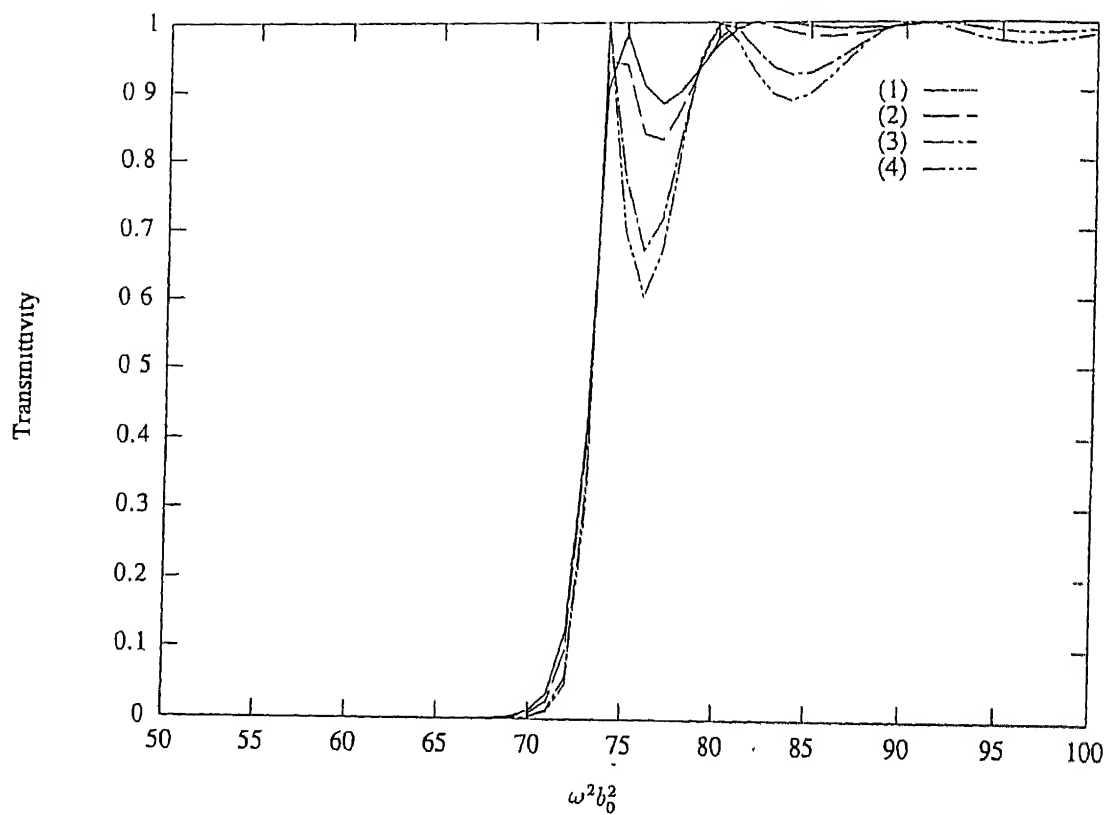
Figure 5.10: $|T|^2$ for $p = 8$ and (1) $n = 8$ (2) $n = 10$ (3) $n = 20$ (4) $n = 40$

opposite happens for lower values of ω. For ωb_o outside the regions between a_i and b_{i+1}, explicit solutions are not known and we are unable to analyse the problem. A similar situation also exists in $3 + 1$ dimensions.

It is important to note the differences between our analysis and the one due to Clement [32]. Clement's basic motivation was to demonstrate the fact that the wormhole's mouth is a 'particle-like' object. In order to do that, he used the scattering of scalar and electromagnetic waves as probes. By analyzing the 'phase-shifts' due to the scattering of incident plane waves he arrived at certain interesting conclusions supporting the conjecture that wormholes are in fact like 'particles'. His work is important in the context of the Wheeler-Misner concept of visualizing classical physics as manifest in just the geometry of spacetime. The context in which wormholes are discussed in recent times are however somewhat different.

(ii) From a purely geometrical viewpoint wormholes are characterized by their shapes in embedding space. These shapes are given by the cross sectional uniformity of the neck in the neighbourhood of the throat, (i.e., for $l \leq b_o$) and also by the rapidity with which the necks eventually turn into flat space. A one parameter generalisation of the standard Ellis geometry(outlined in Chapter 3)has been used to define a class of shapes in embedding space.

It is intuitive that such shapes would lead to interesting effects in the scattering of waves, provided the wavelength is comparable to the throat size. We have found that different shapes translate into specific $1D$ potentials for the radial propagation of waves through the necks. The more uniform the neck, the more uniform (i.e., flatter) the associated potential barrier. A rapid transition of the neck into flat space leads to a spike in the potential, and hence to the possibility of bound states/standing waves. The more rapid the transition the faster the drop in the potential, and the sharper the accompanying spike. Far away from the neck the propagation is of course free and the potentials fall off to zero.

With potentials of this sort, elementary quantum mechanics tell us that the transmission coefficient will exhibit a series of resonances which become less and less prominent as the energy of the wave increases. Angular momentum contributes a centrifugal term to the effective potential which is always repulsive and hence pushes up the height of the barrier. We have explicitly shown that such resonances exist for the class of representative potentials.

As for what all this means for actual wormholes, it is premature to have strong prejudices about the size and shape of these hypothesized objects. However, the above discussion indicates that for wormholes with throat-sizes in the km range, radio-waves coming through would display resonances. The position of these resonances, in what would appear to us as the emission spectra of the objects, would give an indication of throat size, whereas the depth would give an idea of its shape.

For wormholes much larger (i.e. for $b_o/\lambda \rightarrow \infty$) resonances in the emission spectra will be less prominent and will hence give less information. However, in this case the wormhole would represent a large region with a non-trivial gravitational field, which is likely to produce lensing and other effects. These could help in identifying these objects.

(iii) One can also visualize the reflection and transmission of scalar waves in the following alternative way. The wormhole has two asymptotic regions ($l \rightarrow \infty, l \rightarrow -\infty$). Suppose we have an observer in the $l \rightarrow -\infty$ region. He sees a certain wave being sent in through the throat. As he is totally unaware of the existence of another asymptotic region he can think that the incident wave is in a sense partially 'absorbed' and partially reflected. In fact, he can, in principle, use his intellectual abilities to predict that he is in a wormhole geometry and not just in flat space. The existence of a 'tunnel' to the 'other universe' is a primary cause of certain characteristic properties of the reflection and transmission of scalar waves.

(iv) The obvious question that one can ask is 'What happens if we send in

a massive scalar wave?' The answer to this is almost trivial. If one replaces ω^2 by $\omega^2 + m^2 = \omega'^2$ one can repeat the analysis given for the massless case without any further modifications. The parameter a q will have their values in terms of ω'^2. Hence the possible values of ωb_o will change when viewed relative to the massless case. In 3+1 dimensions a similar situation arises. The complete study of 'perturbation' of a wormhole geometry would actually require understanding the 'reflection' and 'transmission' of 'electromagnetic waves' as well as 'spin-half' waves (The Dirac Equations) as well as the problem of general gravitational perturbations.

(v)   Finally, we mention the following analogy. The fact that the geometry for the $n = 2$ case has a 'catenoidal' spacelike section when embedded in R^3 implies that it is a 'minimal surface' (a surface of zero mean curvature). Such surfaces occur when one studies soap films formed between rings. Thus, our study of scalar waves is in principle a study of the vibrational modes of the soap film modulo the fact that appropriate boundary conditions have to be employed for the latter. Using exactly the same analysis (for the $2 + 1$ case) one can actually comment on the stability of such films.

Chapter 6

Lorentzian Wormholes in Higher Dimensional and Higher Order Theories

The results in the earlier chapters are primarily on four dimensional geometries.Moreover , it has been assumed that GR is the theory that explains gravity.The worrisome feature of the matter that threads a wormhole has led people to investigate the status of the WEC as well as the specific characteristics of wormhole geometries in alternative theories of gravity. Hochberg [35],Ghoruku and Soma [38] have discussed such solutions in the context of $\mathcal{R} + \mathcal{R}^2$ theories in four-dimensions. Moffat [36] has recently shown that the violation of WEC persists in his non-symmetric theory of gravitation.

In this Chapter, we first discuss static Lorentzian wormholes in the Einstein-Gauss-Bonnet (EGB) theory of gravity. The action for this theory consists of the usual Einstein-Hilbert term plus the Gauss-Bonnet(GB) combination. In four-dimensions the EGB theory reduces to general relativity . This is because the GB combination reduces to a pure divergence in four-dimensions by virtue of the

Bach identity. Spherically symmetric black hole and cosmological solutions of the field equations of EGB theory have been discussed in detail by various authors [89,90]. Higher dimensional Euclidean wormholes in this theory have been studied by Gonsalez-Diaz [96], and Jianjun and Sicong [95]. Our focus here is on Lorentzian wormholes. We shall use dimensionally extended versions of the metric ansatz and the stress-energy tensor used by Morris and Thorne [14]. The presence of extra dimensions as well as the GB combination leads to the existence of a wide class of solutions. The WEC is violated at least at the throat except for the case in which the coupling coefficient for the GB combination is negative and satisfies a certain inequality containing the wormhole shape function. Unfortunately, even in this case the normalcy of matter persists only upto a certain point beyond which WEC violation sets in.

Since evolving wormholes have been found to have desirable features in four dimensions, it is of interest to discuss their properties in the context of EGB theory and $D > 4$ GR as well. In the first part of the second section we discuss the case without extra compact dimensions. The second part contains a model with extra, contracting ,compact dimensions present in an otherwise inflating wormhole geometry.

6.1   The Field Equations for EGB Theory

The action integral for EGB theory is given as

$$I = \int d^D x \sqrt{-g} [\kappa \mathcal{R} + \alpha (\mathcal{R}_{\mu\nu\rho\sigma} \mathcal{R}^{\mu\nu\rho\sigma} - 4\mathcal{R}_{\mu\nu} \mathcal{R}^{\mu\nu} + \mathcal{R}^2)] + I_{matter} \qquad (6.1)$$

where D is the dimensionality of spacetime and $\kappa > 0$. Henceforth, we choose to work in units $c = \kappa = 1$. The field equations which follow from such an action are

given as

$$
\begin{aligned}
T_{\mu\nu} &= \kappa \left[\mathcal{R}_{\mu\nu} - \frac{1}{2} g_{\mu\nu} \mathcal{R} \right] - \alpha \left[\frac{1}{2} g_{\mu\nu} \left(\mathcal{R}_{\alpha\beta\gamma\delta} \mathcal{R}^{\alpha\beta\gamma\delta} - 4 \mathcal{R}_{\alpha\beta} \mathcal{R}^{\alpha\beta} + \mathcal{R}^2 \right) \right. \\
&\left. - 2 \mathcal{R} \mathcal{R}_{\mu\nu} + 4 \mathcal{R}_{\mu\alpha} \mathcal{R}^{\alpha}{}_{\nu} + 4 \mathcal{R}_{\alpha\beta} \mathcal{R}^{\alpha}{}_{\mu}{}^{\beta}{}_{\nu} - 2 \mathcal{R}_{\mu\alpha\beta\gamma} \mathcal{R}_{\nu}{}^{\alpha\beta\gamma} \right]
\end{aligned}
\tag{6.2}
$$

The α which appears above as the coupling coefficient of the GB combination is positive as long as we consider EGB theory as the low frequency limit of superstring theory [92,93,94] . It is important to note that if EGB theory is assumed as a theory in its own right (it is in fact the first order correction to general relativity as pointed out by Lovelock[88]) there is no restriction on the sign of α. We shall take α with values in various ranges and derive the consequences. A similar stand regarding α has been taken by Wiltshire [90] and Wheeler [89] while discussing the spherically symmetric and cosmological solutions of EGB theory.

Our metric ansatz is that of Morris and Thorne , except that the 2-sphere is replaced by a $(D-2)$-sphere. It is given as

$$
ds^2 = -e^{2\Phi(r)} dt^2 + \frac{dr^2}{1 - \frac{b(r)}{r}} + r^2 d\Omega_{D-2}^2
\tag{6.3}
$$

Here $\Phi(r)$ and $b(r)$ are the same as mentioned in the earlier chapters. $d\Omega_{D-2}^2$ is the metric on the surface of a $(D-2)$-sphere.

We can write Eq 6.3 in the proper orthonormal basis as

$$
ds^2 = -e^0 \otimes e^0 + e^1 \otimes e^1 + \sum_{i=2}^{D-1} e^i \otimes e^i
\tag{6.4}
$$

where the basis 1-forms are

$$
e^0 = e^{\Phi} dt
\tag{6.5}
$$

$$
e^1 = \frac{dr}{\sqrt{1 - \frac{b(r)}{r}}}
\tag{6.6}
$$

$$
e^2 = r d\theta_2
\tag{6.7}
$$

$$
e^i = r \sin\theta_2 \cdots \sin\theta_{i-1} \, d\theta_i
\tag{6.8}
$$

$$e^{D-1} = r \sin \theta_2 \cdots \sin \theta_{D-2} \, d\theta_{D-1} \tag{6.9}$$

In our notation, there is no θ_1. The angular coordinates are denoted by θ_i, where $i = 2, 3, \ldots, D - 1$.

Using the Cartan equations of structure we can derive the curvature 2-forms :

$$\mathcal{R}^0{}_1 = M e^0 \wedge e^1 \tag{6.10}$$

$$\mathcal{R}^0{}_i = N e^0 \wedge e^i \tag{6.11}$$

$$\mathcal{R}^1{}_i = P e^1 \wedge e^i \tag{6.12}$$

$$\mathcal{R}^i{}_j = Q e^i \wedge e^j \tag{6.13}$$

For any fixed i, j can have values $i < j \leq (D - 1)$. M, N, P, Q are

$$M = \left(1 - \frac{b}{r}\right) \left[-\Phi'' - \Phi'^2 + \frac{\Phi'(b'r - b)}{2r(r - b)} \right] \tag{6.14}$$

$$N = -\frac{\Phi'}{r}\left(1 - \frac{b}{r}\right) \tag{6.15}$$

$$P = \frac{1}{2r^3}(b'r - b) \tag{6.16}$$

$$Q = \frac{b}{r^3} \tag{6.17}$$

where a prime denotes differentiation with respect to r. From these curvature 2-forms all components of the full Riemann-Christoffel curvature tensor and hence the Ricci tensor and the Ricci scalar can be derived.

The stress-energy tensor in the static observer's frame is given as

$$T_{00} = \rho(r), \quad T_{11} = \tau(r), \quad T_{ij} = p(r)\delta_{ij} \tag{6.18}$$

where $i, j = 2, 3, \ldots, D - 1$.

The field equations turn out to be the following

$$\rho(r) = (D - 2)\left[\left(\frac{D - 3}{2}\right)Q + P\right] + \bar{\alpha}Q(D - 2)\left[\left(\frac{D - 5}{2}\right)Q + 2P\right] \tag{6.19}$$

$$\tau(r) = -(D-2)\left[\left(\frac{D-3}{2}\right)Q + N\right] - \bar{\alpha}Q(D-2)\left[\left(\frac{D-5}{2}\right)Q + 2N\right] \quad (6.20)$$

$$
\begin{aligned}
p(r) = {} & -M - (D-3)N - (D-3)P - \frac{1}{2}(D-3)(D-4)Q \\
& -\frac{1}{2}(D-5)(D-6)\bar{\alpha}Q^2 - 4(D-5)\bar{\alpha}NP - 2(D-5)\bar{\alpha}PQ \\
& -2(D-5)\bar{\alpha}NQ - 2\bar{\alpha}MQ
\end{aligned}
\quad (6.21)
$$

where $\bar{\alpha} = (D-3)(D-4)\alpha$. One can check that for $D = 4$, Eqs.(6.19), (6.20) and (6.21) reduce to the Einstein field equations . For $\alpha = 0$ and $D > 4$ the field equations are those for higher-dimensional general relativity. Also, the vacuum solutions of the field equations give the standard Boulware-Deser black hole spacetime [91].

6.2 The WEC and Some Static Wormhole Solutions

6.2.1 Exoticity of matter near the throat

In four-dimensional general relativity it was shown in [14] that the 'flaring-out condition' near the throat of the wormhole led to the fact that $\rho_0 + \tau_0 < 0$ where τ_0 and ρ_0 are the values of τ and ρ near the throat which led to WEC violation. From the field equations for EGB theory we get the following expression for $(\rho + \tau)$,

$$\rho + \tau = (D-2)[1 + 2\bar{\alpha}Q][P - N] \quad (6.22)$$

The essential difference between the expression for $\rho + \tau$ in four-dimensional GR and the one for EGB theory is the presence of two extra factors, $(D - 2)$ and $[1 + 2\bar{\alpha}Q]$. The former originates from the dimensionality of the spacetime and the latter from features specific to the EGB theory. The factor $[P - N]$ is exactly

identical to the expression for $\rho + \tau$ in GR. We examine $(\rho + \tau)$ near the throat. This leads to

$$\rho_0 + \tau_0 = (D-2)\left[1 + \frac{2\bar{\alpha}}{b_0{}^2}\right][P-N]_{r=b=b_0} \qquad (6.23)$$

Now $[P-N]_{r=b=b_0} < 0$. Thus, for an EGB wormhole, matter near the throat is exotic or normal according as the quantity $(1 + 2\bar{\alpha}/b_0{}^2)$ is positive or negative respectively . The above-stated conditions can be thought of as constraints on b_0 or α. We prefer to choose α and let this choice determine b_0. If $\alpha > 0$, the quantity $(1 + 2\bar{\alpha}/b_0^2)$ is always positive and WEC is violated near the throat. Also, the mere fact that $(1 + 2\bar{\alpha}/b_0^2) > 0$ does not imply any lower bound on b_0. For α negative, the quantity $(1 - 2|\bar{\alpha}|/b_0^2)$ can be positive or negative. If it is positive then $b_0 > (2|\bar{\alpha}|)^{1/2}$. Otherwise, $b_0 < (2|\bar{\alpha}|)^{1/2}$. Thus, matter can be normal near the throat but, as will be shown below, other constraints forbid the existence of a solution with normal matter everywhere.

The next obvious question to ask is whether it is possible to obtain solutions in EGB theory for which matter is exotic or normal everywhere. One can also investigate the possibility of having solutions with exotic or normal matter confined to a small region in the vicinity of the throat. In the following subsections these situations are discussed.

6.2.2 Solutions with $\alpha > 0$ and $\rho > 0, \rho + \tau < 0$, $\Phi = 0$

From expression 6.20 we notice that if $\alpha > 0$, $\Phi = 0$, then $\tau < 0$ everywhere. This implies that $b' < b/r$ everywhere. Eq.6.19, after some rearrangements, reduces to

$$\rho(r) = (D-2)\frac{X}{2r^3} + (D-2)\bar{\alpha}b(r)\frac{Y}{2r^6} \qquad (6.24)$$

where

$$X = (D-4)b + b'r \qquad (6.25)$$

$$Y = (D-7)b + 2b'r \qquad (6.26)$$

Thus, $\rho(r)$ can be greater than zero, if any of the following hold

(A) $X = 0$, $Y > 0$,

(B) $X < 0$, $Y > 0$; $|X| < \bar{a}bY/r^3$,

(C) $X > 0$, $Y = 0$,

(D) $X > 0$, $Y > 0$,

(E) $X > 0$, $Y < 0$; $X > \bar{a}b|Y|/r^3$

An acceptable zero-tidal force wormhole solution in this case thus has to obey the condition $b' < b/r$, the general constraints for having a wormhole and any one of the above conditions which lead to $\rho > 0$. For the cases (A) and (B) a little amount of analysis will show that we require $D < 1$ for $\rho > 0$, which is impossible. We shall study the remaining three cases below. Our strategy is to begin with the validity of the $\rho > 0$ condition. Then we examine the proposed solutions for the other constraints.

Case(C): In this case $Y = 0$ leads to the differential equation

$$b' = -\frac{(D-7)}{2}\frac{b}{r} \tag{6.27}$$

The unique wormhole solution is

$$b(r) = b_0{}^{(D-5)/2} r^{-(D-7)/2} \tag{6.28}$$

The solution in $D = 5$ is ruled out since it does not satisfy $\frac{b(r)}{r} < 1$ for $r > b_0$

Case(D): The conditions on X and Y give the following inequality

$$b' > -\frac{(D-7)}{2}\frac{b}{r} \tag{6.29}$$

In five-dimensions this becomes $b' > b/r$, whereas $\tau > \rho$ led to $b' < b/r$. Thus, in five-dimensions this kind of solutions are ruled out. For $D \geq 6$ a large variety of solutions are possible. Some examples are:

Power law solution

$$b(r) = b_0{}^{m/D} r^{1-m/D}; \quad 0 < m < \frac{D(D-5)}{2} \tag{6.30}$$

Logarithmic solution

$$b(r) = \frac{r}{\ln r} \ln b_0; \quad b_0 > e^{2/(D-5)} \tag{6.31}$$

Hyperbolic solution

$$b(r) = \frac{b_0}{\tanh b_0} \tanh r. \tag{6.32}$$

However, this solution is valid only for $D \geq 7$. For $D = 6$ it is valid only if $\sinh 2r < 4r$. This implies limiting the range of r upto a certain value r_0. Consequently, no solution is possible with exotic matter everywhere.

Case (E): The conditions $X > 0$ and $Y < 0$ implies

$$-(\frac{D-7}{2}) > \frac{b'r}{b} > -(D-4). \tag{6.33}$$

An example of a solution obeying all conditions is

$$b(r) = b_0{}^{m/D} r^{1-m/D} \tag{6.34}$$

where m is always positive and takes values such that

$$\frac{D(D-5)}{2} < m < D(D-3) \tag{6.35}$$

However the inequality between X and Y leads to

$$b_0 > (12\alpha \frac{m}{2D-m})^{1/2} \tag{6.36}$$

which requires $m < 2D$. This new constraint on m along with Eq.6.35 restricts D such that $4 < D < 9$. The throat radius b_0 is constrained to have a minimum value dependent on α, m and D. The presence of both the GB combination as well as the extra dimensions is visible quite clearly here.

6.2.3 Solutions with $\rho > 0, \rho + \tau < 0$, $\Phi = 0$ and $\alpha < 0$, $(1 + 2Q\bar{\alpha}) > 0$

In this subsection, we look for wormhole solutions with exotic matter everywhere but with $\alpha < 0$. The condition $\tau > \rho$ near the throat implies

$$b_0 > (2|\bar{\alpha}|)^{1/2} \qquad (6.37)$$

For general values of r, $b(r)$ should be such that $b(r) < r^3/(2|\bar{\alpha}|)$.

Just as in the previous section, the solutions in the present case should also satisfy the condition $b' < b/r$ and all the four general constraints. Also, to ensure the positivity of ρ, any one of the following five sets of conditions on X and Y should be satisfied.

(A) $X = 0, \quad Y < 0,$

(B) $X < 0, \quad Y < 0; \quad |X| < b|\bar{\alpha}||Y|/r^3,$

(C) $X > 0, \quad Y = 0,$

(D) $X > 0, \quad Y > 0; \quad X > b|\bar{\alpha}|Y/r^3,$

(E) $X > 0, \quad Y < 0.$

Case(A): In this case, it can be shown that the unique wormhole solution has the form

$$b(r) = b_0{}^{D-3} r^{-(D-4)}. \qquad (6.38)$$

Moreover, as stated above, the throat radius b_0 has a lower limit given by Eq. 6.37 .

Case(B): The extra inequality relation between X and Y along with the conditions $b'r/b < 1$ and $b/r < 1$ lead to the fact that the domain of r is not $[b_0, \infty)$ but $[b_0, r_0)$. Thus, there exists in all cases an upper bound for r. This implies the nonexistence of solutions with matter exotic everywhere.

Case(C): Except for the existence of a lower bound for b_0 , this case is similar to the case (C) of subsection 6.2.2. The solution is given by Eq.6.28 and is valid for $D \geq 6$.

Case(D): This case bears a similarity to the case(D) of 6.2.2. No solution is possible for $D = 5$. All solutions mentioned there for $D \geq 6$ are applicable here. However, there will always be a lower bound on b_0. For every solution we have to choose the appropriate lower bound by comparing Eq.6.37 and the extra inequality relation between X and Y. For example, in the power law solution Eq. 6.30, we have to choose between Eq.6.37 and the inequality

$$b_0 > \left[\mid \alpha \mid \frac{D - 5 - 2m/D}{D - 3 - m/D} \right]^{1/2}. \qquad (6.39)$$

Since the R.H.S. of Eq.6.37 is greater than that of Eq.6.39, the former will give the lower limit for b_0.

Case(E): The only difference between this case and (E) of 6.2.2 is that the lower limit on b_0 here is determined by Eq.6.37. Due to this reason, the power law solution does not have the extra restriction $m < 2D$. It is therefore valid for all $D > 4$.

6.2.4 Solutions with $\rho + \tau > 0$ and $\rho > 0$

It is not possible to have wormhole solutions of the EGB field equations with normal matter everywhere. To have $\rho + \tau > 0$, we need

$$b(r) > \frac{r^3}{2 \mid \bar{\alpha} \mid}. \qquad (6.40)$$

This, together with the fact that $b/r < 1$, implies that any solution obtained in this case will be valid only upto a certain value of r, i.e., $r < (2 \mid \bar{\alpha} \mid)^{1/2}$. A way out of this may be the following. Consider a solution with normal matter extended from the throat radius upto a certain radius r_c so that $b_0 < r_c < (2 \mid \bar{\alpha} \mid)^{1/2}$. At $r = r_c$ join the solution to the vacuum Boulware-Deser spacetime across a surface layer. However, this requires an extension of the Junction-Condition formalism of GR to EGB theory.

6.2.5 Solutions with exotic matter limited to the throat

We can also have solutions with $\rho + \tau < 0$, $\alpha > 0$ such that the exotic matter is limited to the throat region. Following [14], we assume $r_a = b_o + \Delta r$, where Δr is the region of extension of exotic matter near the throat. To get a significant flaring-out(of about 45 degrees) from the throat, we need to have dz/dr at $r = r_a$ is very near to 1, where $z(r)$ describes the $t = $ constant, $\theta = \pi/2$ section of the wormhole spacetime embedded in R^3. This leads to $b' < 0$, once $\Delta r \ll b_0$. It is not possible to have $\rho > 0$, $b' < 0$ and $\Delta r \ll b_0$ simultaneously in four-dimensional GR. Let us consider the corresponding situation in EGB theory for the case $X > 0$, $Y > 0$ and $\alpha > 0$. We require

$$\frac{\mid b' \mid r}{b} < \frac{1}{2}(D - 7) \tag{6.41}$$

to have $\rho > 0$, with $b' < 0$. Combining this with

$$\frac{\Delta r}{b_0}(1 + \mid b' \mid) = 1 \tag{6.42}$$

we get

$$\Delta r > \frac{2}{D - 5}b_0 \tag{6.43}$$

Thus, for $D > 7$, $\Delta r/b_0 < 1$ is not a contradiction. For higher dimensions, we see that $\frac{\Delta r}{b_0}$ becomes progressively smaller. The eventuality mentioned above is possible not only in EGB theory but also in D-dimensional GR, where we have

$$\Delta r > \frac{1}{D - 4}b_0 \tag{6.44}$$

6.3 Evolving Wormholes

6.3.1 $D > 4$ GR and EGB Theory(Without Compact Dimensions)

In $D > 4$ GR the consequence of adding an extra time–dependent conformal factor $\Omega^2(t)$ in the metric given in Eq 6.3 is not too dramatic. The WEC inequalities now contain extra dimensional factors. The form of $F(t)$ remains as in $D = 4$ GR and with $F(t) > 0$ one can easily construct higher dimensional geometries with the throat radii related to the maximum of $[F(t)]^{-1}$ through similar inequalities.

However, in EGB theory , the WEC inequalities are much more complicated. After some amount of algebra one obtains the following set of relations:

$$\rho \geq 0 \Rightarrow (D-2)\left[N_e + \frac{D-3}{2}P_e\right] + \bar{\alpha}P_e(D-2)\left[\frac{D-5}{2}P_e + 2N_e\right] \geq 0 \quad (6.45)$$

$$\rho + \tau \geq 0 \Rightarrow (N_e + M_e)(D-2)[1 + 2\bar{\alpha}P_e] \geq 0 \quad (6.46)$$

$$\begin{aligned} \rho + p \geq 0 \quad \Rightarrow \quad &(D-2)M_e + N_e + (D-3)P_e + \bar{\alpha}\left[4M_eN_e\right. \\ &+ \quad 2(D-4)M_eP_e + 2(D-5)P_e^2 + 6N_eP_e\right] \geq 0 \end{aligned} \quad (6.47)$$

where M_e , N_e and P_e are given as

$$M_e = \frac{1}{\Omega^2}\left[\left(\frac{\dot{\Omega}}{\Omega}\right)^2 - \frac{\ddot{\Omega}}{\Omega}\right] \quad (6.48)$$

$$N_e = \frac{1}{\Omega^2}\left[\left(\frac{\dot{\Omega}}{\Omega}\right)^2 + \frac{b'r - b}{2r^3}\right] \quad (6.49)$$

$$P_e = \frac{1}{\Omega^2}\left[\left(\frac{\dot{\Omega}}{\Omega}\right)^2 + \frac{b}{r^3}\right] \quad (6.50)$$

108

It is quite difficult to make any general statement about the violation/ non-violation of the WEC from the above inequalities. However, for $\alpha > 0$ one notices the fact that the requirement $F(t) > 0$ is still necessary. This is clearly seen from the second WEC inequality, wherein the factor $N_e + M_e$ is essentially the same as in $D = 4$ GR. For $\alpha < 0$, the possibility of avoiding the $F(t) > 0$ constraint exists. What can one say about the other two inequalities ? One simple conclusion is the following.If $M_e \geq 0, N_e \geq 0$ then all three inequalities are satisfied.Contrasting this with the case of ordinary GR (where $N_e + M_e \geq 0$ was sufficient) we find that, here, we end up with an extra pair of constraints apart from the usual one.This may or may not affect the conclusions in comparison with identical situations in GR. For example it can be very easily checked that with $\Omega(t) = \exp \omega t$ there is no difference whereas in the case of $\Omega(t) = t^n$ the conclusions change. We shall not analyse evolving wormholes in EGB theory any further.

6.3.2   The Case of Compact Extra Dimensions

IT is well known from the work of Roman [75] and from the analysis presented in Chapter 4 that with an inflationary scale factor one cannot avoid the violation of the WEC even for a finite interval of time . This is indeed somewhat depressing, because if one believes in the existence of wormholes, then one possible way in which they can appear on macroscopic scales is by growing very large during the inflationary epoch. We now demonstrate through an example that with compact extra dimensions (S^2) an inflationary wormhole can exist for a finite interval of time with matter satisfying the WEC.

The assumption for the metric is :

$$ds^2 = -dt^2 + a_1^2(t) \left(\frac{dr^2}{1 - b/r} + r^2 d\Omega_2^2 \right) + a_2^2(t) \left(d\chi^2 + \sin^2 \chi d\xi^2 \right) \qquad (6.51)$$

where $a_1(t)$ and $a_2(t)$ are the scale factors for the wormhole amd the compact

extra dimensions respectively. We assume

$$a_1(t) = e^{\omega t}, \quad a_2(t) = (t_0 - t)^{1/2}, \quad b(r) = b_0 \qquad (6.52)$$

Instead of writing down the Einstein equation in all its glory, we straightaway move on to the WEC inequalities. $\rho, \tau, p_1, p_2, p_3$ and p_4 are the six non–zero diagonal components of the energy momentum tensor. We have essentially four inequalities as $p_1 = p_2$ and $p_3 = p_4$ by symmetry.

$$\rho \geq 0 \Rightarrow 3\omega^2 + \frac{1 - 3\omega}{t_0 - t} + \frac{1}{4(t_0 - t)^2} \geq 0 \qquad (6.53)$$

$$\rho + \tau \geq 0 \Rightarrow -\frac{b_0 e^{-2\omega t}}{r^3} + \frac{2}{(t_0 - t)}\left[-\omega + \frac{1}{2(t_0 - t)} \right] \geq 0 \qquad (6.54)$$

$$\rho + p_1 \geq 0 \Rightarrow \frac{b_0 e^{-2\omega t}}{2r^3} + \frac{2}{(t_0 - t)}\left[-\omega + \frac{1}{2(t_0 - t)} \right] \geq 0 \qquad (6.55)$$

$$\rho + p_3 \geq 0 \Rightarrow -3\omega^2 + \frac{2 - 3\omega}{t_0 - t} + \frac{1}{2(t_0 - t)^2} \geq 0 \qquad (6.56)$$

The quantity reminiscent of the $F(t)$ is the second term in the second and third inequalities. If this term is positive (which is possible if $t > t_0 - \frac{1}{2\omega}$) then the third inequality is satisfied and the second one yields a bound on the allowed domain of b_0. The first inequality is satisfied for all $\omega \leq \frac{1}{3}$ while the fourth one gives another lower bound on t :

$$t \geq t_0 - \frac{\sqrt{(2 - 3\omega)^2 + 24\omega^2} + (2 - 3\omega)}{12\omega^2} \qquad (6.57)$$

Of the two lower bounds on t one has to choose the more stringent one. For instance if $\omega = \frac{1}{3}$ then the first bound gives $t \geq t_0 - 1.5$ and the second one implies $t \geq t_0 - 2.2$ .Thus , if we assume $t \geq t_0 - 1.5$ the other inequality is automatically satisfied. The wormhole can exist for the interval $t_0 - 1.5 < t < t_0$ with matter satisfying the WEC. The bound on the throat radius is:

$$b_0^2 \geq max\left[\frac{e^{-2\omega t}(t_0 - t)^2}{2\omega t - t_0 - 1/2\omega} \right] \qquad (6.58)$$

Thus we have indicated through the above example that an inflationary worm-hole with compact extra dimensions can exist for a finite interval of time with matter satisfying the WEC.

6.4 Conclusions and Remarks

In conclusion, it is important to figure out the distinguishing features of wormholes in EGB theory as compared to the ones in GR. First we deal with the static case.

For $\rho > 0$, $\rho + \tau < 0$ and $\alpha > 0$, an EGB wormhole exists in five-dimensions only in the case in which the throat radius is constrained to have a minimum value dependent on α. There exist solutions which have a minimum throat radius depending on D only (the logarithmic solution). Solutions with b_0 independent of D or α are also there as well; b_0 here can be arbitrary but finite. On the other hand, for $\rho > 0$, $\rho + \tau < 0$ and $\alpha < 0$ with $1 + 2\bar{\alpha}Q > 0$, the solutions are forced to have a throat radius which is bounded below by a quantity dependent on D and α. Finally, if $\rho + \tau > 0$, $\rho > 0$, $\alpha < 0$ and $1 + 2\bar{\alpha}Q < 0$, all solutions are defined only upto a certain value of $r = r_c$. Beyond $r = r_c$, normal matter cannot exist and a possible way out, as suggested earlier, is the type of solutions with normal matter for $b_0 < r < r_c - \epsilon$ and vacuum for $r > r_c - \epsilon$.

It has been shown in EGB theory as well as in D-dimensional GR ($D > 5$) one can limit exotic matter with $\rho > 0$ to an arbitrarily small region. This was not possible in four-dimensional GR.

The status of WEC in EGB theory, however, remains almost the same as it was in GR. For $\alpha > 0$, it is violated; for $\alpha < 0$ it may or may not be violated at the throat depending on whether $(1 + 2\bar{\alpha}Q)$ is greater or less than zero. Even if WEC is not violated at the throat, one cannot construct EGB wormholes with matter normal everywhere.

It would be interesting to explore the possibility of constructing an EGB wormhole with WEC satisfied everywhere. This implies investigating the solution with normal matter confined to the throat and vacuum elsewhere. We do not know whether the matching of the two different types of solutions would be possible at all.

For evolving wormholes our discussion has been brief. The constraints (WEC) for EGB theory are pretty complicated and general statements are not too easily obtained. We have illustrated some special cases which provide insights into the differences between the conclusions of GR and those for EGB theory. With compact dimensions, the fact that the inflationary wormhole can exist for a finite time interval has been proved. Consequences for other choices of scale factors have not been discussed but are certainly not very difficult to obtain.

Appendix I

Modified Mathieu and Radial Oblate Spheroidal Functions

I.1 Modified Mathieu Functions

Several authors have discussed Mathieu and Modified Mathieu functions in great detail [86,87,84,85].In this appendix we collect some of the material relevant for our purpose.

The original equation which Mathieu had studied while investigating the oscillations on an elliptical lake is:

$$\frac{d^2y}{dz^2} + (a - 2q\cos 2z)y = 0 \qquad (I.1)$$

Replacing z by iz we arrive at the Modified Mathieu equation

$$\frac{d^2y}{dz^2} - (a - 2q\cosh 2z)y = 0 \qquad (I.2)$$

We shall not go any further into discussing the solutions of I.1. Rather we shall concentrate on the solutions of I.2. It is worthwhile to mention that I.1 and I.2

appear when the Helmholtz equation $(\nabla^2 + k^2)$ is separated in elliptic-cylindrical coordinates.

Solutions to I.2 are dependent on the values of a and q (or b and s). In fact, the $b - s$ plot shown in Fig.I.1 demonstrates this fact clearly. The solid lines (marked a_o, a_1, b_1 etc.) on this plot are known as the characteristic lines. Values of (a, q) lying on these lines yield solutions to A1.1 known as Mathieu functions of integral order. These are the functions $Mc_{2n}^{(1)}, Mc_{2n+1}^{(1)}, Ms_{2n}^{(1)}, Ms_{2n+1}^{(1)}$ for a values lying on the $a_{2n}, a_{2n+1}, b_{2n}, b_{2n+1}$ curves respectively. These functions can be represented by infinite series in various ways. The most common of these representations are the 'cosh' or 'sinh' series, the Bessel functions series and the one in terms of products of Bessel functions. The first one of these representations is given below.

$$Mc_{2n}^{(1)} = \frac{(-1)^n A_o^{2n}}{ce_{2n}(\pi/2, q)(ce_{2n}(o, q)} \sum_{k=o}^{\infty} A_{2n}^{2k}(q) \cosh 2kz \qquad (I.3)$$

$$Mc_{2n+1}^{(1)} = \frac{(-1)^{n+1} A_1^{2n+1} \sqrt{q}}{ce_{2n}'(\pi/2, q)(ce_{2n+1}(o, q)} \sum_{k=o}^{\infty} A_{2n+1}^{2k+1}(q) \cosh(2k+1)z \qquad (I.4)$$

$$Ms_{2n}^{(1)} = \frac{(-1)^n q B_2^{2n}}{se_{2n}'(o, q) Se_{2n}'(\pi/2, q)} \sum_{k=o}^{\infty} B_{2n}^{2k}(q) \sinh 2kz \qquad (I.5)$$

$$Ms_{2n+1}^{(1)} = \frac{(-1)^{n+1} B_1^{2n+1} \sqrt{q}}{se_{n+1}''(o, q) se_{2n+1}(\pi/2, q)} \sum_{k=o}^{\infty} B_{2n+1}^{2k+1}(q) \sinh(2k+1)z \qquad (I.6)$$

where $ce(z, q)$ and $se(z, q)$ are the basically periodic solutions of the Mathieu equation. The $Mc_{2n}^{(1)}, Mc_{2n+1}^{(1)}, Ms_{2n}^{(1)}, Ms_{2n+1}^{(1)}$ form the 'basically periodic solutions of the Mathieu equation. $Mc_{2n}^{(1)}$ and $Ms_{2n}^{(1)}$ or any such pair cannot coexist for the same values of (a, q). Thus we require a second solution to the Modified Mathieu equation. These second solutions are the $Mc^{(2)}, Ms^{(2)}$ corresponding to $Mc^{(1)}$ and $Ms^{(1)}$ respectively. The $Mc^{(1)}, Ms^{(1)}$ are even and odd solutions respectively. A theorem due to Ince [86] says that the $Mc^{(2)}$ and $Ms^{(2)}$ are functions which are neither even nor odd. The Bessel function series representations are given below.

114
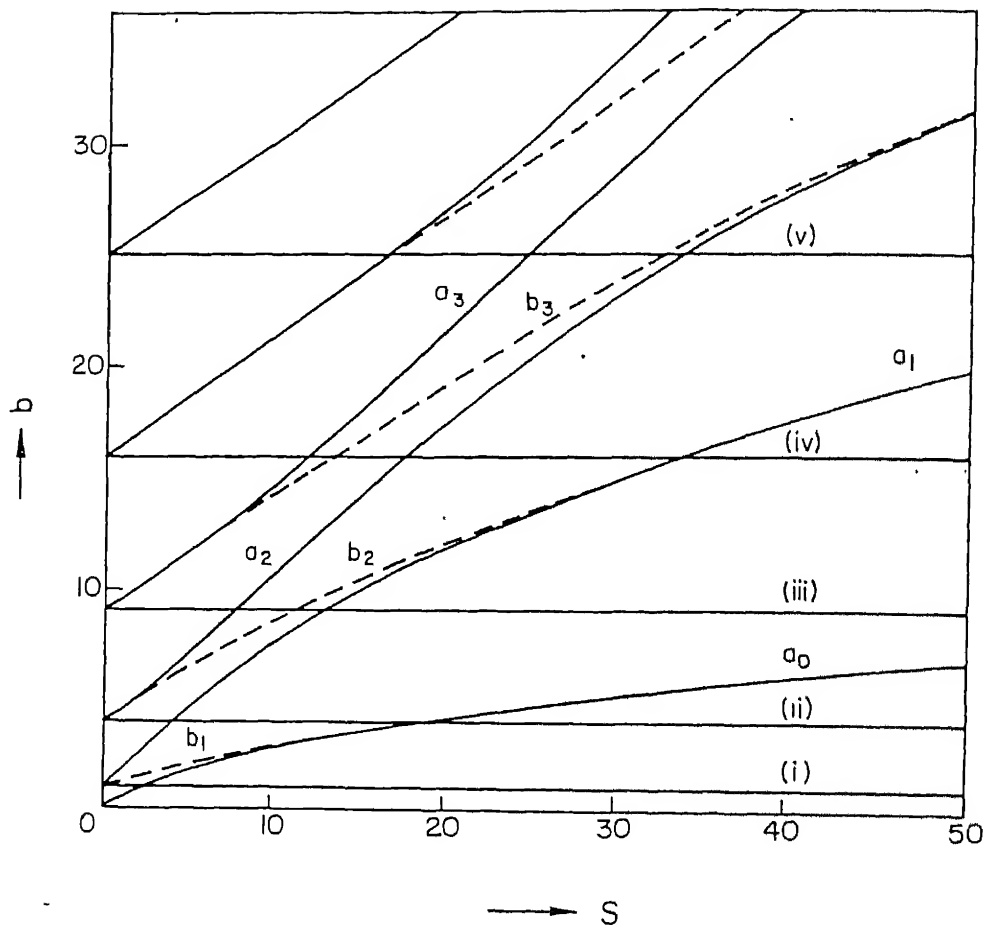
Figure I.1: The b–s plot for the characteristic lines. Here $B = m^2$ and $s = \omega^2 b_0^2$. In relation to a, q we have $a = 4q$ and $a + 2q = m^2$. The regions between the a_i and b_{i+1} curves are the stability regions for the Mathieu functions. (i),(ii),(iii), (iv) and (v) correspond to $m = 1, 2, 3, 4, 5$ respectively(i.e $b = 1, 4, 9, 16, 25$).

The series involving the $'J'$ Bessel functions are valid for all z. On the other hand, the series involving the Neumann (Y Bessel function) functions are valid for $z > 0$. We shall discuss later in this appendix how to analytically continue the $Mc^{(2)}$ or $Ms^{(2)}$ for $z < 0$.

$$Mc_{2n}^{(\imath)} = [ce_{2n}(o,q)]^{-1} \sum_{k=o}^{\infty} (-1)^{k+n} A_{2k}^{2n}(q) Z_{2k}^{(j)}(2\sqrt{q}\cosh z) \qquad (I.7)$$

$$Ms_{2n}^{(\imath)} = [se_{2n}(o,q)]^{-1} \tanh z \sum_{k=1}^{\infty} (-1)^{k+n} 2k B_{2k}^{2n}(q) Z_{2k}^{(j)}(2\sqrt{q}\cosh z) \qquad (I.8)$$

The formulas for a_{2n+1} and b_{2n+1} are exactly identical with $2n \to 2n+1$ and $2k \to 2k+1$. $Z_{2k}^{(j)}$ denotes a 'J' Bessel function for $j = 1$ and aY Bessel function of $j = 2$.

We now move on to the analysis for $z < 0$. This is based on sec 20.6.18 of [80]. Consider two combinations

$$X_1 = Mc_r^{(2)}(z,q) + Mc_r^{(2)}(-z,q) \qquad (I.9)$$

$$X_2 = Ms_r^{(2)}(z,q) - Ms_r^{(2)}(-z,q) \qquad (I.10)$$

X_1 is even and therefore proportional to $Mc_r^{(1)}(z,q)$. X_2 is odd and proportional to $Ms_r^{(1)}(z,q)$. The proportionality factors are evaluated by using the values of the functions at $z = 0$. It turns out that

$$Mc_r^{(2)}(-z,q) = -Mc_r^{(2)}(z,q) - 2f_{e,r} Mc_r^{(2)}(z,q) \qquad (I.11)$$

$$Ms_r^{(2)}(-z,q) = Ms_r^{(2)}(z,q) - 2g_{e,r} Ms_r^{(2)}(z,q) \qquad (I.12)$$

where

$$f_{e,r} = -Mc_r^{(2)}(o,q)/Mc_r^{(1)}(o,q) \qquad (I.13)$$

$$g_{e,r} = \left[\frac{d}{dz}Ms_r^{(2)}(z,q)/\frac{d}{dz}Ms_r^{(1)}(z,q)\right]_{z=0} \qquad (I.14)$$

The asymptotic forms for the function $Mc^{(1)}, Mc^{(2)}, Ms^{(1)}, Ms^{(2)}$ have been discussed earlier and therefore are not repeated here.

Apart from the integral order solutions the Mathieu equation as well as the Modified Mathieu equation has solution of real fractional order. The regions between a_i and b_{i+1} in the plot correspond to the region of stability. Within these regions and away from the characteristic lines we have these fractional order solutions. The functions $Ce_{2n+\beta}$ and $Se_{2n+\beta}$ are not basically periodic and can coexist for the same value of $a_{2n+\beta}$.

I.2 The Radial Oblate Spheroidal Functions

If we separate the Helmholtz equation in oblate spheroidal coordinates (see Pg 752-753 of [80]) the radial equation has the form given in Eq.5.21-22. However, we are concerned with only the $m = 0$ case i.e. the functions V_{on}. Once again as in the Mathieu case we have a set of solutions which are even or odd according to whether n is even or odd. These are known as the first solutions and we denote to them by $V_{on}^{(1)}$. The second solutions are neither even nor odd and correspond to a second set $V_{on}^{(2)}$. Both $V_{on}^{(1)}$ and $V_{on}^{(2)}$ exist for the values of λ_{on} which lie on the characteristic lines shown in Fig I2. The analytical continuation to values of $z < 0$ based on the same analysis as for the case of Modified Mathieu functions. [Unfortunately we are not aware of the existence of tables for the joining factors in this case. Therefore we have to remain satisfied with the analytical expressions only.]

It is useful to make the correspondence between the $V_{on}^{(1)}$ and the $V_{on}^{(2)}$ and the $Mc^{(1)}, Mc^{(2)}, Ms^{(1)}, Ms^{(2)}$ clearer .$V_{on}^{(1)}$ for n even is the analog of $Mc^{(1)}$, $V_{on}^{(1)}$ for n odd is similar to $Ms^{(1)}$. $V_{on}^{(2)}$ (n even) and $V_{on}^{(2)}$ (n odd) correspond to $Mc^{(2)}$ and

$Ms^{(2)}$ respectively. The series representations for the $V_{on}^{(i)}$ ($i = 1, 2$) are given in [81] and [83] .Leitner and Spence [81] have discussed the oblate spheroidal wave functions in great detail. The reader interested in spheroidal wave functions in general is referred to [83,82,84,85].
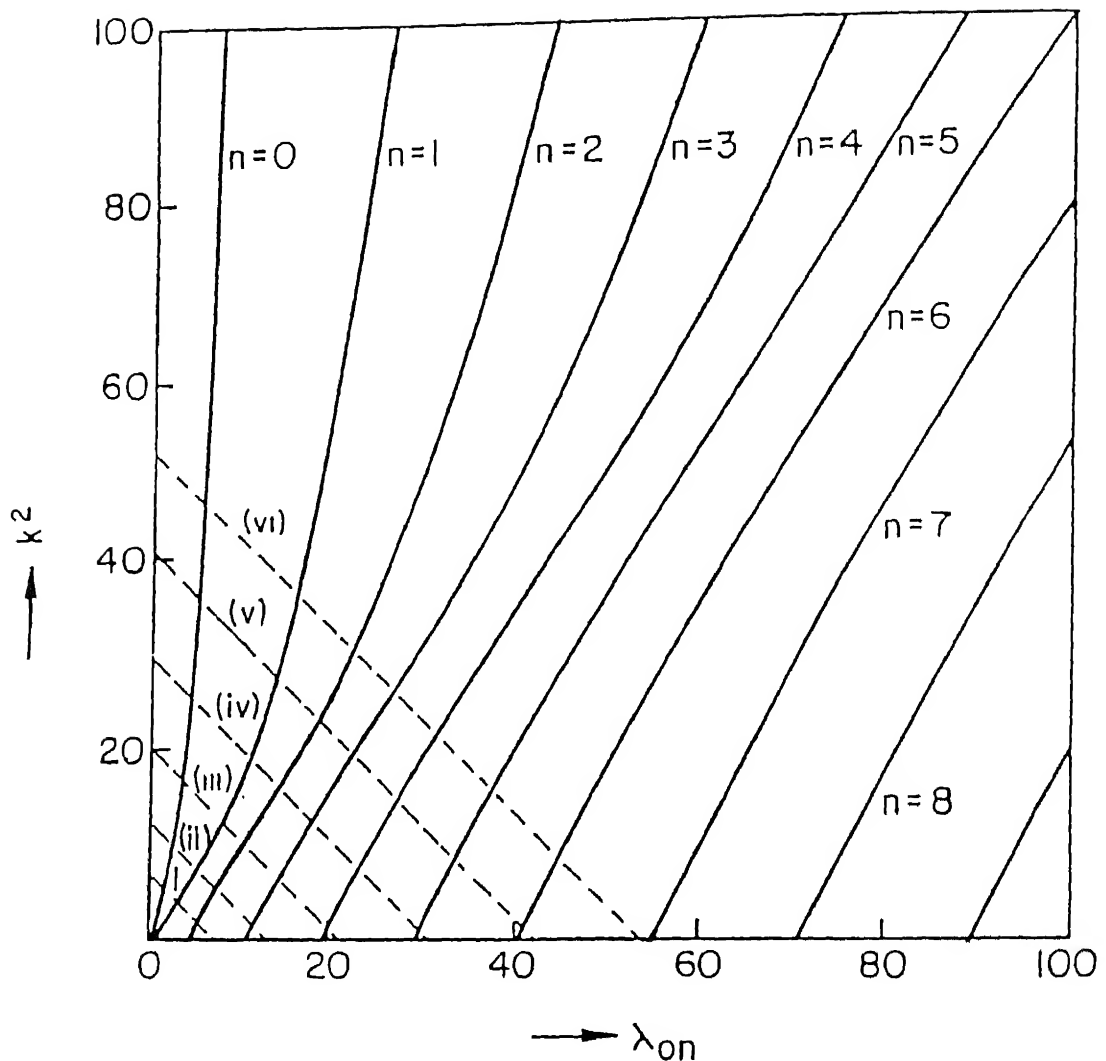
Figure I.2: $\lambda_{0n}-k^2$ plot for the characteristic lines for the oblate spheroidal functions with $m = 0$.(i),(ii),(iii),(iv),(v) and (vi) refer to the straight lines $\lambda_{0n} = -k^2 + p(p + 1)$ where $p = 2, 3, 4, 5, 6, 7$.

Appendix II

The Numerical Method

In this appendix we briefly outline the numerical method used in evaluating the reflection and transmission coefficients.

The differential equation we have to solve in order to obtain the reflection and transmission coefficients is of the usual Schroedinger type .This is given as

$$\frac{d^2\Psi}{dl^2} + \left(k^2 - V(l)\right) = 0 \qquad \cdot \tag{II.1}$$

where $V(l)$ has the generic form of a potential barrier situated at $l = 0$ and asymptotically($l \rightarrow \pm\infty$) falling off to zero. The asymptotic boundary conditions are :

$$\Psi(l) \;=\; I[e^{ikl} + \alpha e^{-ikl}] \qquad for \quad l \rightarrow -\infty \tag{II.2}$$

$$I\beta e^{ikl} \qquad for \quad l \rightarrow \infty \tag{II.3}$$

In other words, we have an plane wave incident from the left(-ve values of l) part of which gets reflected and the remaining part transmitted to the right (+ve l region).In the above i,α,β are complex quantities. without any loss of generality we can assume $I\beta = 1$.

We now convert this problem into two separate problems by defining $\Psi = U + \imath V$, where U, V are real functions of l and satisfy the differential equation independently. From Eqn II.3 we obtain the asymptotic conditions for U, V. These are

$$U = 1 \qquad , U' = 0 \tag{II.4}$$

$$V = 0 \qquad , V' = k \tag{II.5}$$

at $l = 100 \times \frac{2\pi}{k}$

Given these initial values we numerically solve the differential equation with the relevant potential and obtain n function values for U and V over one period of oscillation of the $l \rightarrow -\infty$ solution. n is taken to be very large(in our computations it is 10000). The amplitude of Ψ at each n value is therefore given as

$$A(i) = \sqrt{(U^2(i) + V^2(i))} \tag{II.6}$$

where i varies from 1 to $n + 1$.

We notice that $A(\imath)$ undergoes an oscillation with maximum and minimum values given as

$$A_{max} = I[1 + |\alpha|] \tag{II.7}$$

$$A_{min} = I[1 - |\alpha|] \tag{II.8}$$

Thus the reflection amnd transmission coefficients turn out to be

$$|R|^2 = |\alpha|^2 = \left[\frac{A_{max} - A_{min}}{A_{max} + A_{min}}\right]^2 \tag{II.9}$$

$$|T|^2 = |\beta|^2 = \frac{4 A_{max} A_{min}}{[A_{max} + A_{min}]^2} \tag{II.10}$$

The differential equations were solved using standard NAG Library routines available at the Computer Centre, IIT Kanpur. Scanning the values of $A(i)$ over one period gives A_{max} and A_{min} and hence R and T.
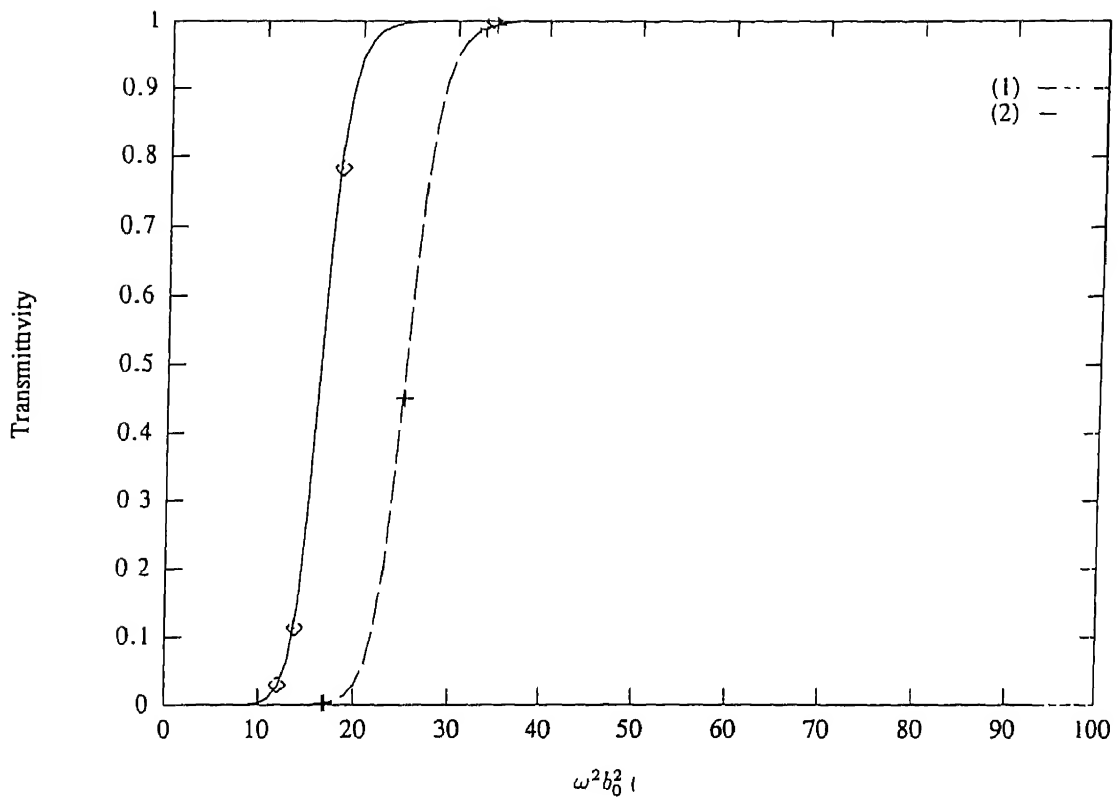
Figure II.1: Comparison between numerical and analytical results:$(1)|T|^{2}$for $n = 2, m = 4$ $(2)|T|^{2}$for $n = 2, m = 5$;the encircled/crossed points denote the analytical values.

Fortunately for us we have a way of checking the correctness of our numerical method.The analytically obtained values for R in Table 1 Chapter 5 can be compared with the numerical results obtained with the method outlined here.Fig II.1 shows the comparison for a few cases .The continuous curves are the numerical results and the encircled points are the analytical values.

Bibliography

[1] C.W.Misner and J.A.Wheeler , Annals of Physics **2**, 525 (1957)

[2] J.A.Wheeler , Annals of Physics **2**, 604 (1957)

[3] J.A.Wheeler , Geometrodynamics (Academic, New York, 1962)

[4] S.W.Hawking , Physical Review **D** **37**,904 (1988)

[5] S.B.Giddings and A.Strominger , Nuclear Physics **B** **306**,890 (1988)

[6] M.S.Morris , K.S.Thorne and U.Yurtsever , Physical Review Letters **61**, 1466 (1988)

[7] S.Coleman , Nuclear Physics **B** **310**,643 (1988)

[8] S.W.Hawking and G.F.R.Ellis , The Large Scale Structure of Spacetime (Cambridge University Press,Cambridge,U.K, 1973)

[9] R.Schoen and S.T.Yau , Communications in Mathematical Physics , **79**,47 (1981);R.Schoen and S.T Yau , Communications in Mathematical Physics , **79**,231 (1981); E.Witten , Communications in MAthematical Physics , **84**,223 (1982)

[10] H Epstein,V.Glaser and A.Yaffe , Nuovo Cimento **36**,2296 (1965)

[11] H.B.G.Casimir , Proc. K. Ned. Akad. Wet **51**,793 (1948)

[12] L.S.Brown and G.J.Maclay , Physical Review **184**,1272 (1969)

[13] T.A.Roman , Physical Review **D 33**,3526 (1986) ; Physical Review **D 37**,546 (1988)

[14] M.S.Morris and K.S.Thorne , American Journal of Physics **56**,395 (1988)

[15] J.L.Friedman,M.S.Morris,I.D.Novikov,F.Echeverria,G.Klinkhammer, K.S.Thorne and U.Yurtsever , Physical Review **42**,1915 (1990)

[16] J.L.Friedman and M.S.Morris , Physical Review Letters **66**,401 (1991)

. [17] D.Boulware , Physical Review **D 46**,4421 (1992)

[18] J.L.Friedman ,N.Papastamatiou,J.Z.Simon , Physical Review **D 46**,4442 (1992)

[19] J.L.Friedman ,N.Papastamatiou,J.Z.Simon , Physical Review **D 46**,4456 (1992)

[20] J.R.Gott III , Physical Review Letters **66**,1126 (1991)

[21] S.Deser, R.Jackiw and G.t'Hooft , Physical Review Letters **62**,220 (1992)

[22] R.P.Geroch , Journal of Mathematical Physics **8**,782 (1967)

[23] F.J.Tipler , Annals of Physics **108**,1 (1977)

[24] G.Y.Rainich , Transactions of the American Mathematical Society **27**,106 (1925)

[25] G.Y.Rainich , The Mathematics of Relativity (Wiley,New York,1950)

[26] J.D.Brown, C.P.Burgess, A.Kshirsagar, B.F.Whiting and J.W.York Nuclear Physics **B 328**,213 (1989)

124

[27] A.K.Gupta,J.Hughes,J.Preskill and M.B.Wise , Nuclear Physics **B** **333**,195 (1990)

[28] R.C.Myers , Nuclear Physics **B** **323**,225 (1989)

[29] A.Hosoya and T.Ogura , Physics Letters **B** **225**,117 (1989)

[30] J.Preskill , Nuclear Physics **323**,141 (1989)

[31] H.Ellis , Journal of Mathematical Physics **14**,104 (1973)

[32] G.Clement , International Journal of Theoretical Physics (1984)

[33] M.Visser , Physical Review **D** **39**,3182 (1989)

[34] M.Visser , Nuclear Physics **B** **328**,203 (1989)

[35] D.Hochberg , Physics Letters **B** **251**,349 (1990)

[36] J.W.Moffat and T.Svoboda , Physical Review **D** **44**,429 (1991)

[37] D.Hochberg and T.W. Kephart , Physics Letters **B** **268** ,377 (1991)

[38] K. Ghoruku and T.Soma ,Physical Review **D46**,1507 (1992)

[39] I.D.Novikov Soviet Physics JETP **68**,439 (1989)

[40] V.P.Frolov and I.D.Novikov , Physical Review **D42**,1057 1990)

[41] A.Ori , Physical Review Letters **71**,2517 (1993)

[42] F.Echeverria,G.Klinkhammer and K.S.Thorne , Physical Review **D** **44** ,1077 (1991)

[43] V.Frolov , Physical Review **D** **43**,(1991)

[44] S.Y.Kim , Physical Review **D** **46**,2428 (1993)

[45] S.Y.Kim and K.S.Thorne , Physical Review **D** 43,3929 (1991)

[46] S.W.Hawking , Physical Review **D** 46,603 (1992)

[47] A.Anderson and B.DeWitt , Foundations of Physics **16**,91 (1986); C.Manogue,E.Copland and T.Dray , Pramana–Journal of Physics **30**,279 (1988)

[48] R.Sorkin , Physical Review **D33**,978 (1986)

[49] E.Witten , Nuclear Physics **B323**,113 (1989)

[50] Y.Fujiwara, S.Higuchi, A.Hosoya, T.Mishima and M.Siino , Physical Review **D** 44,1763 (1992)

[51] P.Yodzis , Communications in Mathematical Physics **26**,39 (1972);General Relativity and Gravitation 4,299 (1973)

[52] G.T.Horowitz , Classical and Quantum Gravity **8**,587 (1991)

[53] C.V.Vishveshwara , Journal of Mathematical Physics **9**, 1319 (1968)

[54] L.Flamm , Physik. Z. ,**17**,448 (1916)

[55] A.K.Raychaudhuri , Physical Review **98**,1123 (1955)

[56] Ya.B.Zel'dovich , Soviet Physics JETP **14**,1143 (1962)

[57] Ya.B.Zel'dovich and L.P.Pitaevskii , Communications in Mathematical Physics **23**,185 (1971)

[58] F.J.Tipler , Physical Review **D17**,2521 (1978)

[59] A.Borde , Classical and Quantum Gravity **4**,343 (1987)

[60] L.Parker and S.A.Fulling , Physical Review **D7**,2357 (1973)

126

[61] G.L.Murphy , Physical Review **D8**,4231 (1973)

[62] J.D.Bekenstein , Physical Review **D11**,2072 (1975)

[63] P.C.W.Davies and S.A.Fulling , Proceedings of the Royal Society , London **A356**,237 (1977)

[64] S.A.Fulling and P.C.W.Davies , Proceedings of the Royal Society , London **A348**,393 (1976)

[65] S.M.Wagh and N.Dadhich , Physical Review **D32**,1863 (1985)

[66] B.Rose , Classical and Quantum Gravity **3**,975 (1986) ; **4**,1019 (1987)

[67] L.A.Wu, H.J.Kimble, J.L.Hall and H.Wu , Physical Review Letters **57**,2520 (1986)

[68] T.A.Roman and P.G.Bergmann , Physical Review **D 28**,1265 (1983)

[69] G.Klinkhammer , Physical Review **D43**,2542 (1991)

[70] U.Yurtsever , Classical and Quantum Gravity **7**,L251 (1990)

[71] R.M.Wald and U.Yurtsever , Physical Review **D 44**,403 (1991)

[72] N.Sen , Annalen der Physik **73**,365 (1924); C.Lanczos , Phys. Zeits.**23**,539 (1922) ; C.Lanczos , Annalen der Physik **74**,518 (1924); S.O'Brien and J.L. Synge Communications of the Dublin Institute of Advanced Studies **A 9** (1952) ; W.Israel , Nuovo Cimento **64** ,1 (1966)

[73] C.W.Misner,K.S.Thorne and J.A.Wheeler , Gravitation (W.H.Freeman,San Francisco,1973)

[74] D.Hochberg and T.W.Kephart , Physical Review Letters **70**, (1993)

[75] T.A.Roman , Physical Review **D 47**,1370 (1993)

[76] R.M.Wald , General Relativity (University of Chicago Press,Chicago, 1985)

[77] K.S.Thorne ,Black Holes and Timewarps (W.W.Norton, 1994)

[78] D.Deutsch and M.Lockwood , Scientific American **270** ,68 (1994)

[79] National Bureau of Standards , Tables Relating to Mathieu Functions (Columbia University Press , New York ,1951)

[80] M.Abramowitz and I.A.Stegun , Eds. , Handbook of Mathematical Functions and Formulas,Graphs and Mathematical Tables (Dover Publications,New York,1965)

[81] A.Leitner and R.D.Spence , Journal of The Franklin Institute **249** ,229 (1950)

[82] J.A.Stratton,P.M.Morse,L.J.Chu and R.A.Hutner, Elliptic Cylinder and Spheroidal Wave Functions (Wiley,New York,1941)

[83] C.Flammer , Spheroidal Wave Functions (Stanford University Press, Stanford,CA ,1957)

[84] P.M.Morse and H.Feshbach , Methods of Theoretical Physics (McGraw Hill ,New York,1953)

[85] A.Erdelyi , Ed. , Higher Transcendental Functions (McGraw Hill , New York,1953)Vol. 3

[86] N.W.MacLachlan , Theory and Applications of Mathieu Functions, (Dover Publications,New York ,1964)

[87] F.M.Arscott , Periodic Differential Equations, (The Macmillan Company, New York ,1964)

[88] D.Lovelock , Journal of Mathematical Physics **12**,498 (1971); Journal of Mathematical Physics **13**,874 (1972)

[89] J.T.Wheeler , Nuclear Physics **B 268**,737 (1986)

[90] D.L.Wiltshire , Physical Review **D 38**,2445 (1988)

[91] D.G.Boulware and S.Deser , Physical Review Letters **55**,2656 (1985)

[92] J.Scherk and J.H.Schwartz , Nuclear Physics **81**,118 (1974)

[93] B.Zwiebach , Physics Letters **B 156**,315 (1985)

[94] B.Zumino , Physics Reports **137**,109 (1986)

[95] X.Jianjun and D.Sicong , Modern Physics Letters **A 6**,2197 (1991)

[96] P Gonsalez Diaz , Physics Letters **B 247**,251 (1990)

ERRATA

Ch.no	Pg.no	Line/Eqn./Fig.no	The Correction
1	12	12	'distance' is misspelt
2	16	18	'Eq. 2.1.1' should be replaced by 'Eq. 2.1'
2	18	Eq 2.9	$z(r) = b_0 cosh^{-1}(\frac{r}{b_0})$ is the correct Eqn.
2	20	Eq 2.13	The $\frac{1}{4\pi a}$ factor in ξ should be $\frac{1}{2\pi a}$
2	24	18	'attempts 'is misspelt
2	24	24	(i) should be replaced by 2.1
3	37	3	Eq (5) should be replaced by Eqn.3.10
3	42	4	(curves (1)...) should read as (curves (3)...)
3	42	8	(curve (2)) should read as (curve (3))
3	42	17	(curve (3)) should read as (curve (1))
3	53	26	'cannot' should be replaced by 'can'
3	53	27	'at any cost' should be deleted
5	86	Tab. 5.1	$|T|^2 = .5373$ for m=2, $s_m = 4.25$
5	86	Tab. 5.1	$|T|^2 = .0020$ for m=5, $s_m = 16.75$
5	86	3	$|R|$ should be replaced by $|T|^2$
5	87	8	5.58 should read as 5.55
6	104	2	$\tau > \rho$ should read as $-\tau > \rho$
6	109	Eq. 6.58	$b_0^2 \geq max \left[\frac{e^{-2\omega t}(t_0 - t)^2}{\omega(t - t_0 + \frac{1}{2\omega})}\right]$ is the correct Eqn.
I	113	6	'A1.1 ..Mathieu' should read 'I.2 ..Modified Mathieu'
I	113	18	'Mathieu' should be replaced by 'Modified Mathieu'
I	114	Fig I.1	'B' should be replaced by 'b'
II	119	Eq.II.1	$\frac{d^2\Psi}{dl^2} + (k^2 - V(l))\Psi = 0$ is the correct Eqn.
II	119	13	'i,α,β' should be replaced by 'I,α,β'
II	120	3	'Eq.II.3 'should be replaced by 'Eqs II.2,II.3'